A Study of Inclement Weather Impacts on Freeway Free-Flow Speed

By

Hossam ElDin Hablas

Thesis submitted to the Faculty of the Virginia Polytechnic Institute and State University in partial fulfillment of the requirements for the degree of

Master of Science in Civil and Environmental Engineering

Hesham Rakha, Chair

Mazen Arafeh, Co-Chair

Antoine Hobeika, Member

Montasir Abbas, Member.

June 25, 2007

Blacksburg, Virginia

Keywords: Loop Detectors, Free-Flow Speed, Weather, and Speed Adjustment Factors.

A Study of Inclement Weather Impacts on Freeway Free-Flow Speed

Hossam ElDin Hablas

ABSTRACT

The research presented in this thesis attempts to investigate the impact of detector failure frequency and failure duration on the accuracy of loop detector speed, flow, and density measurements using a Monte Carlo simulation approach. The inputs to the model are the frequency of failures and failure duration. Several regression models were developed to relate loop detector accuracy to detector failure data. The results showed that the models were consistent and similar for the same location with an R square that ranged between 86% and 94% for all models and in comparing two locations, the differences between the regression models were minor except for the flow model errors, the location had the same trend but the magnitude of the flow RMSE increased by 7.5 to 15%.

The second part of the research effort attempts to quantify the impact of inclement weather (precipitation and visibility) on traffic stream free-flow speeds along freeway sections. The analysis is conducted using weather (precipitation and visibility) and loop detector data (speed) obtained from Baltimore, Minneapolis/St. Paul, and Seattle, US. The results demonstrate that visibility alone has a minimum impact on free-flow speed with reductions in the range of 1 to 3%. These reductions only appear as the visibility level falls below 1.2 km. The study demonstrates that the impact of snow is more significant than that of rain for similar intensity levels. Reductions caused by rain are in the neighborhood of 2 to 5% depending on the precipitation intensity while reductions caused by snow are in the neighborhood of 6 to 20%. With regards to freezing rain, higher reductions in free-flow speed were observed when compared to rain and snow. Specifically, the free-flow speed was reduced by 14% at the onset of freezing rain precipitation with a maximum decrease of 27% at freezing rain intensity of about 0.53 cm/h for Baltimore and as the case of Seattle the reduction was found to be constant with 31%.

Finally, the paper derives free-flow speed reduction factors that vary as a function of the precipitation type and intensity level. These reduction factors can be incorporated within the Highway Capacity Manual's procedures.

Acknowledgements

All Praise is due to Allah, we thank him, seek his guidance and forgiveness.

I would like to express all my gratitude to my advisor Dr. Hesham Rakha who had been very helpful to me in each stage of this research, financially and academically. I learned a lot from him, he always gives me the sincere advice and he was always there for me when I needed him.

Also my gratitude goes to Dr. Mazen Arafeh who gave me plenty of support and encouraged me a lot during that research. Finally I would like to express my deepest appreciation to my mother, my wife, and my children for helping me and for setting up a good study atmosphere in order to finish my degree.

Attribution

Two of the committee members aided in the writing and research behind several of the chapters of this thesis. A brief description of their background and their contributions are included here.

Prof. Hesham Rakha, Ph.D. (Department of Civil Engineering, Virginia Tech) is the primary Advisor and Committee Chair. Prof. Rakha provided the research direction for all work during the author's graduate study. Furthermore, Prof. Rakha also directed the composition of the chapters, extensively edited each chapter in this thesis and is the corresponding author of all papers published.

Dr. Mazen Arafeh, Ph.D. (Virginia Tech Transportation Institute, Virginia Tech) is senior research associate in the Center for Sustainable Mobility (CSM) worked in collaboration with the author on a project supported from Federal Highway Administration (FHWA). Dr Arafeh contributed to the regression statistics models in Chapter 4 and Chapter 5.

Table of Contents

List of Tables

List of Figures

Chapter 1: Introduction

1.1 Problem Statement

It is common knowledge that inclement weather affects the traffic stream Free-Flow Speed (FFS) along a roadway. However, it is not clear how these various forms of inclement weather impact traffic stream FFS.

Although previous research efforts provide substantial evidence that freeway speed reductions can be observed under snowy and rainy conditions, these research efforts were either conducted outside the United States or were limited in scope because they did not use long-term data to quantify the weather impact on traffic stream speed.

Chapter 23 in the Highway Capacity Manual 2000 (HCM) asserts that a basic freeway segment speed design is achieved under base conditions which are good weather, good visibility, and no incidents or accidents. In Determining Free-Flow Speed (FFS), the HCM defines the FFS as "the mean speed of passenger cars measured during low to moderate flows (up to 1,300 pc/h/ln)." Two methods are used to determine the FFS according to the HCM, the first is field measurement and the second is estimation using a set of guidelines provided in the HCM.

There are certain conditions in order to conduct the speed field measurements, which are beyond the scope of this research; however readers may refer to the HCM to get an overview of the approach. On the other hand the second method of determining the FFS is estimating the speed indirectly on the basis of the physical characteristics of the freeway. Equation 1 is used to estimate the FFS

$$FFS = BFFS - f_{LW} - f_{LC} - f_N - f_{ID}$$

Where *FFS* is the free-flow speed (km/h); *BFFS* is the base free-flow speed, 110 km/h (urban) or 120 km/h (rural); $f_{LW}$is the adjustment factor for lane width (km/h); f_{LC} is the adjustment factor for right-shoulder lateral clearance (km/h); f_N is the adjustment factor for number of lanes (km/h); and f_{ID} is the adjustment factor for interchange density (km/h).

Estimation of FFS for an existing or future freeway segment is accomplished by adjusting a base free-flow speed downward to reflect the influence of four factors: lane width, lateral clearance, number of lanes, and interchange density.

The proposed research effort is important because it develops FFS inclement weather adjustment factors that may be incorporated within the HCM 2000.

1.2 Previous Research Initiatives

HCM2000 specifies that "the base conditions under which the full capacity of a basic freeway segment is achieved are good weather, good visibility, and no incidents or accidents". Only in Chapter 22 – Freeway Facilities there is a brief accounting for the effect of inclement weather in the form of speed-flow curves for different weather conditions. HCM2000 suggests that free-flow speed (FFS) is reduced by 10 km/h (6 mph) in light rain, and by 19 km/h (12 mph) in heavy rain. A more detailed description of earlier research efforts are provided in the second chapter (literature review) of the thesis.

A key input to the analysis is loop detector data. Consequently, the research effort also investigates the impact of detector failure frequency and duration on the accuracy of loop detector speed, flow, and density measurements. Several research efforts examined the reliability of detectors on freeways. Tests for screening traffic characteristic data is grouped into two categories:

Threshold value tests in order to determine the acceptance of data by using minimum and maximum acceptable values of volume, speed, and occupancy, and

Tests based on basic traffic flow theory such as the average vehicle effective length (AVEL).

1.3 Thesis Objectives

The objectives of the thesis are five-fold:

1. Characterize the impact of detector failures on the accuracy of detector output in an attempt to provide a systematic approach for predicting the accuracy of loop detector data.
2. Characterize the impact of precipitation type (rain, freezing rain, and snow) and intensity levels on the free-flow speed of freeway sections.
3. Characterize the impact of visibility levels on the free-flow speed of freeway sections.
4. Investigate the regional differences in inclement weather impacts on traffic stream behavior.
5. Develop inclement weather FFS adjustment factors that can be incorporated within the HCM procedures.

1.4 Research Contributions

The two main contributions of this research effort are:

1 Developing a framework for predicting the accuracy of loop detector data. The input parameters to this framework are the average and standard deviation of the time interval between failures and the average duration of failures.

2 Freeway FFS inclement weather adjustment factors that can be incorporated within the HCM procedures. These factors account for precipitation type and intensity level, visibility level, and US regional differences.

1.5 Thesis layout

This thesis is organized into six chapters. The second chapter provides a review of the previous related work concerning loop detector accuracy and the impact of the inclement weather on the traffic stream FFS. Chapter three describes the different sources of weather data and describes how weather data are gathered, the various instrumentations required to gather weather data, and the types of data that are gathered. The fourth chapter presents a sensitivity analysis on what are the effects of loop detector failure durations and frequencies on the accuracy of loop detector measurements. The fifth chapter combines traffic and weather data in order to develop FFS inclement weather adjustment factors. Finally, the sixth chapter concludes with the conclusions of the study and recommendations for further research.

Chapter 2: Literature Review

Given that the evaluation of the impact of inclement weather on traffic stream free-flow speed hinges on two data sources – loop detector and weather data – this chapter first describes the state-of-the-art literature on the accuracy of loop detector speed, flow, and occupancy measurements. In addition, the state-of-practice studies on inclement weather impacts on traffic stream behavior are presented and analyzed in order to identify research needs and opportunities.

2.1 Loop Detector Accuracy Analysis

An important device used for electronic surveillance is the inductance loop detector. The data derived from inductance loop detectors are typically screened in order to enhance the data quality used in support of transportation applications.

Tests for screening traffic characteristic data are grouped into two categories: threshold value tests and tests based on basic traffic flow theory. These two screening approaches are described briefly in the following sections.

For the first category the most commonly used approach is to determine minimum and maximum acceptable values of volume, speed, and/or occupancy. Any data outside these ranges are regarded as invalid. For example, Coifman [1] introduced a method that identifies detector errors using dual loop speed trap data to compute the detector on-time at both the upstream and downstream detectors in the same lane. Detector errors are identified by differences in on times that exceed a certain threshold (taken to be 1/30s).

Turochy and Smith [2] combined the thresholds value test and basic traffic flow principles to remove erroneous observations from loop detector data. In their screening methodology they used 5 tests, two of them used the threshold values and two tests used basic traffic flow theory and the fifth test combined both thresholds and traffic flow theory principles.

For the first test they use a maximum occupancy threshold to examine the occupancy values in individual records, and then they used an overall maximum volume threshold and compared it against the 20-s volume measurements. The third test screened out the values that had zero speeds that were accompanied with positive volume measurements, the fourth test examined the maximum volume threshold with zero occupancy values, and the last test examined the feasibility of the Average Effective Vehicle Length (AEVL) (the summation of the vehicle length and the detector length) calculated using traffic flow theory and should be in the range of

5 – 12 meters (16.5 – 40 ft), any calculated value not within the mentioned range would flag data as erroneous.

A study done by Jacobson *et al.* [3] applied one test to screen the data using a feasible range of volume values in different occupancy intervals by using volume-occupancy ratios to test 20 sec volume and occupancy measurements. The algorithm was composed of two parts; the first one screened the 20 sec data. The algorithm detected an error if one of the following conditions occurred:

1. 20-s volumes greater than 17 veh/20s.
2. 20-s volume/occupancy ratio was outside the threshold ranges for four occupancy ranges (0-7.9 sec) (8-25.9 sec) (26-35.9 sec) (greater than 36 sec).
3. 20-s volumes were greater than 1 veh/20 s when the occupancies were between 0 – 0.1 percent.

The second part screened the 5-min data by screening the 5-min occupancies. If they were greater than 90 percent, they were considered as errors.

In 2002 Coifman and Dhoorjaty [4] introduced a series of detector validation tests that can be applied to dual loop detectors and partially to single loop detectors. They introduced eight tests, five of which can be applied to single loop detectors and all eight can be applied to dual loop detectors. The first test compares the pulse at the downstream loop against the upstream loop pulse that preceded it to identify any intervening pulses, if no intervening pulses exist the loop detectors are considered to be working fine, otherwise an error is recorded. After matching the pulses the speed from both detectors are calculated and from it the effective vehicle length is calculated. The second test compares the measured individual speeds and compares it with the median speed of 11 vehicles centered on the subject vehicle, if the individual speed deviates from the median by 32 km/h (20 mph) it is considered as a measurement error. The third test uses the headway versus the on-time to identify potential errors. Specifically, the uncongested regime is identified by on-times less than 0.3 sec and headways greater than 8s, while the congested regime is characterized by on-times greater than 1.3s. If an individual speed measurement falls in the uncongested regime and has a speed value less than 72 km/h (45 mph); it is considered as an erroneous measurement. The fourth test sets a range of feasible vehicle lengths between 10 and 90 ft and if the calculated vehicle length falls outside this range, it is considered an error. The fifth test sets a feasible range of values for the headway (min = 0.75

sec) and the on-time (min = 0.16 sec). The sixth test uses a normalized calculation of the vehicle length from the dual detectors $(L_1-L_2)/(L_1+L_2)$; if it is close to zero, the loops are working properly. The seventh test calculates the cumulative distribution function (CDF) for the vehicle length and compares it with another CDF calculated for the previous day but at the same time to detect any changes in the detector performance. The last test checks the workability of a detector by counting the number of pulses at one loop since the last pulse at upstream loop and detects errors.

A study done by Chen *et al*. [5] described a method that detects bad data samples and imputes missing or bad samples from a grid of clean data. According to the study "The diagnostic algorithm uses the volume-occupancy values to detect errors and impute missing data using neighboring loop detector measurements in combination with linear regression to predict missing data." Also a recent study conducted by Ishak [6] presented an approach derived from a fuzzy clustering concept to measure the level of uncertainties associated with dual loop detector readings, the algorithm is "model free because it does not use a mathematical model for the three parameters speed, volume, and occupancy. Instead, the approach clusters data into highly concentrated region observations, and then parameters are derived from both the membership grade and the decaying function of the normalized Euclidean distance by which the level of certainty is determined."

Despite of the numerous research efforts that have been devoted to identify erroneous loop detector data there appears to be no research efforts aimed at quantifying the effect of loop detector failures on the traffic stream parameter measurements. Consequently, Chapter 4 addresses this need by attempting to quantify the impact of loop detector failures on the system accuracy.

2.2 Impact of Inclement Weather on Free flow Speed.

Weather affects the operation of the transportation system by changing the driving setting as well as the performance of drivers, who adjust their individual headways and target speeds in response to specific weather events. The individual reactions of these drivers to weather, in turn, directly impacts overall system performance.

For freeways, the HCM2000 [7] specifies that "the base conditions under which the full capacity of a basic freeway segment is achieved are good weather, good visibility, and no incidents or

accidents". Only in Chapter 22 – Freeway Facilities is there a brief accounting for the effect of inclement weather on traffic stream behavior in the form of speed-flow curves for different weather conditions. The HCM2000 suggests that free-flow speed (FFS) is reduced by 10 km/h (6 mph) in light rain, and by 19 km/h (12 mph) in heavy rain.

In 1977 an FHWA report [8] cited in [9] presented the economic impacts of adverse weather on each type of facility and recommended speed reductions as summarized in Table 1

Table 1 : Impact of Inclement Weather on Traffic Stream Parameters.

	Reduction (%)
Dry	0
Wet	0
Wet and Snowing	13
Wet and Slushy	22
Slushy in wheel Paths	30
Snowy and sticking	35
Snowy and packed	42

Ibrahim and Hall [10] in 1994 analyzed freeway operations under inclement weather conditions on a section of the Queen Elizabeth Way (QEW) in Mississauga, Ontario. Three traffic stream variables, namely: volume, occupancy, and speed, were analyzed at 30-s intervals. Two sites with measured speeds and flow data and outside the influence of ramp or weaving sections were selected for analysis. Uncongested traffic data from 10 AM to 4 PM were used. The type and intensity of precipitation were accounted for. Weather conditions were categorized into six types: clear, light rain, heavy rain, light snow, heavy snow, and snowstorms.

The intensity of rainfall was indicated by accumulation on rain gauges while the intensity of snow was measured using visibility as a distinguishing criterion.

The study demonstrated that both the flow-occupancy and speed-flow relationships were affected by weather conditions. The degree of the effect corresponded to the severity of weather conditions. Light rain caused minimal effects on both relationships. Light rain caused a drop in speed of less than 2 km/h (1.2 mph). Heavy rain caused serious speed reductions varying from 5 to 10 km/h (3.1 mph to 6.2 mph). Light snow caused a 3 km/h drop and heavy snow caused a 37-42 km/h (23.12 – 26.23 mph) 35% –40% reduction in speeds. The duration of weather data was limited because they only used six clear days and, two rainy, and two snowy days.

Also Lamm *et al*. [11] examined 24 curved road sections of rural two-lane highways during both dry and wet conditions to study the effect of inclement weather on traffic stream behavior. They found no statistical difference in the operating speeds between those two conditions. Their data

were collected when visibility was not affected by heavy rain, which may explain the lack of difference in the measured speeds.

According to [9] "Brilon and Ponzlet [12] reported in 1996 on a study of fluctuations of average speeds from 15 stations on German autobahns. Ten 4-lane (two lanes per direction) sections and five 6- lane sections were monitored continuously between 1991 and 1993. Weather data were obtained from meteorological stations located about 5 to 50 km (3 to 31 miles) away from each observed area. Although, there were not perfect sources of weather data, they provided sufficient information to classify the weather conditions into five categories: dry, wet, dry or wet, somewhat snowy, and snow and ice. The influence of several independent factors was examined with ANOVA and several comprehensive models were developed that accounted for year, month, day type (weekday, Saturday, day before holiday, and holiday), location, daylight vs. darkness, traffic density, percentage of heavy vehicles, and weather in five categories as defined above. The study concluded that wet roadway conditions caused a speed reduction of about 9.5 km/h (5.9 mph) on 2-lane freeways, and about 12 km/h (7.46mph) on 3-lane freeways. Speed reduction was greater in darkness, average speed dropped by about 5 km/h (3.1 mph) in darkness."

Knapp and Smithson [13] selected a bridge over Interstate 35 as a study site for analysis purposes. The bridge had low volumes of traffic and was at least 26 feet wide (to allow data collection activities without closing the roadway). The data were collected with a mobile video traffic data collection and interpretation system which required a set of markings with known spacing to be identified on the roadway. These markings were painted on the shoulder by the data collection team prior to the beginning of the winter season. The data were collected during the 1998/1999 winter season when there was some type of snowfall.

The visibility and roadway snow cover data were manually collected, but the traffic volume, vehicle speed, and vehicle headway data were measured using the mobile video data collection and interpretation equipment. Overall, more than 27 hours of data were collected during the seven winter storm events.

Traffic flow characteristics were obtained for Interstate 35 northbound lanes at the site, and for a combination of both lanes. The traffic volume data were summarized into 15-minute volumes and then expressed as an equivalent hourly rate.

The average headway between vehicles in each lane, average vehicle gap for both lanes, and average vehicle speed were also calculated for the same 15-minute time periods.

Driver visibility, greater or less than 0.4 km (¼-mile) was also manually estimated by the data collection team every 15 minutes through the identification or sighting of a landmark at a distance of 0.4 km (¼-mile). Roadway pavement surface conditions were approximated by viewing the videotape and estimating the amount of snow cover on the roadway cross section. An average percentage of cross section snow cover was estimated for each 15-minute data collection time period.

The average winter weather vehicle speed was approximately 96.4 km/h (59.9 mph) while the typical average vehicle speed, was approximately 115.1 km/h (71.5 mph) producing a reduction in average speed of approximately 16%, and the average weather standard deviation was found to be 12.2 km/h (7.57 mph) while the typical standard deviation was only 2.99 km/h (1.86 mph). These differences represent an increase of 307%.

According to [9] "In 1998, May [14] (cited in [19],[20]) synthesized the effects of adverse weather conditions on freeway capacity based on previous work." May's FFS recommendations for HCM2000 are summarized in Table 2.

Table 2 : May's FFS recommendations for HCM2000.

	FFS (km/h)	**Reduction (%)**
Clear and dry	120	0
Light rain and light snow	110	8.33
Heavy rain	100	16.67
Heavy snow	70	41.67

Hawkins [15] -cited in [9]- "reported in 1988 about the relationship between vehicle speeds and weather conditions on UK's M1 motorway in Nottinghamshire. Weather conditions were classified into nine conditions with clear visibility and dry pavement as the base case. Speed began to drop when visibility was reduced to about 300 m (984 ft), with all lanes showing a reduction of between 25% and 30% as visibility reached 100 m (328 ft). Both light and steady or heavy rain were reported to cause a speed reduction of about 4 km/h (2.5 mph) on the slow and center lanes and about 6 km/h (3.7 mph) on the fast lane. Greater impacts on speeds were reported as a result of snow or slush - speed reduction of 30 km/h to 40 km/h (18.6 mph to 24.9 mph)."

Galin [16] in the late 1970s analyzed several factors that could affect speeds on Australian two-lane rural roads using multiple regression analysis. According to [9] "Analysis of speeds was performed by considering two weather conditions: dry and wet pavement. Wet conditions caused a drop of the average travel speeds of about 7 km/h (4.35 mph). However, this result may be of limited significance because base conditions were not clearly defined and the number of observed data was small (27 to 72 vehicles.)"

According to [9] "Olson et al. [17] in 1984 investigated the differences between speed distributions on wet and dry pavements in daytime. The study locations were a set of 26 permanent speed-monitoring stations, which included 7 interstate highways, 15 rural arterials, and 4 rural collectors in Illinois. Speed data in days with rain and adjacent dry days were analyzed. The analysis accounted for time-of-day effects. Although several dates with high probability of rain over a large portion of Illinois were collected, information on rainfall intensity was not available. Days were classified as "dry" or "rain." The mean speed, speed at various percentiles, and standard deviation were estimated. The Kolmogorov-Smirnov test was used to investigate differences between wet and dry day speed distributions. No differences among the daily speed distribution on dry and rainy days that were significant at a 95% confidence level were found.

Kyte et al. [18] measured prevailing free-flow speeds during clear conditions and in rain, snow, fog, low visibility, and high wind conditions. Data were collected between 1996 and 2000 from a level grade 4-lane section of I-84. Volumes were usually below 500 vphpl. Count and speed by lane, time, and vehicle length data were measured. Weather and visibility sensors were located in the same area to measure wind speed, direction, air temperature, relative humidity, roadway surface condition, the type and amount of precipitation, and visibility. The developed speed model includes several weather factors:

Speed = 100.2 - 16.4 x *snow* - 4.54 x *wet* + 0.77 x *vis* - 0.34 x *wind*

Where, *Speed* is the passenger-car speed in km/h; *Snow* is a binary variable indicating presence of snow on the roadway; *Wet* is a binary variable indicating that the pavement is wet; *Vis* is a visibility variable that equals 0.28 km (919 ft) when visibility ≥ 0.28 km or equals the actual visibility distance when visibility < 0.28 km; *Wind* is a binary variable indicating that wind speed exceeds 24 km/h (15 mph).

Speed decreased by 9.5 km/h (5.9 mph) when the pavement was wet. Speed decreased by 11.7 km/h (7.3 mph) when wind speed exceeded 24 km/h (15 mph). Speed decreased by 0.77 km/h (0.48 mph) for every 0.01 km (33 ft) below the critical visibility of 0.28 km.

Kyte, et al. [19] reported in 2001 on the effects of weather-related factors such as visibility, road surface condition, precipitation, and wind speed on free-flow speeds. Data were collected during two winter periods, 1997-1998 and 1998-1999, as part of an ITS field operation test of a storm warning system, located on an isolated section on I-84 in southeastern Idaho.

Sensors were installed to obtain traffic, visibility, roadway, and weather data. Normal conditions included no precipitation, dry roadway, visibility greater than 0.37 km (0.23 mile), and wind speed less than 16 km/h (9.94 mph). The average speed for passenger cars was 117.1 km/h (72.8 mph) and average truck speed was 98.8 km/h (61.4 mph). The mean speed for all vehicles was 109.0 km/h (67.7 mph). Light rain caused a drop in speed between 14.1 and 19.5 km/h (8.8 to 12.1 mph). Heavy rain caused a drop in speed of about 31.6 km/h (19.6 mph). The study used the freeway section of I-84 but was limited to rural freeway sections, and did not classify precipitation by intensity."

Similarly Liang, et al. [20] studied a 15-mile segment of Interstate 84 in Idaho. Traffic volume data were collected by ATRs, and visibility by two point detection systems and one laser ranging device from December 1995 to April 1996. Speed data from foggy days revealed an average

speed reduction of 8 km/h (5 mph) when compared to average clear day speed and an average speed reduction of 19.2 km/h (11.9 mph) was observed during snow events.

A recent study, Agarwal, et al. [21] was done on the freeway road network of the Twin Cities that is managed by the Traffic Management Center. It contains a number of roadside and in-pavement ITS field devices and includes several interstates and trunk highways built to freeway design standards. Unlike prior research, this study used a larger dataset of four years (January 2000 to April 2004) of traffic and weather information and categorized the impacts of weather variables by intensity ranges.

The study area has around 4,000 detector loops installed in freeway lanes that collect traffic data (volume and occupancy) for every 30-second time interval. These data were archived by the University of Minnesota Duluth for the Traffic Management Center. Weather records were obtained from five RWIS sites operated by the Minnesota Department of Transportation (Mn/DOT) and three ASOS sites at airports near the highway system and managed by the National Climatic Data Center.

The weather data reported by ASOS sites were not organized by a specific time interval, but provided information on the amount of precipitation (cm/hour) and the start and end timings of precipitation.

Once the data were collected and examined for appreciable flow-occupancy and speed-flow relationships, average freeway operating speeds were computed for all detectors near an ASOS site for every weather category. These average values were then compared to evaluate the percent reductions in freeway capacities and speeds due to varying rain and snow intensities.

According to the study "The rain data were divided into four categories (0, less than 0.0254, 0.0254–0.635, and greater than 0.635 cm/hour) for the analysis of the impacts of rain on freeway speeds. The database contained approximately 50,000, 1,400, 1,250, and 200 records for the above-defined rain categories by intensity values for each selected detector.

The freeway detector sites near the airports (Minneapolis-St. Paul International [MSP], Minneapolis Crystal [MIC], and St. Paul Downtown [STP]) were selected for this research effort. These sites showed statistically significant average speed reductions of 1%–2%, 2%–4%, and 4%–7% were found for freeway sites near the airports (MSP, MIC, and STP) for trace, light, and heavy rain, respectively. Statistical analysis showed that differences in speeds for light and heavy rain (0.0254 –0.635 and more than 0.635 cm/hour) were not statistically significant."

Datasets on snowfall events were categorized into five categories of none, trace, light, moderate, and heavy (0, less than/equal to 0.127, 0.1524 – 0.254, 0.2794 – 0.635, and greater than 0.635 cm/hour, respectively). The database contained approximately 50,000, 900, 550, 300, and 125 records for these snow categories for each selected detector.

The study showed speed reductions of 3%–5%, 7%–9%, and 8%–10% for trace, light, and moderate snow, respectively.

According to the study "Data for low visibility conditions, due to fog events, were categorized into four different groups (> 1.6, 1.6 – 0.816, 0.8 – 0.4, and < 0.4 Km) for freeway sites. The databases contained approximately 50,000, 110, 100, 300, and 60 records for above visibility categories for each selected detector.

Freeway sites near the Minneapolis Crystal Airport showed statistically significant reductions of reductions of 6.63%, 7.10%, and 11.78% were noted for three groups of visibility ranges when compared with visibility greater than one mile."

FHWA's Weather Management web site [22] contains comprehensive summaries of the effect of weather on traffic systems but sources for the information are not cited. The site reports the following impacts:

1. Freeways: Light rain reduces speed by approximately 10%.
2. Freeways: Heavy rain decreases speed by approximately 16%.
3. Freeway speeds are reduced by approximately 10% in light snow and by 40% in heavy snow.

Finally, another study conducted by Unrau and Andrey [23] used data from the Gardiner Expressway, a six-lane, limited-access highway that provides access to Toronto, to study the impact on inclement weather on traffic stream behavior. The Expressway had a speed limit of 90 km/h and an annual average daily vehicle count of 90,000 vehicles.

An initial analysis was done on one site that was chosen for the study (dw0060), located on the western portion of the Gardiner, based on the criteria that the site had almost complete data coverage and -as the study indicated- "minimal effect of road curvature, or grade, and merging maneuvers". For the purposes of analysis, only the median lane, or the lane closest to the center median, was included for each direction of traffic. The analysis included weekdays only (Monday through Friday).

Dual-loop detectors provided information in 20-second intervals for three variables: traffic vehicle count (volume); space mean speed (km/h); occupancy, which is an indication of traffic density. All information was aggregated to 5-minute intervals in order to be consistent with previous studies. Traffic volume and space mean speed were used directly as two indicators of traffic conditions. They also calculated the standard deviation of the 20-second average speeds and was also calculated for each 5-minute interval and used as a measure of the relative variability of speed in a traffic stream.

The weather data were obtained from one station - Pearson International Airport- located 16.1 km (10 miles) from the study site. The records were supplemented with data from Bloor St. station located 3.1 km (1.94 miles) from the study if there were any missing data from the Pearson airport data. To test the suitability of the Pearson data for the current study, the hourly precipitation observations taken at the City Centre Airport -located 1.1 km (0.7 mile) from the site - were compared with hourly accumulation data for Pearson. In total, only five percent differed in terms of their recordings of whether or not rainfall occurred.

According to the study "There were a total of 230 hours of observations – 115 hours of rainfall and 115 matched control hours. Of these 115 hours of rainfall, 105 were classified as light (0.1 – 2.4 mm total accumulation). The remaining hours were classified as moderate or heavy. Light rainfall was only considered because of the fairly undersized sample for heavy precipitation.

For the analysis each 5-minute time interval with rainfall was matched with the same clock time either one week before or after the period of rainfall, the relationships between speed, volume and occupancy was first explored in order to create subsets of observations according to traffic regime—uncongested, congested and queue discharge. The number of observations that were combined for dry and light rain was 1792 and 1823 data points, respectively.

The speed-volume relationships were modeled for each of the two datasets and a quadratic trend line was fit to the data, first for dry conditions and then for light rainfall. The R^2 of these models was 0.55 for dry conditions and 0.52 for light rainfall; the equations are as follows where X represents 5-minute volume counts:

Average Speed during Dry Uncongested Conditions = $-.0018X^2 + .1265X + 91.302$

Average Speed during Light Rain, Uncongested Conditions = $-.0018X^2 + .0744X + 89.286$"

The study concluded that at night in uncongested conditions, average speed is reduced by only 2.5 km/h (<3%) in light rain, and for daytime uncongested conditions, light rainfall is associated with an average speed reduction of 8 km/h (~10%).

The results of the various studies are summarized in Table 3 These results are normalized and presented in percentage reductions in speed relative to the base free-flow speed. These results will be compared to the results of the analysis presented in Chapter 5 later in the thesis. By analyzing the results of the table a number of conclusions can be derived. First, the results of the studies differ considerably, which suggests for the potential for regional differences in driver response to adverse weather conditions. Second, most studies did not have access to high resolution weather data or analyzed very small sample sizes.

Table 3: Summary of speed reduction findings from previous research.

Study	*Year*	*Country*	**Speed Reduction**
Ibrahim and Hall	1994	Canada	Light rain 2 %
			Heavy Rain 5-10%
			Light Snow 2.8%
			Heavy snow 35 -40%
Lamm *et al.*	1990	US	None in Light rain
Brilon and Ponzlet	1996	Germany	2 lane freeway 7.6 %
			3 lane freeway 9.6 %
			In dark 4 %
Knapp and Smithson	1998	US	Snow event 21 %
Hawkins	1988	UK	light and steady or heavy rain 6km/h
			Snow or slush 30 – 40 km/h
Liang et al.	1998		Fog 7.5 %
			Snow event 18 %
Galin	1981	Australia	Wet pavement 8 %
Olson *et al*.	1984	US	None in rainy days
Kyte *et al*.	2001	US	light rain 13 %
			Heavy rain 29 %
Kyte *et al*.	2001	US	Light rain with strong wind 9 %
Agarwal *et al*.	2006	US	Trace rain 1 - 2 %
			Light rain 2 – 4 %
			Heavy rain 4 – 7 %
			Trace snow 3 – 5 %
			Light snow 7 – 9 %
			Moderate snow 8-10%
Unrau and Andrey	2006	Canada	Light rain/ Day 10%
			Light rain/ Night <3%
FHWA's Weather Management web site	Accessed 2007	US	Light rain 10%
			Heavy rain 16%
			Light snow 10%
			Heavy snow 40%
HCM 2000	2000	US	Light rain 9.6 %
			Heavy rain 18.3%

2.3 Summary

A review of the literature has revealed the following deficiencies in the state-of-knowledge:

1. No study has attempted to relate the accuracy of loop detector data to loop detector failure frequency and duration as a function of the traffic stream level of congestion.
2. No studies have quantified the impact of freezing rain on traffic stream free-flow speed.
3. No studies have looked at regional differences associated with inclement weather impacts on free-flow speed.

4. Studies have not looked at changes in the variance of free-flow speed as a function of inclement weather.

The research presented in this thesis will attempt to address these deficiencies.

Chapter 3: Weather Data Analysis

Given that the study of inclement weather impacts on traffic stream behavior entails the usage of weather data, this chapter describes the various weather monitoring systems and how these data are gathered and measured.

3.1 Introduction

As was mentioned earlier in the thesis, low visibility, precipitation, high winds, and extreme temperature affect driver capabilities, sight distance, vehicle performance, and infrastructure characteristics. Changes to vision and control are the two primary effects on individual drivers. Fog, smog, and active precipitation, as well as splash and spray from other vehicles traveling on wet pavement, reduce highway visibility. High winds and poor traction from precipitation on the roadways reduce driver control and vehicle performance. These conditions alter driver behavior. Additionally, weather events can impact physical roadway geometry and traffic control devices (i.e., narrowed or blocked lanes, shortened acceleration/deceleration lanes, blocked signs and signals, or power outages to control devices), which in turn can lead to changes in traffic flow. Weather impacts mobility by reducing capacity and speeds, increasing headway, and increasing travel time and delay.

3.2 Definition

Weather comprises all the various phenomena that occur in the atmosphere of a planet. "Weather" is normally taken to mean the activity of these phenomena over a period of time of up to a few days. The average weather over a longer period is known as the climate. This aspect of weather is studied with great detail by climatologists, for any signs of climate change. [24]

Kyte *et al*. [19] defined the weather events as "any meteorological occurrence that causes weather conditions to degrade from the "ideal" weather condition." The ideal weather condition is defined as having the following conditions: (a) no precipitation; (b) dry roadway; (c) good visibility (greater than 0.4 km); and (d) winds less than 16 km/h.

3.3 How is Weather Measured?

Weather scientists or meteorologists measure temperature, rainfall, air pressure, humidity (the amount of moisture in the air), sunshine, and cloudiness. The weather instruments (weather

tools) used for weather measurement include the anemometer, thermometer, hygrometer, barometer, and rain gage.

Because this study uses the Automated Surface Observing System (ASOS) to measure the various weather parameters, the next section briefly describes the Automated Surface Observing System (ASOS).

3.4 The Automated Surface Observing System (ASOS)

The Automated Surface Observing System (ASOS) program is a joint effort between the National Weather Service (NWS), the Federal Aviation Administration (FAA), and the Department of Defense (DOD). The ASOS system serves as the nation's primary surface weather observing network. ASOS is designed to support weather forecast activities and aviation operations and, at the same time, supports the needs of the meteorological, hydrological, and climate research communities.

With the largest and most modern complement of weather sensors, ASOS has notably expanded the information available to forecasters and the aviation society. For example, the ASOS network has more than doubled the number of full-time surface weather observing locations.

According to the ASOS Guide "The ASOS system works non-stop, updates observations every minute, 24 hours a day, every day of the year, gathering more information on the atmosphere. Thus, ASOS information helps the National Weather Service (NWS) to increase the accuracy and timeliness of its forecasts and warnings--the overriding goal of the NWS modernization.

The primary concern of the aviation community is safety, and weather conditions often threaten that safety. A basic strength of ASOS is that critical aviation weather parameters are measured where they are needed most: airport runway touchdown zone(s)."

ASOS detects significant changes, disseminating hourly and special observations via the networks. Additionally, ASOS routinely and automatically provides computer-generated voice observations directly to aircrafts in the vicinity of airports, using FAA ground-to-air radio. These messages are also available via a telephone dial-in port. ASOS observes, formats, archives and transmits observations automatically. ASOS transmits a special report when conditions exceed preselected weather element thresholds, e.g., the visibility decreases to less than 3 miles [25].

3.5 System Description and Components

According to the ASOS guide "the ASOS performs all the basic observing functions, including the acquisition, processing, distribution, transmission, and documentation of data.

The ASOS consists of three main components.

1. Sensor group(s), consisting of individual weather sensors and a Data Collection Package (DCP)
2. The Acquisition Control Unit (ACU)
3. The Operator Interface Device (OID)"

Every ASOS contains the following instruments: (a) cloud height indicator sensor, (b) visibility sensor, (c) precipitation identifier sensor, (d) pressure sensors, (e) temperature/dew-point sensor, (f) wind direction/speed sensor, (g) rainfall accumulation sensor, and (h) freezing rain sensors.

3.6 Weather Observation Elements

3.6.1 Visibility

Visibility is reported in statue miles (SM) and fractions (space between whole miles and fractions); always followed by SM to indicate statute miles; values less than 1/4 mile are reported as M1/4SM.

3.6.2 Weather Data

According to the ASOS pilot guide "*ASOS reports precipitation type as rain (RA), which is liquid precipitation that does not freeze; snow (SN) as frozen precipitation other than hail; and precipitation of unknown type (UP). The precipitation type is concatenated by the precipitation intensity level as follows: light takes a minus sign (-), moderate takes no sign, heavy takes the plus sign (+); fog (FG); freezing fog (FRFG- temperature below 32F); Mist (BR); Haze (HZ); and Squall (SQ). In addition, the precipitation is augmented by the type of observer: Funnel Cloud/Tornado/Waterspout (FC); Thunderstorm (TS); Hail (GR); Small hail (GS; < 1/4 inch); Freezing Rain (FZRA).*" [26]

In addition, the ASOS provides a detailed report about the sky condition, temperature, dew-point, and altimeter setting (pressure in inches of mercury (Hg)). The specifics of how visibility is measured will be described later in the chapter.

3.7 Sensor and Measurement Description

This section describes the various sensors used to gather the various weather data and how these data are measured and gathered.

3.7.1 Visibility

ASOS visibility is based on light scattering. The visibility sensor projects a beam of light over a very short distance, and the light that is scattered is detected by a receiver. The amount of light scattered and then received by the sensor is converted into a visibility value.

A measurement using the forward scatter sensor is taken every 30 seconds. ASOS derives one-minute averages for the extinction coefficient and a day vs. night indication. A photocell on the visibility sensor turns on at dawn and off at dusk to alert the sensor whether to use day or night equations for visibility. A one-minute average visibility is calculated and the value is stored for the next 10 minutes. Finally, ASOS computes a running 10-minute harmonic mean once per minute from the stored data to provide the latest visibility. A harmonic mean is used rather than an arithmetic mean because it is more responsive to rapidly decreasing visibility conditions. The value obtained from this computation is then rounded down to the nearest reportable visibility value. This visibility is stored in memory for 31 days for the METAR reports. Eight one-minute data samples in the last 10 minutes are required to form a report.

The newest visibility value is checked against that reported in the last METAR report to flag if any visibility thresholds were exceeded. If so, ASOS generates a SPECI report. If visibility is variable enough, ASOS also generates an appropriate remark.

At airport locations with control towers, tower visibility is entered to ASOS and compared with surface visibility. If tower visibility is less than 4 miles and is less than surface visibility, tower visibility is entered in the body of the METAR report. If surface visibility is less than tower visibility, surface visibility is retained in the body of the METAR report.

The location of the visibility sensor is critical. The sensor should be located in the area of most concern. Therefore, most primary visibility sensors are placed near the touchdown zone of the primary instrument runway. The sensor must be located at least 10 feet above ground level.

Visibility in METAR is reported in quarter-mile increments up to two miles, then at 2.5 miles, then at every mile to a maximum of 10 miles. Visibilities greater than 10 miles are still reported

as 10 miles. Values less than a quarter mile are reported as a quarter mile. Visibilities are always rounded down to the next reportable value if needed.

The strength of the ASOS visibility sensor is its consistency of observation, when compared to other ASOS sites. Variations due to human observation are eliminated [27].

3.7.2 Present Weather and Obstructions to Vision

There are two ASOS present weather sensors. The Precipitation Identifier (PI) sensor discriminates between rain (RA) and snow (SN). The Freezing Rain (FZRA) sensor detects freezing rain. ASOS evaluates multiple sensor data and infers the presence of obstructions to vision.

The PI sensor has the capability to detect and report -RA, RA, +RA, -SN, SN, +SN. When rain and snow are mixed and the prevailing precipitation type cannot be determined, ASOS will report UP.

The Freezing Rain sensor measures accumulation rates as low as 0.01 inches per hour. If freezing rain is detected and the PI sensor indicates no precipitation or rain, then freezing rain is reported. If freezing rain is detected when the PI indicates snow, then snow is reported.

Obstructions to vision are not directly measured by ASOS, but inferred from measurements of visibility, temperature, and dew point. There are only two reported by ASOS: Fog (FG) and Haze (HZ), and only when the visibility is below 7 statute miles. [28]

3.7.3 Precipitation Accumulation

ASOS uses a Heated Tipping Bucket precipitation gauge which is constructed from anodized aluminum and stainless steel to provide years of precision recording for any type of precipitation. According to globaspec.com "*The tipping bucket is molded from a specially-formulated plastic that has a very low surface tension coefficient. The weight of the water required to make the bucket tip produces a momentary switch closure that is equal to 0.01 inch/0.25mm of rainfall. This momentary pulse may be used in a system to determine either rainfall amount and/or rate. The same tip that produces the pulse also dumps the bucket so that the gauge never requires emptying.*

The tipping bucket sensor is mounted on stainless steel instrument bearings and housed in an anodized aluminum case. The unit has a built in bubble level to facilitate installation. An insect/debri screen is also provided; the gauge is heated with two molded rubber electric heaters

which are controlled by a built-in thermostat. These heaters are factory set to operate at 35° F. (1° C.)." [29]

The PI sensor reports data every minute as a 10-minue moving average and stores the data in memory for 12 hours. If more than three data items are missing, the algorithm reports "missing", if there is equal number of different type is reported in the last 10 minutes the heavier is reported meaning if we have 3 samples of rain and three samples of snow the snow would be reported.

After the determination of the precipitation type the algorithm calculate the intensity (light-moderate-heavy) and it is determined from the highest common intensity derived from three or more samples of data. The precipitation type and rate are reported as an average rate over a 5-minute interval, for example if the rain type is determined and there are three heavy rain and one moderate rain in the past five minutes then it would report a heavy rain in the METAR report, also if the most recent 5 minutes of sensor data contains one light snow and two heavy snow reports, the light snow would be reported in the ASOS METAR report.

3.8 Field Data Description

The data used in this study were obtained from three major metropolitan areas in the US; the Twin Cities, MN, Seattle, WA, and Baltimore, MD. For each city two sets of data were obtained for the analysis: traffic data and weather data. Weather data were available from two sources; the Road Weather Information System (RWIS) operated by DOTs and the Automated Surface Observing System (ASOS) stations located at airports. An initial analysis of RWIS data in the Twin Cities Area revealed that the precipitation and visibility readings were either missing or invalid. Consequently, only the ASOS data were utilized for the entire analysis in order to maintain a level of consistency across the various locations. For each study area two years worth of data were utilized for the analysis. The highest total precipitation years were selected for the analysis. Using this criterion the following years were selected for the study; 2002 and 2004 for the Twin Cities, 2003 and 2004 for Seattle, and 2002 and 2003 for Baltimore. The analysis included data for 2004 because this represented the latest available 5- min. weather data at the time of the study for the Twin Cities and Seattle Areas. The analysis also included data for 2003 and 2002 because these years had the highest annual precipitation rates in the 5-year time frame for which weather data were available. In the case of Baltimore the analysis was confined to 2002 and 2003 because traffic and weather data were only available for these two years.

The weather data were then filtered to remove any negative numbers and categorized into rain, snow, and freezing rain. The data were validated against the average annual precipitation of rain and snow using data obtained from the National Climatic Data Center (NCDC). Figure 1 demonstrates that the highest annual rainfall is observed in Baltimore, followed by Seattle, and then Minneapolis. The data also demonstrated that the processed data has an accuracy of 78 %, 89%, and 80%, in the case of Baltimore, Seattle, and Minneapolis, respectively when compared to the NCDC data.

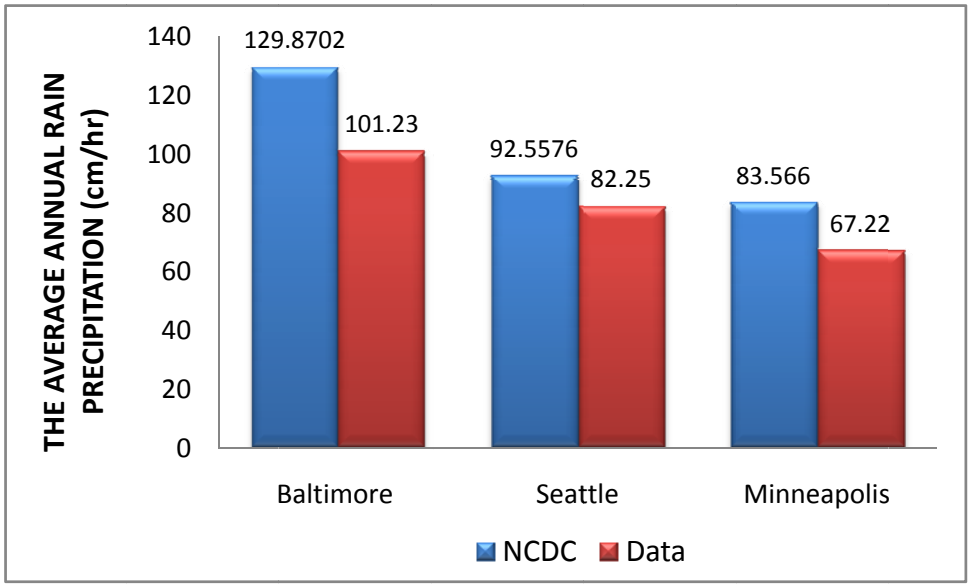

Figure 1: Comparison of average annual rain precipitation between the three cities and the NCDC.

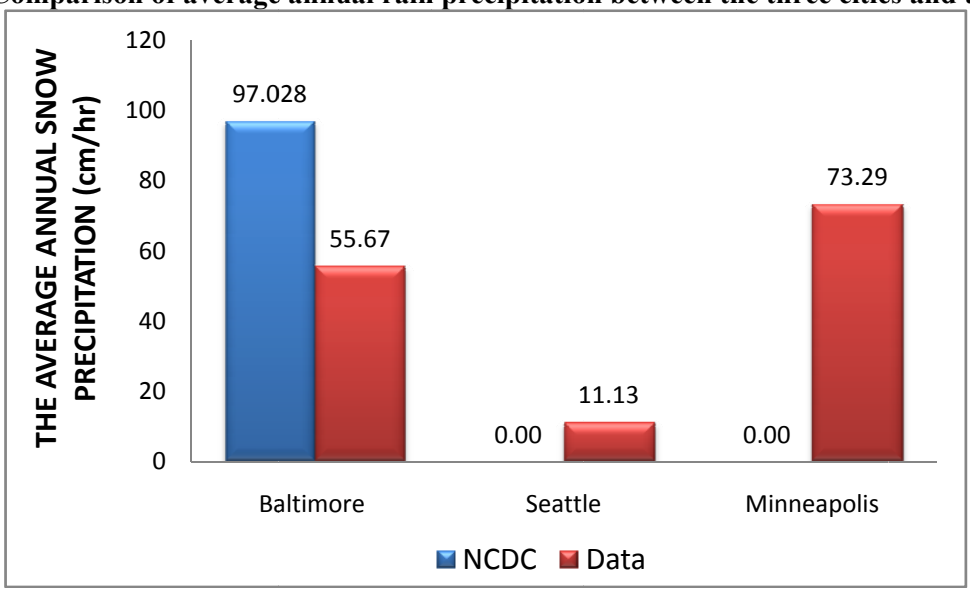

Figure 2: Comparison of the snow average precipitation between the three cities and the NCDC

In the case of snow data, the NCDC did not provide snow precipitation data for Seattle and Minneapolis. Furthermore the difference between the estimated annual rates and those reported by NCDC for Baltimore were almost 43%.

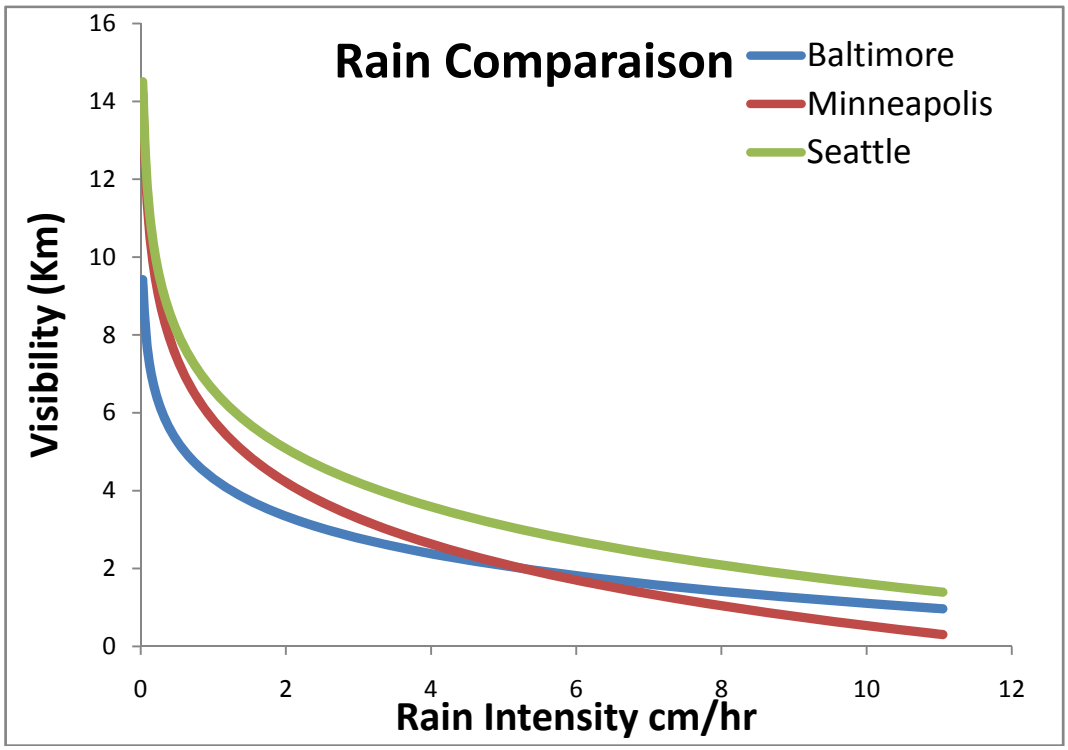

Figure 3: Rain trend line comparison

Using the weather data relationships between precipitation intensity and visibility levels were derived. Specifically, Figure 3 illustrates the various relationships that were derived from the data for the three cities (Baltimore, Seattle, and Minneapolis) using the corresponding visibility reported at the time of precipitation. The relationships clearly demonstrate, as would be expected, that the visibility level decreases as the rain precipitation level increases. Similarly, Figure 4 demonstrates similar trends for snow precipitation; however, regional differences are more evident in the case of snow precipitation in comparison to rain precipitation. One possible explanation for these differences could be the lack of significant data in the case of Minneapolis and Seattle.

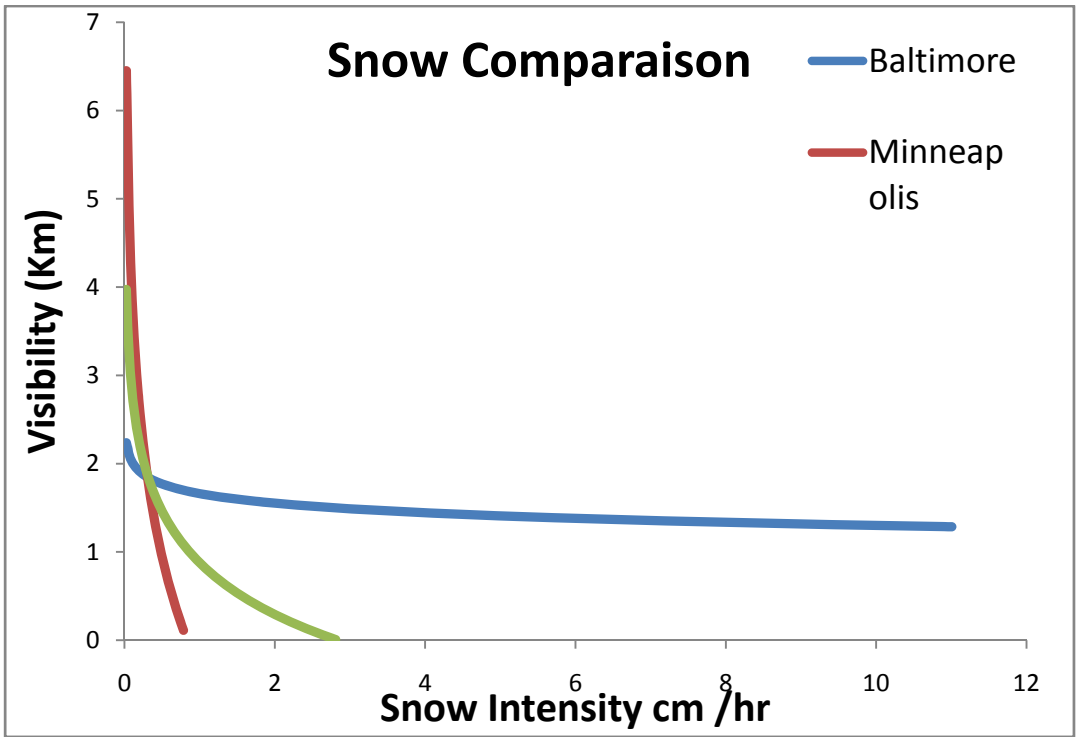

Figure 4: Snow trend line comparison

In addition, the correlation coefficient between visibility and the rain levels was computed, as summarized in Table 4.The results clearly demonstrate, as would be expected, a negative correlation between visibility and precipitation levels. Furthermore, the rain data were stratified into 9 equally-sized bins to compute the correlation coefficient between visibility and precipitation intensity level, as summarized in Table 5. Again, the results demonstrate a high level of negative correlation between visibility level and precipitation intensity, with larger reductions in visibility levels for snow precipitation in comparison to rain.

Table 4: Correlation Coefficient for the Raw Data between the Rain, Snow, Freezing Rain and the Visibility.

	Visibility		
	Baltimore	Seattle	Minneapolis
Rain	-0.207	-0.314	-0.247
Snow	-0.235	-0.168	-0.156
Freezing Rain		-0.355	

Table 5: Correlation Coefficients between the Mean Rain and Snow and the Corresponding Mean Visibility.

	Baltimore	Minneapolis	Seattle
Rain	-0.426	-0.869	-0.906
Snow	-0.884	-0.952	-0.751

Chapter 4: Loop Detector Data Accuracy Analysis

Hablas H., Rakha H., and Arafeh M.

Abstract

While the literature demonstrates that several researchers have investigated the issue of loop detector data reliability and the screening of erroneous loop detector data, no attempts have been made to relate loop detector accuracy to detector failure. Consequently, this paper attempts to quantify the accuracy of loop detector data as a function of detector failure duration and frequency using Monte Carlo simulation.

The research concluded, as would be expected, that the polling interval density, flow, and space mean speed RMSEs increase as the frequency and duration of failures increase. Furthermore, the research demonstrated that the density and flow RMSEs increase as the level of congestion increases while the space-mean speed RMSE decreases. Finally, the research developed regression models that predict the accuracy of loop detector measurements. The input parameters to these models are the failure frequency, the failure duration, and the traffic stream density. The results demonstrate that the models are consistent across the various locations and lanes with coefficients of determination that range between 86% and 94%.

A sensitivity analysis of the models revealed that the errors are insensitive to the error function, location, (speed and density), the lane, or the polling interval that is used to aggregate the data. Alternatively, the location had the same trend but the magnitude of the flow RMSE increased by 7.5 to 15%.

4.1 Introduction

An extremely important question that requires addressing is how accurate are loop detector data? This chapter attempts to answer this question using raw detector pulse data to establish relationships between traffic congestion levels, detector failure durations, and detector failure frequencies on detector accuracy.

Several previous research efforts have attempted to establish the level of reliability of loop detector data using various filtering and screening techniques. However, no research efforts have related loop detector accuracy to detector failure behavior.

In order to conduct such a research effort, detector pulse data are required. These unique data are typically not available and thus the research presented in this paper is unique in the approach that is used and the data that are utilized for the study.

4.2 Background

An important device used for electronic surveillance is the inductance loop detector. The data derived from inductance loop detectors are typically screened in order to enhance data quality in support of transportation applications.

Tests for screening traffic characteristic data are grouped into two categories: threshold value tests and tests based on basic traffic flow theory. For example, Coifman [1] introduced a method that identifies detector errors using dual loop speed trap data to compute the detector on-time at both the upstream and downstream detectors in the same lane. Detector errors are identified by differences in on times that exceed a certain threshold (taken to be 1/30s).

Turochy and Smith [2] combined the thresholds value test and basic traffic flow principles to remove erroneous observations from loop detector data. In their screening methodology they used 5 tests, two of these tests used the threshold values and two tests used basic traffic flow theory and the fifth test combined both thresholds and traffic flow theory principles. For the first test they used a maximum occupancy threshold to examine the occupancy values in individual records, and then they used an overall maximum volume threshold and compared it against the 20-s volume measurements. The third test screened values that had zero speeds that were accompanied with positive volume measurements, the fourth test examined the maximum volume threshold with zero occupancy values, and the last test examined the feasibility of the Average Effective Vehicle Length (AEVL) (the summation of the vehicle length and the detector length) calculated using traffic flow theory and should be in the range of 5 – 12 meters (16.5 – 40 ft), any calculated value not within the mentioned range would flag data as erroneous.

4.3 Field Data Description

This section describes the unique field data that were utilized for the study. The data were gathered from a section of the I-880 freeway in Los Angeles, California. The data are unique in that they include individual detector activations at a resolution of 60 Hertz as opposed to aggregated 20- or 30-s data. In addition to the raw pulse data a detector failure log was also

provided. The failure log indicated the start and end times of each failure at a resolution of 1 second.

The freeway section was composed of 5 lanes and the data were gathered from two dual-loop detector stations 540 m (1800 ft) apart (location 1 and location 2) with no on- or off-ramps between the two stations, as illustrated in Figure 5.

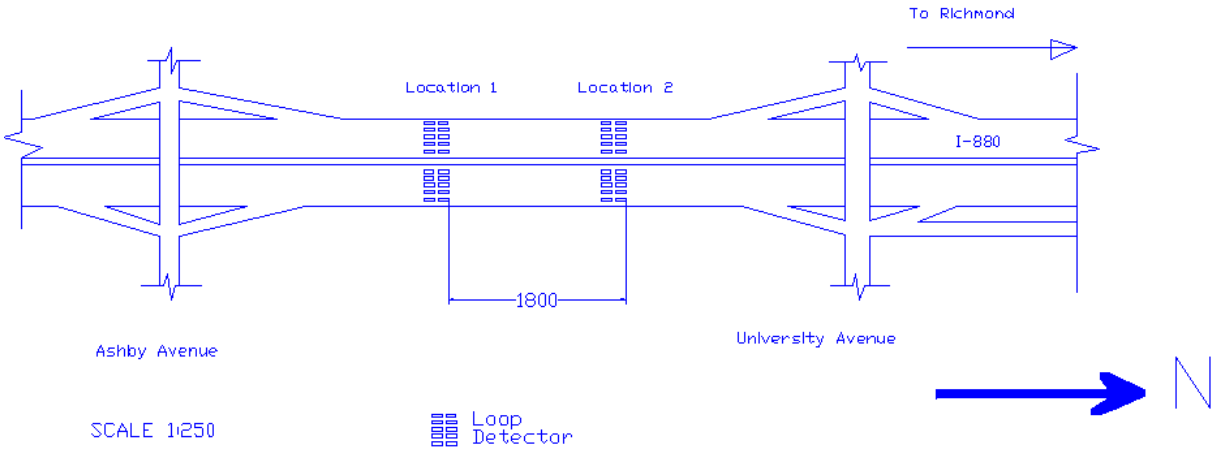

Figure 5: Layout of the site

The data were reported for a single day for each of the two locations. The data were initially filtered to remove any data during detector failures and to remove erroneous data to create a dataset of error-free data, as demonstrated in Table 6. The first column shows the on/off pulse indicator, where a value of one indicates the time instant that a vehicle occupies a loop detector while a zero indication represents the time instant the vehicle clears the loop detector.

Having explained that, the second row provides the time stamp at which the flag was observed at a $1/60^{th}$ of a second resolution. For example, the first vehicle activates the loop detector at instant 266/60 s and occupies the detector for the duration of 11/60 s ((277-266)/60). Using the detector activation data error-free aggregated traffic stream parameters (space-mean speed, flow, and density) were estimated. These parameters served as the base error-free traffic stream parameters that were used for comparison purposes.

Table 6: Sample of Error Free Raw Data

ON/OFF Flag	Time ($1/60^{th}$ s)
1	266
0	277
1	922
0	932
1	2272
0	2282
1	2477
0	2489
1	5439
0	5451
1	7273
0	7282
1	7919
0	7929
1	8683
0	8696
1	9431
0	9442
1	10487
0	10497
1	11019
0	11029
1	11721
0	11731
1	13818
0	13830
1	14534

Alternatively, the detector failure log provides the start and end times of detector failures at a 1-second level of resolution, as illustrated in Table 7. In this case the first column shows the time that the failure started and the second column shows time stamp that the failure ended. For example, the third failure started after 455 s after midnight and ended 460 s after midnight lasting for a total of 5 seconds. In the cases that the failure start and end times were identical (as is the case with the first failure), the failure duration was assumed to last for 1 second.

Table 7: Sample of Failure Log for Location 1

Failure Start Time (s)	Failure End Time (s)
58	58
447	447
455	460
542	542
697	697
992	992
1024	1024
1285	1285
1411	1411
1493	1493
1533	1534
1570	1570
1613	1613
1655	1655
1700	1700
1703	1703
1839	1839
1868	1869
1871	1871
1879	1879
1906	1906
2013	2013
2124	2124
2128	2128
2194	2194
2221	2221
2262	2262

4.4 Methodology

The methodology used for the analysis, as illustrated in Figure 6, can be summarized as follows:

1. Decompose the daily data into hourly data categorized by location and lane.
2. Identify the key input parameters for each hour: (a) the traffic stream density as a measure of the level of congestion, (b) the mean and variance of detector failure spacing, and (c) the range of detector failure durations.
3. Calibrate a Lognormal failure spacing distribution to the hourly detector failure data.

4. Develop a relationship between failure frequency and failure spacing mean and standard deviation derived from the lognormal calibrated distributions for each detector station and lane combination.
5. Using a Monte Carlo simulation approach introduce detector failures into the hour/location/lane combination error-free data.
6. Compute polling interval traffic stream space-mean speeds, flows, and densities and compare to error-free data estimated parameters, the basic polling interval that was used is 20 seconds and an additional analysis was done for polling interval equal to 30 sec and 1 min on lane 3 only.
7. Compute an hour/location/lane specific Route Mean Square Error (RMSE) relative to error-free data parameter estimates.
8. Develop statistical regression models to relate loop detector accuracy to detector failure duration, detector failure spacing mean and standard deviation, and traffic stream density.

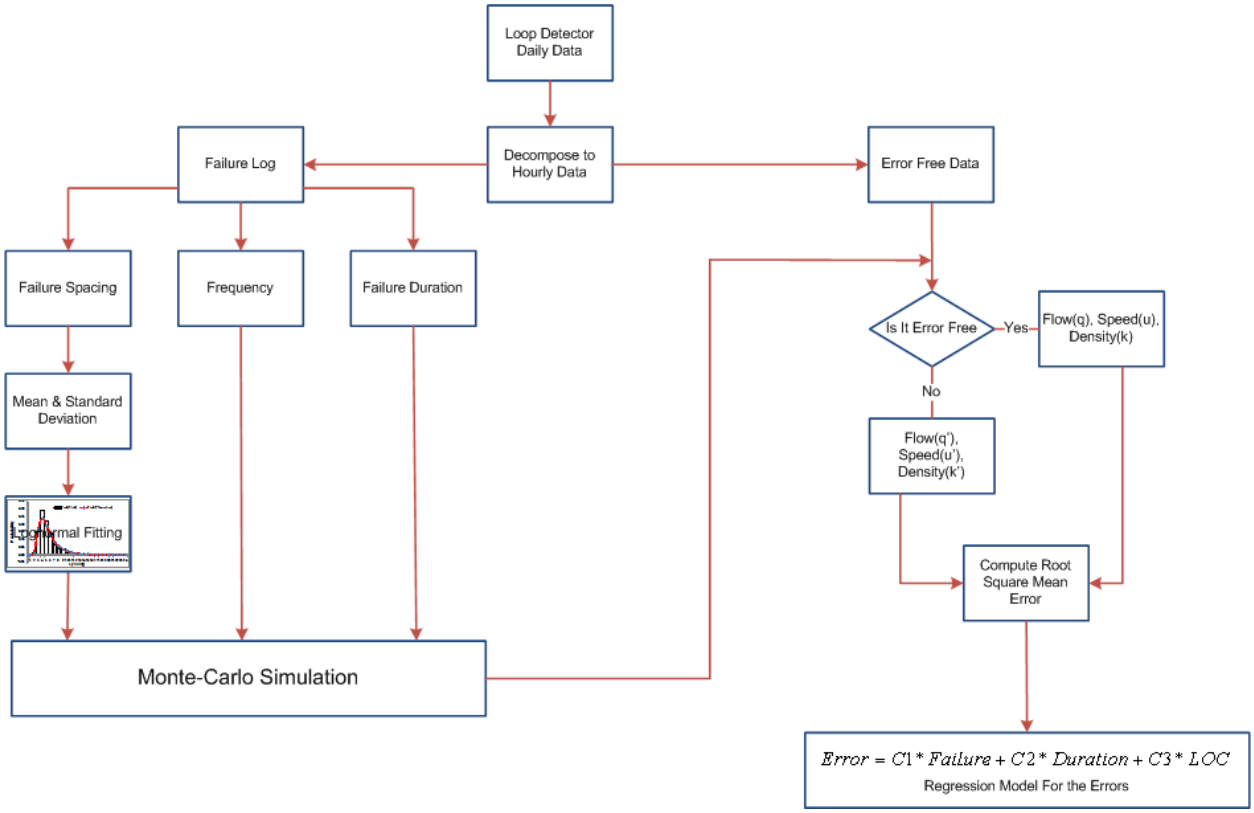

Figure 6: Loop Detector Analysis Methodology

The specifics of each of the eight steps are described in the following sections.

1. The failure log was decomposed into an hourly data set, and for each hour the number of failures was computed together with the time spacing between two consecutive failures,

as summarized in Table 8. The first row illustrates the hour ID while the remainder rows present the time spacing between every two consecutive failures and the last row shows the number of failures (frequency) that occurred in that hour. For example, in the case of the ninth hour (first column) 7 failures occurred with failure spacing ranging between 13 and 2466 s spacing.

Table 8: Sample of Hourly Spacing Data.

9	**10**	**11**	**12**	**13**	**14**	**15**	**16**
33	236	20	836	167	443	423	1186
13	116	271	601	543	8	301	338
74	54	450	652	559	5	957	78
231	4818	278	498	730	611	481	319
442		328	2307	661	37	250	184
309		166			1202	34	107
2466		381			365	277	260
					751	705	384
							30
							52
							30
							19
							4104
7	**4**	**7**	**5**	**5**	**8**	**8**	**13**

2. For each hour the minimum and the maximum failure temporal spacing was computed to provide a range of failure spacing. This range was divided into an equal number of bins across all analysis hours. The number of failures in each bin was then computed and the probability of failure was computed by dividing the number of failures in a bin by the total number of failures, as shown in Table 9. Column 1 of the table shows the failure spacing bin, while, column 2 shows the bin probability, and the third column shows the frequency of failures in a bin.

Table 9: Number of Failures Observed in Each Bin and Their Probability.

Failure Spacing (s)	Probability	Frequency
0.000	0.000	0
0.999	0.000	0
1.999	0.000	0
2.999	0.093	59
3.999	0.174	110
4.999	0.179	113
5.999	0.153	97
6.999	0.114	72
7.999	0.082	52
8.999	0.041	26
9.999	0.038	24
10.999	0.036	23
11.999	0.033	21
12.999	0.013	8
13.999	0.008	5
14.999	0.011	7
15.999	0.008	5
16.999	0.003	2
17.999	0.003	2
18.999	0.005	3
19.999	0.003	2
20.999	0.000	0
21.999	0.003	2
22.999	0.000	0
		633

3. Fit a lognormal distribution to the failure spacing probability, as illustrated in Figure 7. The fitting of the distribution was achieved my minimizing the sum of squared error (SSE) between the theoretical distribution and observed probability histogram. In the figure, the x-axis shows the spacing between failures and the y-axis shows the probability of each failure. The histogram illustrates the field observed probabilities (number of failures for a specific spacing range divided by the total number of failures) and the red line shows the theoretical lognormal distribution super-imposed on the field data.

   Typically in the case of a random process, the Poisson distribution is utilized to represent the count of random events within a specific time interval and a negative or shifted negative exponential distribution describes the spacing between these events. However, as demonstrated in Figure 7 the field observed data build up gradually from its lower limit and furthermore is non-symmetric. Consequently, a lognormal distribution was considered for the analysis.

   A lognormal distribution requires two parameters, namely: the mean (μ) and standard deviation (σ) of the log-transformed data. The pdf of the detector spacing (S) function is given by

$$f(S) = \begin{cases} \dfrac{1}{\sqrt{2\pi}\sigma S}\exp\left[-\dfrac{(\ln S - \mu)^2}{2\sigma^2}\right], & S > 0 \\ 0, & \text{otherwise} \end{cases}$$

Where the variance is greater than zero. The mean and variance of the lognormal random variable can then be computed as

$E(S) = \mu_L = e^{\mu+\sigma^2/2}$, and

$V(S) = \sigma_L^2 = e^{2\mu+\sigma^2}\left(e^{\sigma^2} - 1\right)$.

Here μ and σ are the mean and standard deviation of the log-transformed spacing data, respectively; μ_L and σ_L are the mean and standard deviation of the lognormal random variable, respectively; and *S* is the failure spacing.

The mean and standard deviation of the log-transformed spacing can be computed as

$\mu = \ln\left(\dfrac{\mu_L^2}{\sqrt{\mu_L^2 + \sigma_L^2}}\right)$, and

$\sigma^2 = \ln\left(\dfrac{\mu_L^2 + \sigma_L^2}{\mu_L^2}\right)$.

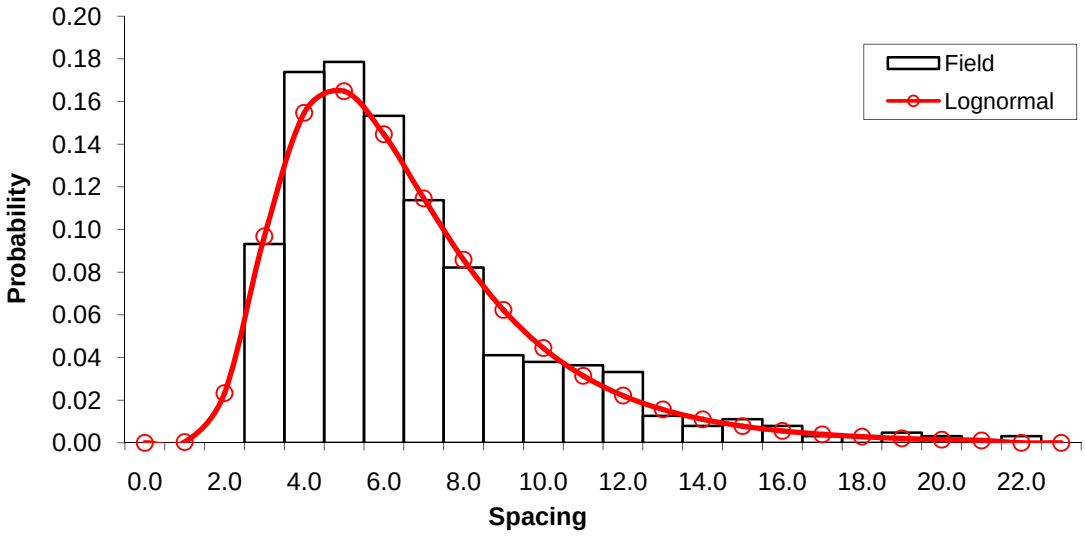

Figure 7: Lognormal Distribution Fit

4. Calibrate the lognormal distribution mean and the standard deviation by minimizing the computed Chi-Square error (Chi-2). Compare the computed Chi-square error to the theoretical Chi-square error for the identified degrees of freedom (Chi-1) as shown in Table 10. For example, for one of the hours the mean and the standard deviation were

computed as 1.685 and 0.50, respectively with a probability of almost 98% demonstrating that the lognormal distribution provides a good fit to the data.

Table 10: Mean and Standard Deviation and Compared Chi-Square.

Mean	1.685	Z	757.69
Std Dev	0.50	**Prob.**	98.4%
		Chi-1	22.36
		Chi-2	4.53

The calibration procedure was applied to each hour to compute the lognormal distribution mean and the standard deviation, as summarized in Table 11. In Table 11 the data are sorted based on the failure frequency in ascending order. As would be expected as the log-transformed mean decreases as a function of the failure frequency.

Table 11: Mean and Standard Deviation for the Entire Day.

Failure Frequency (Failures/h)	Mean (μ)	Std. Dev. (σ)
7	3.50	2.05
8	3.06	1.90
8	3.70	1.01
19	3.90	1.69
24	3.78	1.17
28	4.62	1.00
65	3.75	0.58
165	3.11	0.91
187	2.91	0.96
448	1.86	0.77
558	1.68	0.77
572	1.63	0.40
624	1.99	0.52
631	1.69	0.50

Recognizing the fact that the failure spacing is inversely proportional to the failure frequency, the following relationship can be derived

$$E(S) = \frac{3600}{F}.$$

Here E(*S*) is the expected spacing over all realizations in units seconds while *F* is the frequency of failures in units of failures per hour.

Solving for the failure frequency, the following relationship can be established

$$F = \frac{3600}{\exp\left(\mu + \frac{\sigma^2}{2}\right)}.$$

By taking the log-transformation of both sides of the equation and re-arranging the terms we derive

$$\mu = -\ln(F) + \left[\ln(3600) - \frac{\sigma^2}{2}\right] = -\ln(F) + C$$

Where C is a constant for a specific variance.

Consequently, a logarithmic function should be sufficient to relate the mean of the log-transformed data to the failure frequency, as illustrated in Figure 8 and Figure 9.

The x-axis represents the frequency of failures while the y-axis represents the mean and standard deviation of the log-transformed failure spacing. The two figures demonstrate consistency across the two locations with R^2 values ranging from 67% for location 1 to almost 95% for location 2. Similarly, the two trend lines for the standard deviations are similar with R^2 values of 68% and 80% for locations 1 and 2, respectively.

The equations of the trend lines for both locations were then used to compute the lognormal distribution mean and the standard deviation for a specific failure frequency while conducting the Monte Carlo simulation that is described in the next step.

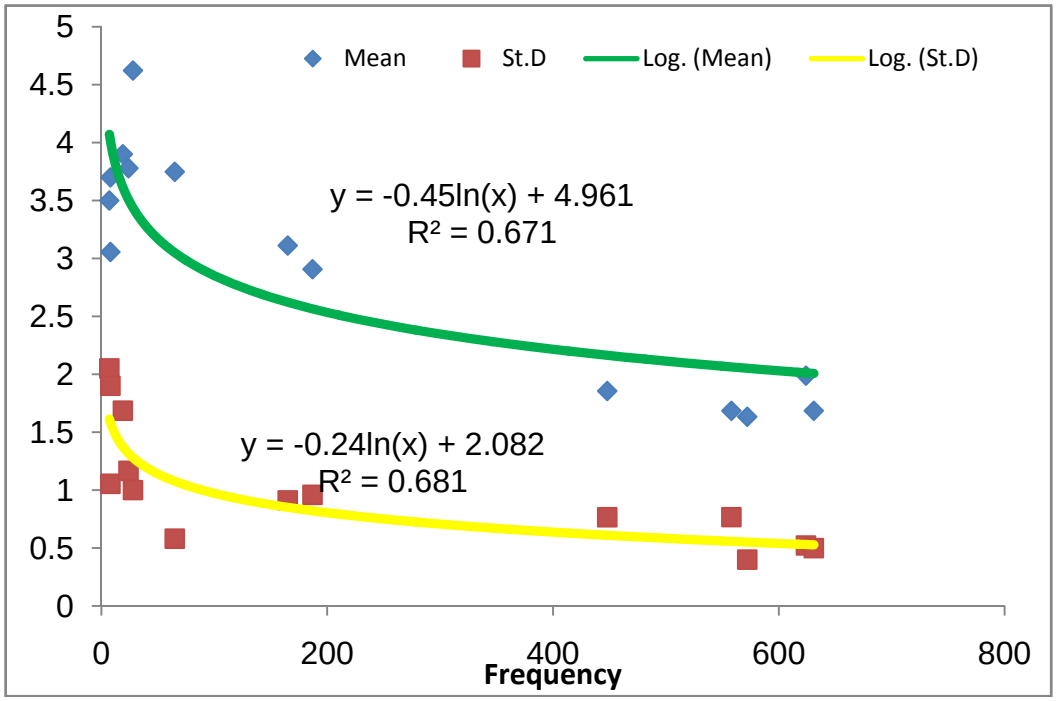

Figure 8: Lognormal Distribution Fit for the Mean and the Standard Deviation for Location 1

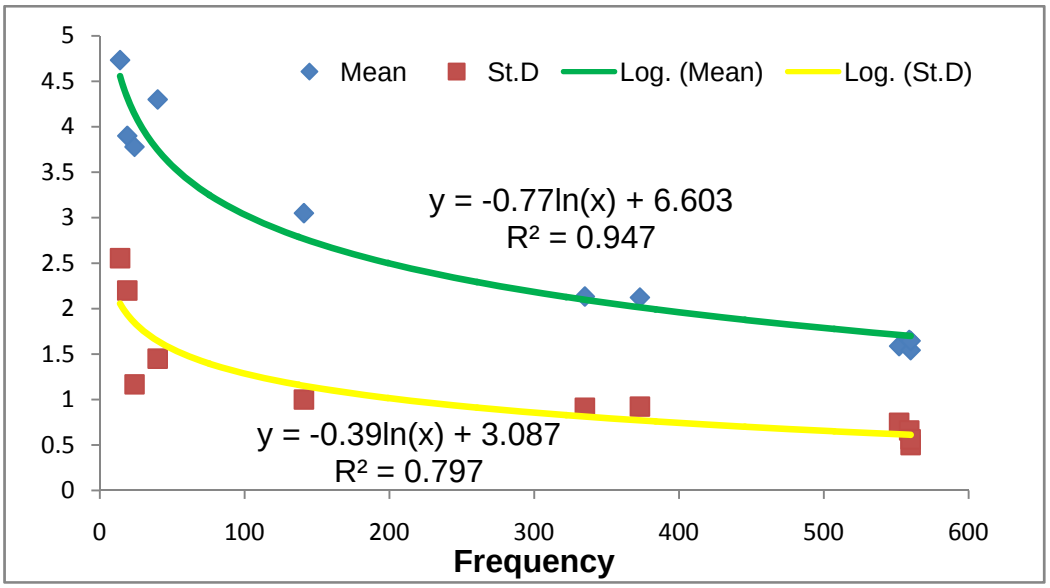

Figure 9: Lognormal Distribution Fit for the Mean and the Standard Deviation for Location 2

5. The next step in the analysis involved conducting a Monte Carlo simulation by introducing failures into the error-free data at different failure frequencies (using the relationships developed in step 4).

   In generating the lognormal random variables a method due to Box and Muller was applied. This technique is simple and easy to program. The method involves generating a standard normal variate and then converting the standard normal variate to a normal variate with mean μ and variance σ^2. Once we generate a normal variable X characterized by N (μ, σ^2) we can generate the spacing variable (S) as $S=e^X$. Using Matlab the X normal variable was generated and from it the spacing variable was computed by taking the exponent of variable X.

   The simulation considered failure durations that varied from a minimum to a maximum value. A total of 30 repetitions were made for each failure frequency/duration combination. A sample application of the failures to the data is illustrated in Figure 10. The figure illustrates the time interval within the fourth hour on the x axis and the detector indication (0 or 1) on the y axis. The detector activation flag is a binary 0-1 variable that is 1 when the vehicle occupies the loop detector and 0 when the detector is not activated. The gap between the 4.3 and 4.6 reading along the x axis was formed due to the introduced failures.

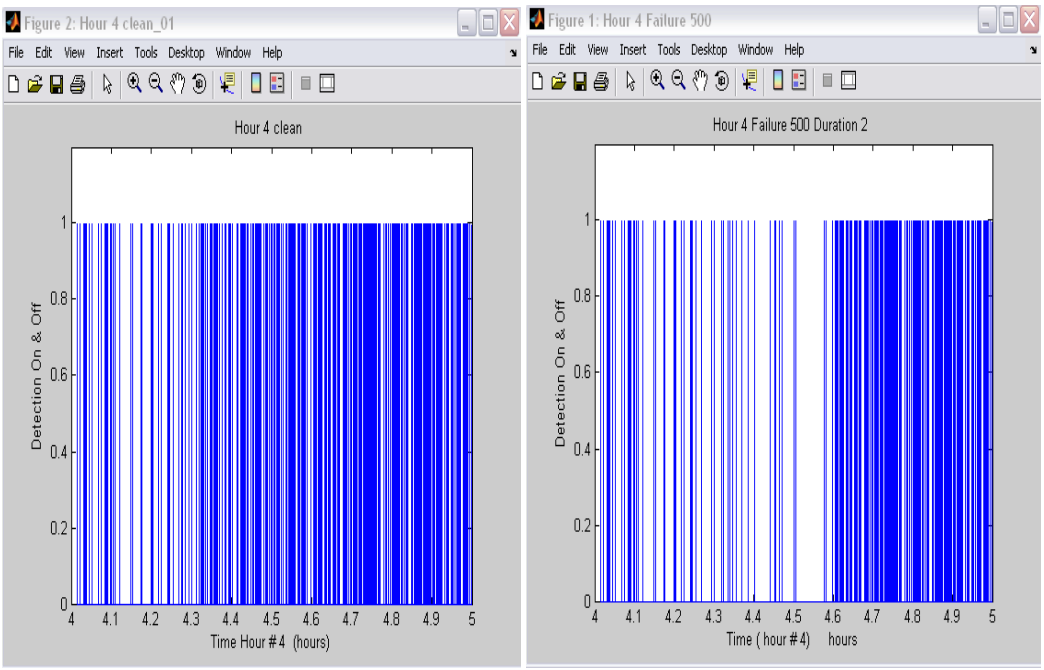

Figure 10: Comparison Before and After Introducing Failures

6. 20-second traffic stream parameters (space-mean speed, flow, and density) were computed for each hour/location combination and compared to the parameter estimates using the error-free data. The analysis was also repeated for one station using varying levels of data aggregation, as will be described later in the paper.
7. The root mean square error (RMSE) over the 30 repetitions was then computed for each failure frequency/spacing combination for each location/lane combination.
8. The data constructed in step 7 were then stratified by traffic stream density, failure frequency, and failure duration to construct statistical models that predict the RMSE. The structure of the model is of the form

   $$E = C_1 \times F + C_2 \times D + C_3 \times k\,.$$

   Where E is the RMSE (km/h in the case of space-mean speed, veh/h/lane in the case of flow, and veh/km/lane in the case of density), F is the failure frequency (failures/h), D is the failure duration (s), k is the traffic stream density (veh/km/lane), and C_1, C_2, and C_3 are model calibrated parameters.

4.5 Model Validation

Prior to conducting the Monte Carlo simulation, a validation exercise was applied in an attempt to validate the random number generation procedures. Specifically, considering a failure

frequency of 500 failures/h, eight independent sets of failure spacing were generated using the regression models that were described earlier. The generated data were then analyzed as follows:

A. Determine the minimum and the maximum spacing values.
B. Divide the range between the min and max values into 23 equally sized bins.
C. Determine the frequency of observations in each bin and the corresponding probability.
D. Construct the simulated histogram of bins and their corresponding probability.
E. Compare the simulated probability distribution to the theoretical distribution that was used to generate the random numbers, as illustrated in Table 12. The first column shows the ID number of the generated spacing, the second column shows the mean, the third column shows the simulated standard deviation, the forth column summarizes the theoretical Chi-square value for the degrees of freedom, the fifth column shows the observed Chi-square value, and the final column presents the probability of observing this Chi-square value. The results clearly demonstrate that the generated failure spacing distribution is consistent with the theoretical lognormal distribution.

Table 12: Comparison Between the 8 Generated Spacing using Matlab.

Repetition	Mean	Std. Dev.	Chi-Square		Probability
			Theoretical	Observed	
1	2.65	0.67	19.68	3.35	98.53
2	2.68	0.69	19.68	7.74	73.68
3	2.76	0.67	18.31	3.73	95.86
4	2.68	0.66	21.03	5.20	95.11
5	2.66	0.63	18.31	5.11	88.34
6	2.79	0.67	18.31	5.08	88.56
7	2.70	0.67	22.36	11.80	54.43
8	2.67	0.67	18.31	5.55	85.17

To further illustrate the results graphically, Figure 11 presents the generated and theoretical failure spacing distribution super-imposed on the generated failures. The figure clearly demonstrates that the proposed random number generation module was consistent with the theoretical distribution.

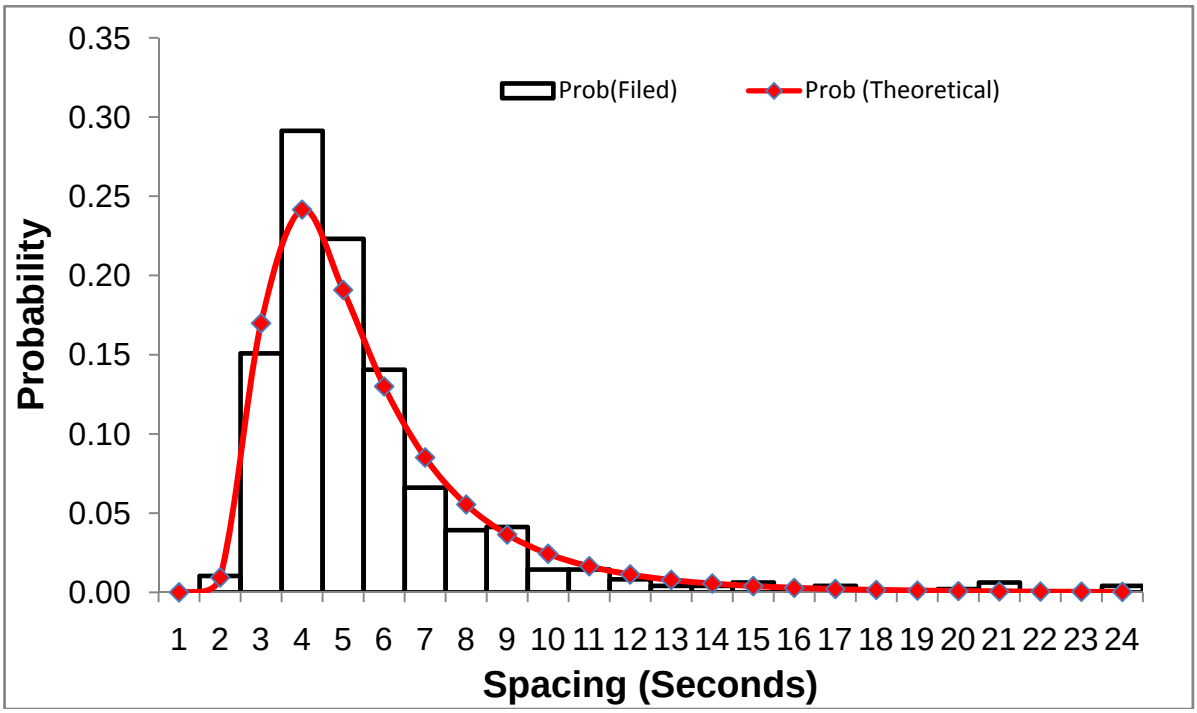

Figure 11: Lognormal Distribution fitting for the Failure Spacing

4.6 Study Findings

This section describes the findings of the study for each of the three traffic stream parameters, namely: density, flow, and space-mean speed.

4.6.1 Traffic Stream Density

Statistical regression models were developed in order to predict the Root Mean Square Error (RMSE). The structure of the model is of the form

$$E = C_1 \times F + C_2 \times D + C_3 \times k\,.$$

Where E is the density RMSE (veh/km/lane), F is the failure frequency (failures/h), D is the failure duration (s), k is the traffic stream density (veh/km/lane), and C_1, C_2, and C_3 are model calibrated parameters.

Table 13 and Table 14 show the parameters C_1, C_2, and C_3 of the regression models that have been developed for density (k), the first column shows the function ID, where function 1 and 2 represent the mean and standard deviations for locations 1 and 2, respectively. The second column shows the location, at which the errors were applied, locations 1 and 2, respectively. The third column shows the regression model coefficients and also the *Pseaudo-*R^2 labels of the model and column 4 through 8 show the calibrated coefficient values for the different lanes.

Table 13: Model Coefficients and R Square of the Density Measurement using Function 1.

			Lane				
			1	**2**	**3**	**4**	**5**
Function 1	**L1**	C_1	0.0030	0.0046	0.0034	0.0032	0.0032
		C_2	0.14	0.21	0.17	0.16	0.16
		C_3	0.53	0.50	0.50	0.51	0.51
		R^2 (%)	88.90	89.10	88.80	88.90	88.90
	L2	C_1	0.0030	0.0046	0.0036	0.0035	0.0033
		C_2	0.13	0.21	0.18	0.17	0.17
		C_3	0.52	0.50	0.50	0.51	0.53
		R^2 (%)	89.30	89.20	88.80	88.90	88.80

Table 14: Model Coefficients and R Square of the Density Measurement using Function 2.

			Lane				
			1	2	3	4	5
Function 2	**L1**	C_1	0.0032	0.0047	0.0037	0.0035	0.0035
		C_2	0.13	0.20	0.17	0.16	0.16
		C_3	0.53	0.50	0.50	0.51	0.51
		R^2 (%)	88.70	88.90	88.60	88.70	88.70
	L2	C_1	0.0031	0.0048	0.0038	0.0037	0.0035
		C_2	0.13	0.21	0.18	0.17	0.16
		C_3	0.52	0.50	0.50	0.51	0.51
		R^2 (%)	89.10	89.00	88.50	88.70	88.70

As illustrated in Figure 12, the traffic stream density error increases as the three parameters (failure frequency, failure duration, and level of congestion (measured as traffic stream density)) increase. All models have a good fit (R square is almost 89% for all models). Figure 12 shows a sample of the density error regression models using the failure spacing mean and the standard deviation that was developed using the second location data (function 2) and a failure duration of 5 seconds. The x-axis is the traffic stream density (veh/km/lane), the y-axis is the failure frequency (number of failures per hour), and the z-axis is the predicted RMSE of the density (veh/km/lane). The figure clearly demonstrates that the traffic stream density error increases as the level of congestion and the frequency of failures increases.

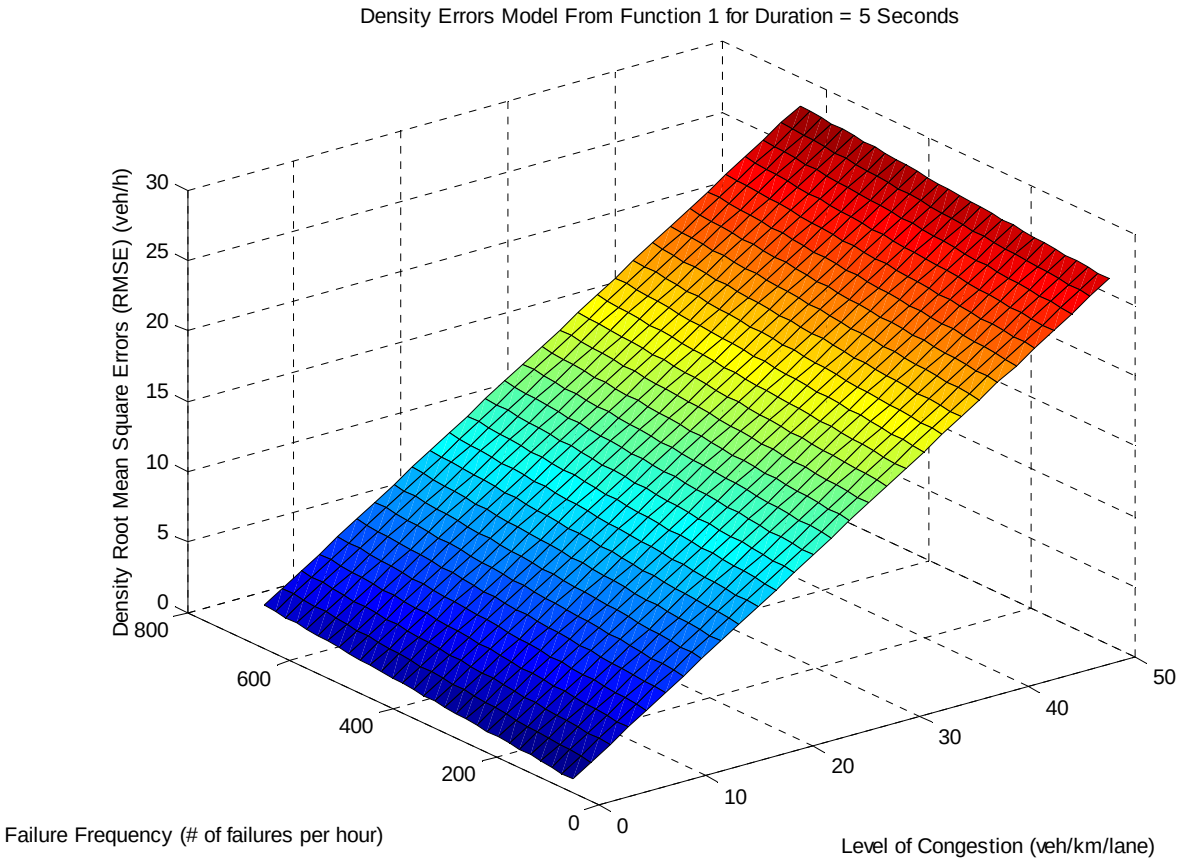

Figure 12: Density Errors Model Sample for Duration = 5 Seconds

In order to observe the effect of failure duration on the aggregated traffic stream density accuracy, the regression model for lane 3 is compared for a variety of failure durations as shown in Figure 13.

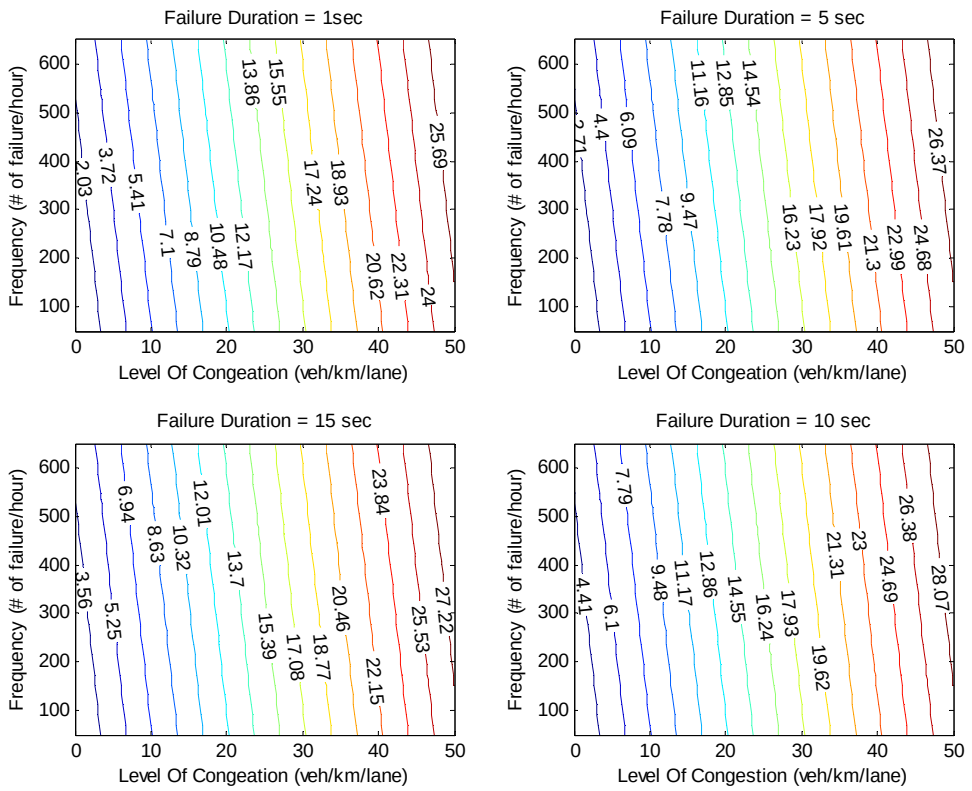

Figure 13 : Comparison between Density Errors with Different Failure Duration.

In the figure, the x-axis represents a measure of the roadway level of congestion –density – (veh/km/lane), the y-axis represents the failure frequency (failures per hour), and the z-axis represents the aggregated density RMSE (veh/km/lane). As illustrated in Figure 13, the density error increases as the failure duration and frequency increases.

The next step in the analysis was to investigate the potential for differences in detector accuracy using different raw datasets. Specifically, the density error using loop detector data at both locations was computed considering an identical error spacing function. The results, which are illustrated in Figure 14, illustrate a high level of similarity considering a failure duration of 5 seconds. In the figure, the x-axis represents a measure of congestion - density- (veh/km/lane), the y-axis represents the failure frequency (number of failures per hour), and the contour lines represent the resulting density RMSE. Again the differences in RMSE between the two locations are small (less than 2 %).

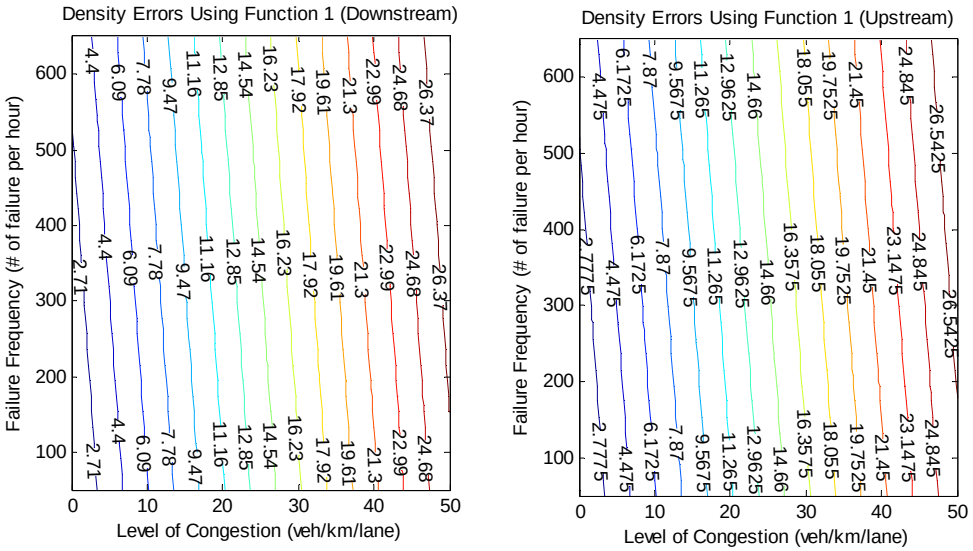

Figure 14: Comparison between Density Errors in Downstream and Upstream Using Function 1.

A further comparison was made by introducing different failure spacing functions using different datasets. Again, as was the case in the previous analysis the difference in the error function is minor, as illustrated in Figure 15. While the results are limited to two datasets and two failure spacing functions, the results do indicate that the loop detector density RMSE appears to be insensitive to the raw measurements dataset and the failure spacing function.

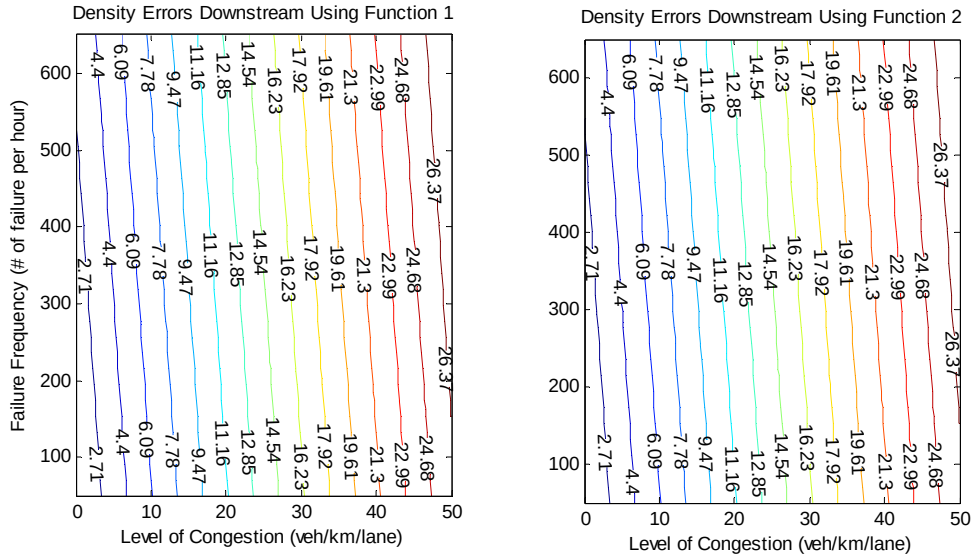

Figure 15: Comparison between Density Errors Using Function 1 and 2 for the same location (Downstream).

A final analysis was conducted to quantify the potential for differences in the accuracy of loop detector density measurements considering different polling intervals. Specifically, three polling intervals 20-, 30-, and 60-s were considered in the analysis because these represent typical polling intervals utilized at Freeway Traffic Management Centers (FTMSs), as illustrated Figure

16. The x-axis represents the level of congestion, the y-axis represents the failure frequency, and the contour lines represent the density errors. The figure demonstrates clearly that, as was the case with the other parameters, the polling interval has a marginal impact on the density polling estimates (less than 1 %). In addition,

Table 15 summarizes the coefficients of model for each polling interval. As is evident from the table the model coefficients are very similar. Specifically Table 16,

shows that the confidence limits for the three model coefficients for each of the three polling intervals overlap and thus there appears to be insufficient statistical evidence to conclude that the polling interval has any impact on loop detector traffic stream density measurements.

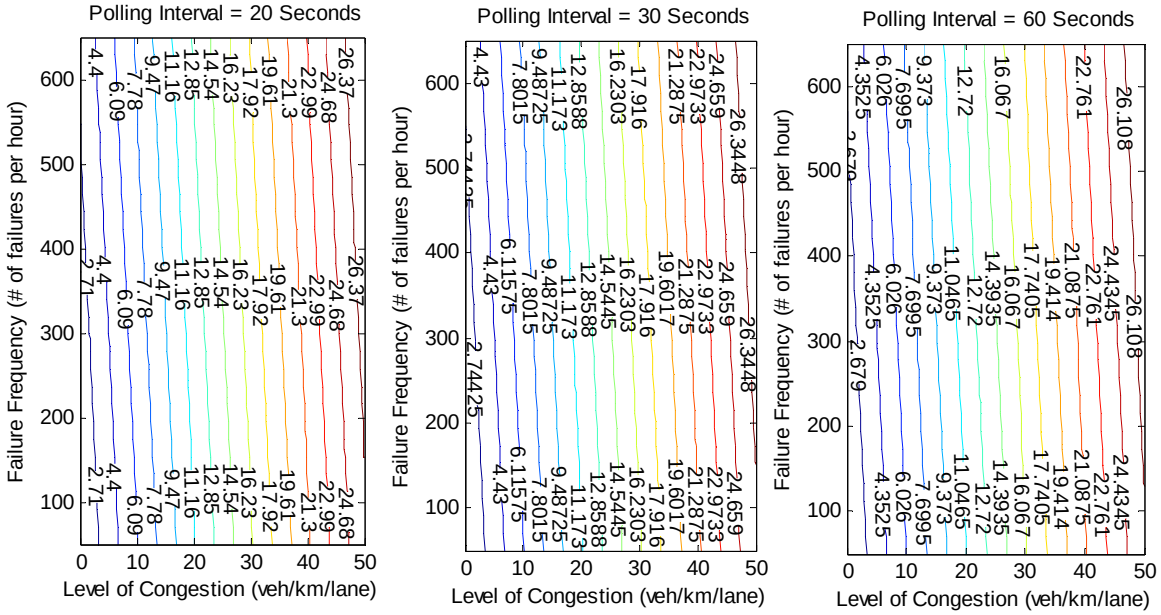

Figure 16: Comparison between Density Errors using different Poling Intervals.

Table 15: Calibrated Coefficients for Density Models for Different Polling Intervals.

	20	30	60
C1	0.00340	0.00337	0.00321
C2	0.170	0.178	0.169
C3	0.500	0.499	0.497

Table 16: Upper and Lower Limits for the Polling Intervals Coefficient for Density Models.

Density	MODELS					
	20SEC		30SEC		60SEC	
	LL	UL	LL	UL	LL	UL
C1	0.003	0.0042	0.0028	0.0039	0.0026	0.0038
C2	0.1699	0.1984	0.1641	0.1924	0.1549	0.1827
C3	0.491	0.513	0.4882	0.5101	0.4857	0.5074

4.6.2 Traffic Stream Flow

Statistical regression models were developed in order to predict the Root Mean Square Errors (RMSE). The structure of the model is of the form

$$E = C_1 \times F + C_2 \times D + C_3 \times k\,.$$

Where E is the flow RMSE (veh/h), F is the failure frequency (failures/h), D is the failure duration (s), k is the traffic stream density (veh/km/lane), and C_1, C_2, and C_3 are model calibrated parameters. Table 17 and Table 18 show the parameters C_1, C_2, and C_3 of the regression models that have been developed for flow (q), the first column shows the function ID, where function 1 and 2 represent the mean and standard deviations for locations 1 and 2, respectively. The second column shows the location, at which the errors were applied, locations 1 and 2, respectively. The third column shows the regression model coefficients and also the *Pseaudo-*R^2 labels of the model and column 4 through 8 show the calibrated coefficient values for the different lanes.

Table 17: Model Coefficients and R Square of the Flow Measurement using Function 1.

			Lane				
			1	2	3	4	5
Function 1	**L1**	**C_1**	0.47	0.99	0.77	0.72	0.72
		C_2	16.60	31.20	25.30	23.60	23.60
		C_3	38.80	19.30	15.90	21.40	21.40
		R^2 (%)	88.40	86.30	88.20	87.30	87.33
	L2	**C_1**	0.46	0.98	0.84	0.73	0.63
		C_2	16.30	31.00	26.80	24.20	21.40
		C_3	38.20	19.10	17.20	20.60	23.80
		R^2 (%)	88.50	86.60	87.40	87.40	86.70

Table 18: Model Coefficients and R Square of the Flow Measurement using Function 2.

			Lane				
			1	2	3	4	5
Function 2	L1	C_1	0.48	1.00	0.86	0.73	0.73
		C_2	16.10	30.80	26.60	23.90	23.40
		C_3	38.00	18.90	17.00	20.50	21.20
		R^2 (%)	88.40	86.50	87.30	87.30	87.20
	L2	C_1	0.48	1.00	0.85	0.75	0.73
		C_2	16.10	30.80	26.60	23.90	23.40
		C_3	38.00	18.90	17.00	20.50	21.20
		R^2 (%)	88.40	86.50	87.30	87.30	87.20

As illustrated in Figure 17, the traffic stream density error increases as the three parameters (failure frequency, failure duration, and Level of Congestion (measured as traffic stream density)) increase. All models have a good fit (R square is almost 87% for all models). Figure 17 shows a sample of the flow error regression models using the failure spacing mean and the standard deviation that was developed using the location 2 data (function 2) and a failure duration of 5 seconds. The x-axis is the traffic stream density (veh/km/lane), the y-axis is the failure frequency (number of failures per hour), and the z-axis is the predicted RMSE of the flow (veh/h). The figure clearly demonstrates that traffic stream flow error increases as the level of congestion and the frequency of failures increases.

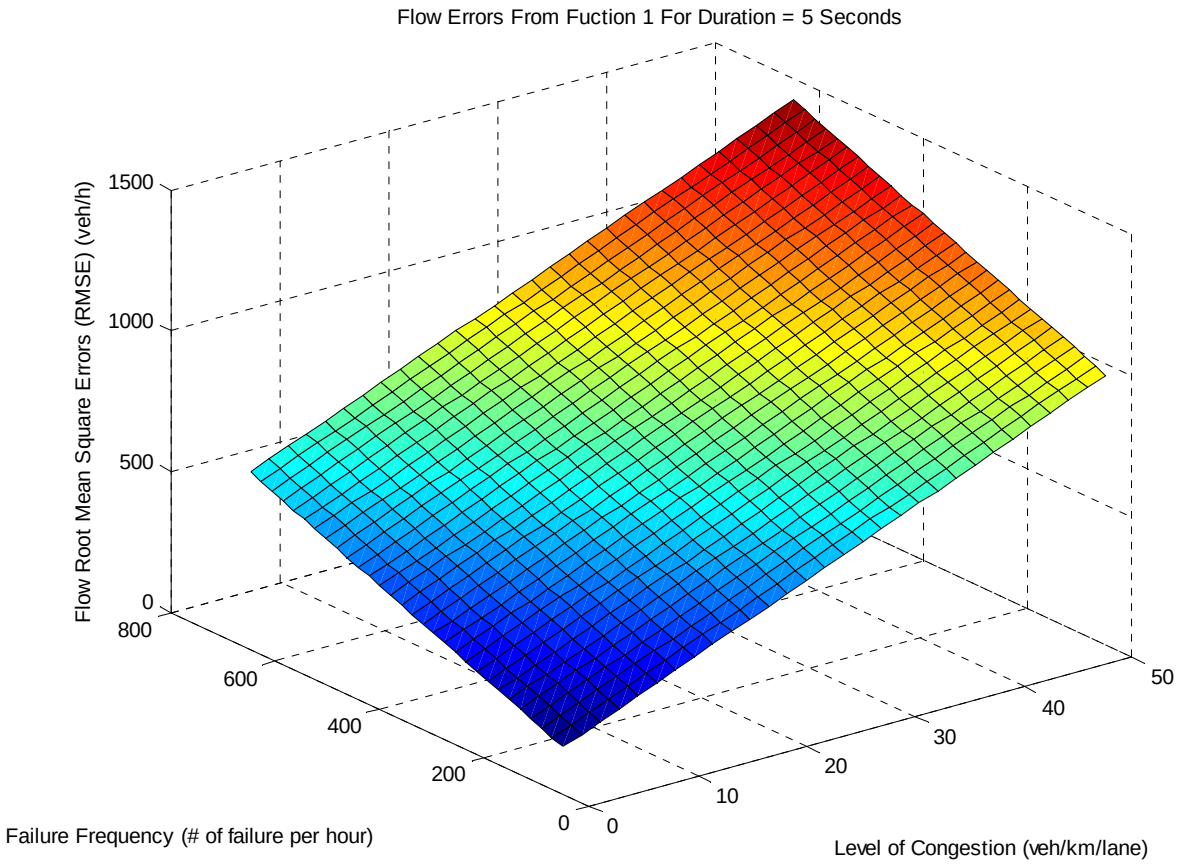

Figure 17: Flow Errors Sample Model for Duration = 5 Seconds.

In order to observe the effect of failure duration on the aggregated traffic stream flow accuracy, the regression model for lane 3 is compared for a variety of failure durations as shown in Figure 18, in the figure, the x-axis represents a measure of the roadway level of congestion –density – (veh/km/lane), the y-axis represents the failure frequency (failures per hour), and the z-axis represents the aggregated flow RMSE (veh/h). As illustrated in Figure 18, the flow error increases as the failure duration and frequency increases.

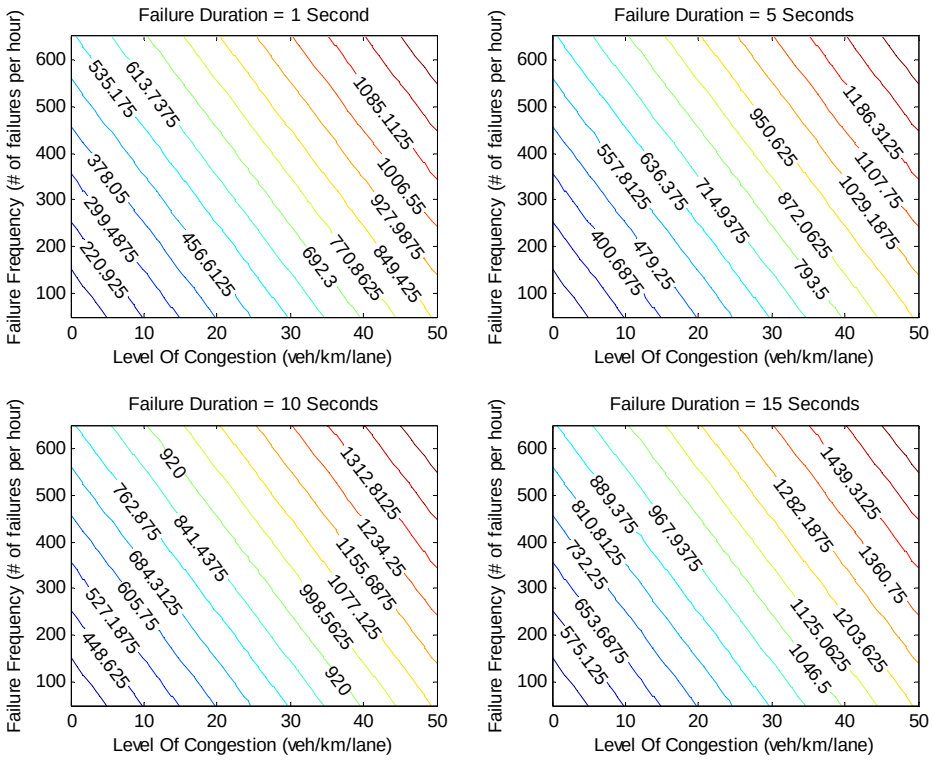

Figure 18: Flow Errors for Different Durations.

The next step in the analysis was to investigate the potential for differences in detector accuracy using different raw datasets. Specifically, the flow error using loop detector data at both locations was computed considering an identical error spacing function. The results, which are illustrated in Figure 19, illustrate a high level of similarity considering failure duration equal to 5 seconds. In the figure, the x-axis represents a measure of congestion - density- (veh/km/lane), the y-axis represents the failure frequency (number of failures per hour), and the contour lines represent the resulting flow RMSE. Again the differences in RMSE between the two locations are in the range from 7.5 to 15 %.

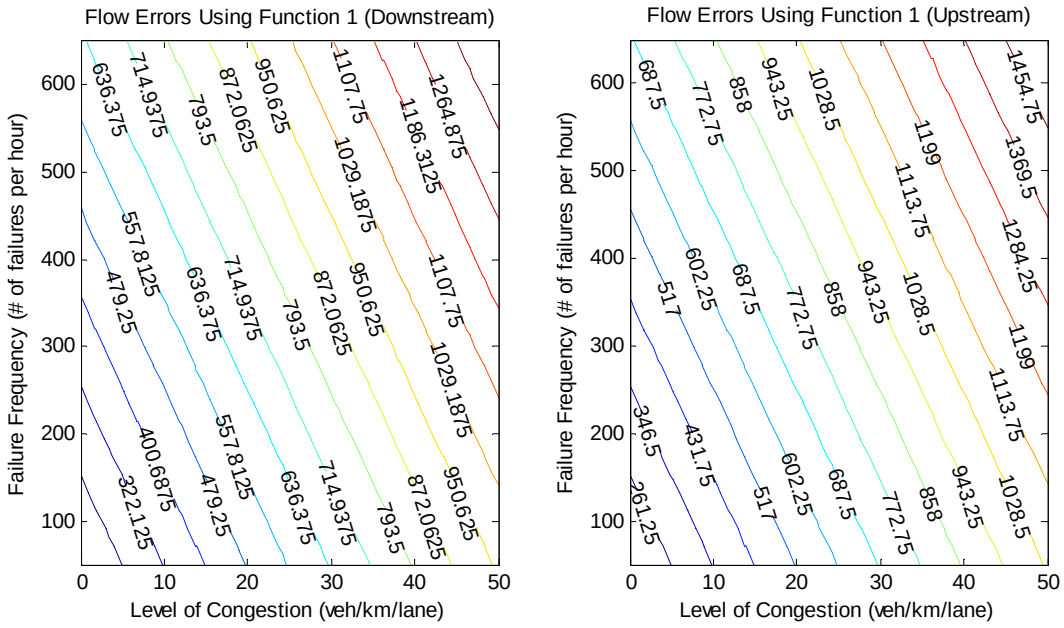

Figure 19: Flow Errors Using Function 1 Upstream and Downstream.

A further comparison was made by introducing different failure spacing functions using different datasets. Again, as was the case in the previous analysis the difference in the error function is minor, as illustrated in Figure 20. While the results are limited to two datasets and two failure spacing functions, the results do indicate that the loop detector flow RMSE appears to be insensitive to the raw measurements dataset and the failure spacing function.

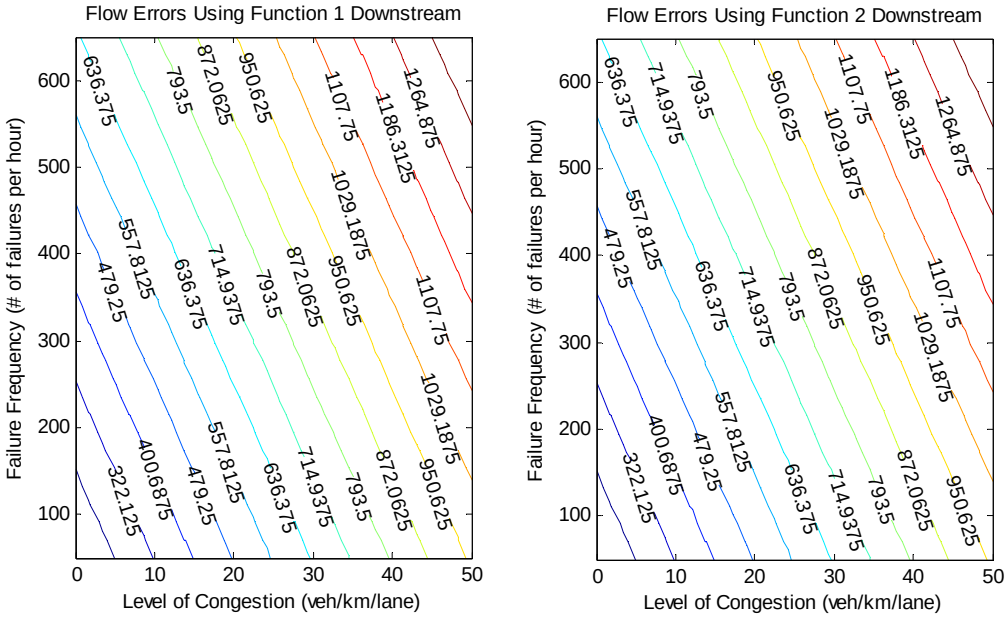

Figure 20: Flow Errors Using Different Functions.

A final analysis was conducted to quantify the potential for differences in the accuracy of loop detector flow measurements considering different polling intervals. Specifically, three polling intervals 20-, 30-, and 60-s were considered in the analysis because these represent typical polling intervals utilized at FTMSs, as illustrated Figure 21. The x-axis represents the level of congestion, the y-axis represents the failure frequency, and the contour lines represent the flow errors. The figure demonstrates clearly that, as was the case with the other parameters, the polling interval has a marginal impact on the flow polling estimates (less than 1.5 %). In addition,

Table 19 summarizes the coefficients of model for each polling interval. As is evident from the table the model coefficients are very similar. Specifically, Table 20 shows that the confidence limits for the three model coefficients for each of the three polling intervals overlap and thus there appears to be insufficient statistical evidence to conclude that the polling interval has any impact on loop detector traffic stream density measurements.

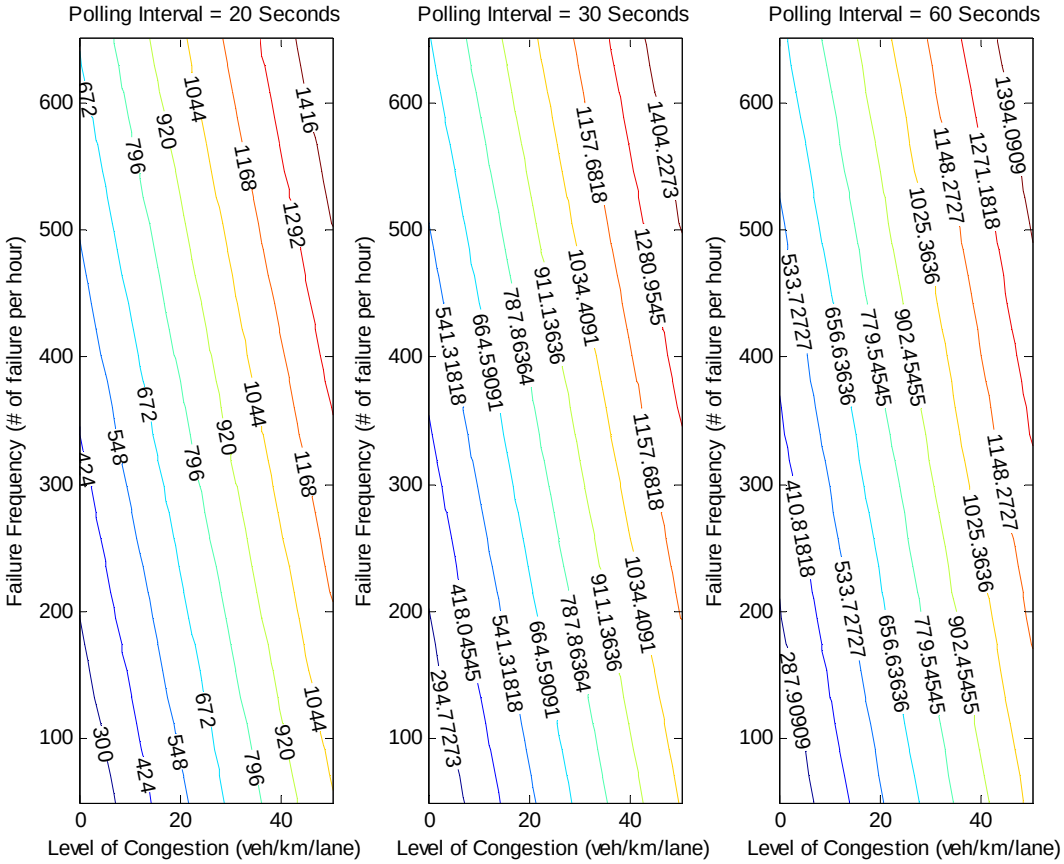

Figure 21: Comparison of Flow Errors using different Polling Intervals.

Table 19: Calibrated Coefficient for Flow Models for Different Polling Intervals.

	20	30	60
C1	0.84	0.81	0.77
C2	26.8	26.2	25.3
C3	17.2	17.4	17.8

Table 20: Upper and Lower Limits for the Polling Intervals Coefficient for Flow Models.

FLOW	MODELS					
	20SEC		30SEC		60SEC	
	LL	UL	UL	LL	UL	LL
C1	0.7966	0.8781	0.769	0.8504	0.7305	0.8118
C2	25.849	27.839	25.235	27.226	24.34	26.327
C3	16.425	17.96	16.618	18.159	17.029	18.584

4.6.3 Traffic Stream Speed:

Statistical regression models were developed in order to predict the Root Square Mean Errors (RMSE). The structure of the model is of the form

$$E = C_1 \times F + C_2 \times D + C_3 \times k\,.$$

Where E is the space mean speed RMSE (km/h), F is the failure frequency (failures/h), D is the failure duration (s), k is the traffic stream density (veh/km/lane), and C_1, C_2, and C_3 are model calibrated parameters.

Table 21 and Table 22 show the parameters C_1, C_2, and C_3 of the regression models that have been developed for space mean speed (u), the first column shows the function ID, where function 1 and 2 represent the mean and standard deviations for locations 1 and 2, respectively. The second column shows the location, at which the errors were applied, locations 1 and 2, respectively. The third column shows the regression model coefficients and also the *Pseaudo-*R^2 labels of the model and column 4 through 8 show the calibrated coefficient values for the different lanes.

Table 21: Model Coefficients and R Square of the Speed Measurement for Function 1.

			Lane				
			1	2	3	4	5
Function 1	L1	C_1	0.1600	0.1610	0.1530	0.1470	0.1470
		C_2	3.36	3.33	3.21	3.08	3.07
		C_3	-0.15	-0.31	-0.38	-0.21	-0.21
		R^2 (%)	94.60	93.90	94.20	94.30	94.30
	L2	C_1	0.1600	0.1600	0.1500	0.1700	0.1400
		C_2	3.33	3.28	3.20	3.05	2.86
		C_3	-0.15	-0.29	-0.37	-0.21	-0.11
		R^2 (%)	94.60	94.00	94.20	94.30	94.00

Table 22: Model Coefficients and R Square of the Speed Measurement for Function 2.

			Lane				
			1	2	3	4	5
Function 2	L1	C_1	0.1700	0.1700	0.1600	0.1500	0.1500
		B	3.30	3.22	3.13	3.00	3.00
		C	-0.26	-0.35	-0.41	-0.25	-0.26
		R (%)	94.60	93.90	94.20	94.40	94.40
	L2	C_1	0.1630	0.1650	0.1570	0.1510	0.1510
		B	3.25	3.18	3.10	2.97	3.00
		C	-0.22	-0.32	-0.41	-0.20	-0.25
		R (%)	94.60	94.00	94.20	94.30	94.40

As illustrated in Figure 22, the traffic stream space mean speed error increases as the two parameters (failure frequency, failure duration), and decreases as the Level of Congestion (measured as traffic stream density increases. All models have a good fit (R square is almost 94% for all models). Figure 22 shows a sample of the density error regression models using the failure spacing mean and the standard deviation that was developed using the location 2 data (function 2) and a failure duration of 5 seconds. The x-axis is the traffic stream density (veh/km/lane), the y-axis is the failure frequency (number of failures per hour), and the z-axis is the predicted RMSE of the space mean speed (km/h). The figure clearly demonstrates that traffic stream space mean speed error increases as the frequency of failures increases and decreases as the level of congestion increases.

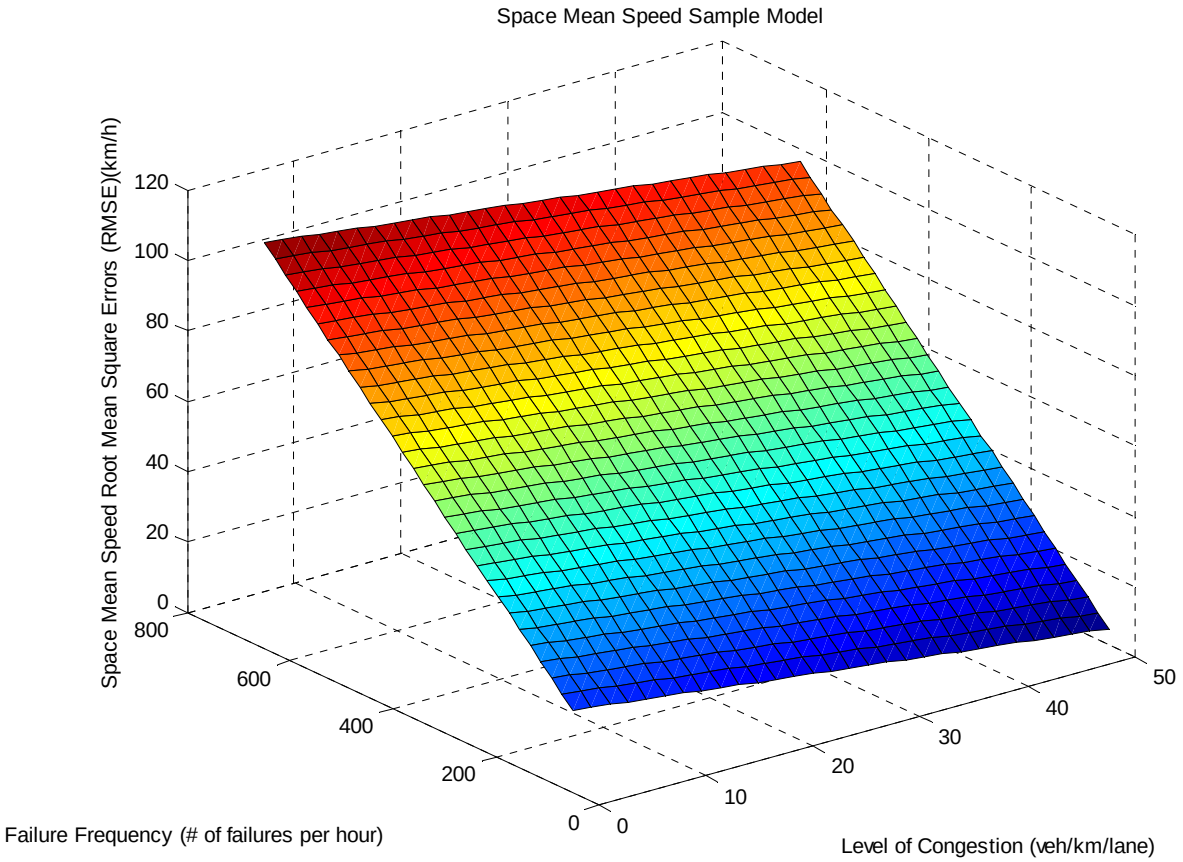

Figure 22: Space Mean Speed Sample Model.

In order to observe the effect of failure duration on the aggregated traffic stream space mean speed accuracy, the regression model for lane 3 is compared for a variety of failure durations as shown in Figure 23, in the figure, the x-axis represents a measure of the roadway level of congestion –density – (veh/km/lane), the y-axis represents the failure frequency (failures per hour), and the z-axis represents the aggregated space mean speed RMSE (km/h). As illustrated in Figure 23, the space mean speed error increases as the failure duration and frequency increases.

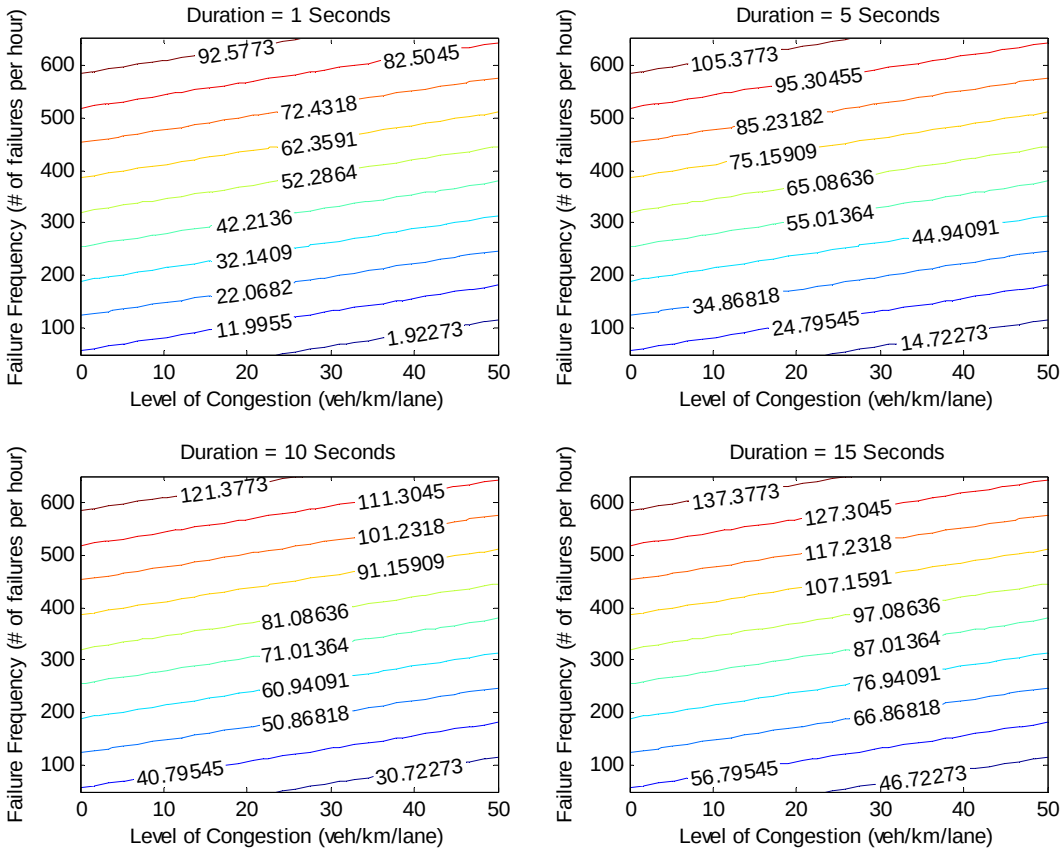

Figure 23: Space Mean Speed Errors for Different Failure Durations.

The next step in the analysis was to investigate the potential for differences detector accuracy using different raw datasets. Specifically, the space mean speed error using loop detector data at both locations was computed considering an identical error spacing function. The results, which are illustrated in Figure 24, illustrate a high level of similarity considering failure duration equal to 5 seconds. In the figure, the x-axis represents a measure of congestion - density- (veh/km/lane), the y-axis represents the failure frequency (number of failures per hour), and the contour lines represent the resulting space mean speed RMSE. Again the differences in RMSE between the two locations are less than 1.7 %.

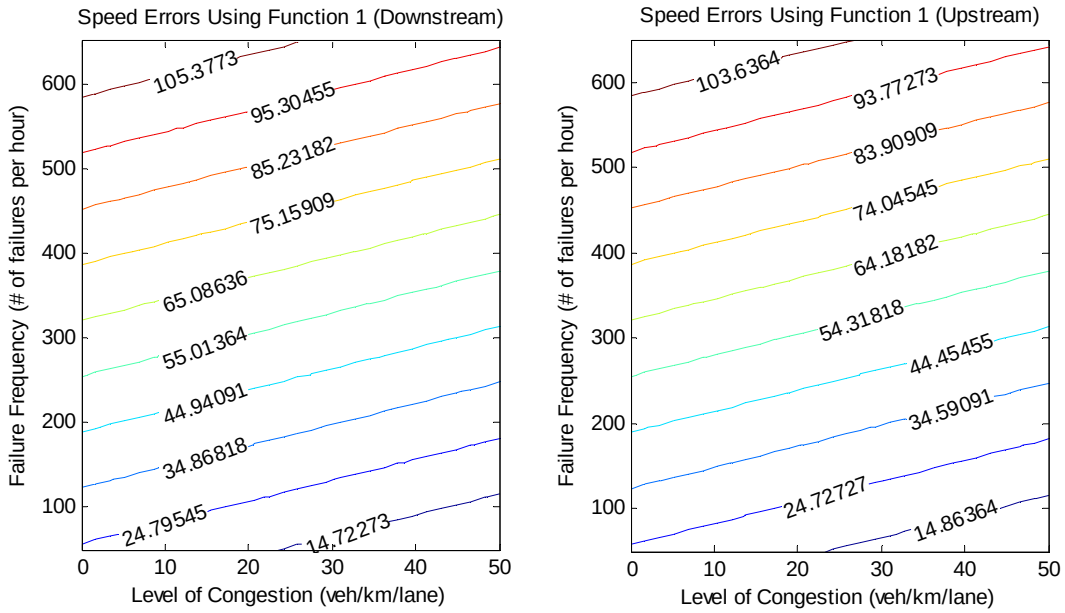

Figure 24: Space Mean Speed Errors using Function 1 (Downstream and Upstream).

A further comparison was made by introducing different failure spacing functions using different datasets. Again, as was the case in the previous analysis the difference in the error function is minor, as illustrated in Figure 25. While the results are limited to two datasets and two failure spacing functions, the results do indicate that the loop detector space mean speed RMSE appears to be insensitive to the raw measurements dataset and the failure spacing function.

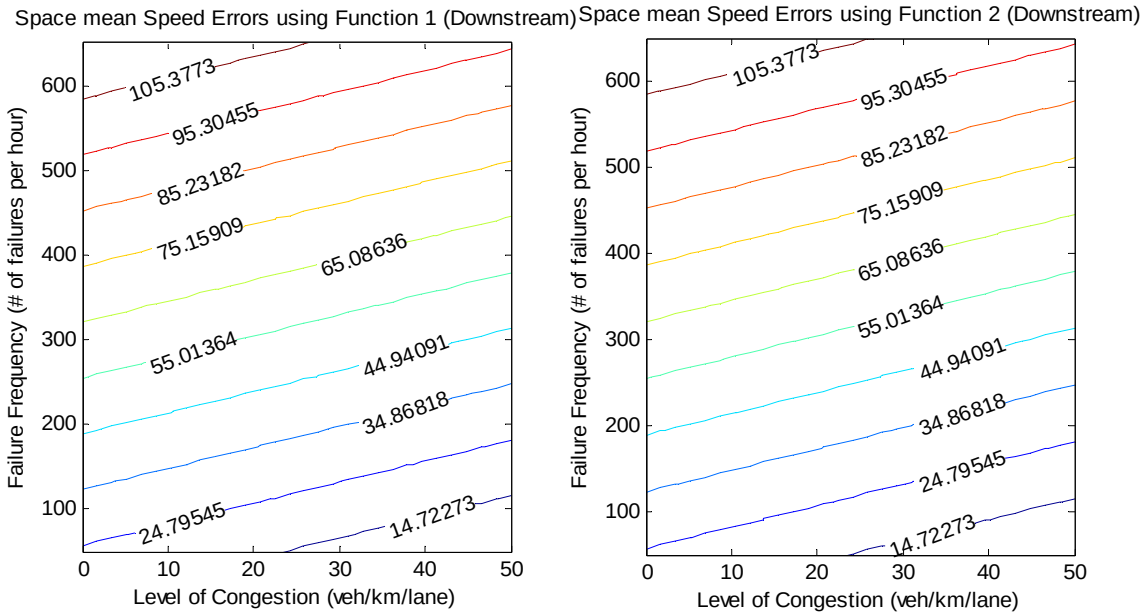

Figure 25: Speed Errors Using Different Functions.

A final analysis was conducted to quantify the potential for differences in the accuracy of loop detector space mean speed measurements considering different polling intervals. Specifically, three polling intervals 20-, 30-, and 60-s were considered in the analysis because these represent typical polling intervals utilized at FTMSs, as illustrated Figure 26. The x-axis represents the level of congestion, the y-axis represents the failure frequency, and the contour lines represent the space mean speed errors. The figure demonstrates clearly that, the polling interval has an impact on the space mean speed errors estimates with errors in the range of10 to 15%. In addition, Table 23 summarizes the model coefficients for each polling interval. As is evident from the table the model coefficients are very similar. Specifically, Table 24 shows that the confidence limits for the three model coefficients for each of the three polling intervals overlap and thus there appears to be insufficient statistical evidence to conclude that the polling interval has any impact on loop detector traffic stream density measurements.

All the above figures, 20 seconds polling interval was used. Other analysis using polling intervals equal to 30 seconds and 1 minute were done and the space mean speed errors were calculated and compared with the 20 seconds polling interval in order to examine the effect of the level of aggregation on the errors. Figure 26 shows the flow errors using different aggregation levels (20, 30, and 60 seconds), the x-axis is the level of congestion, y-axis is the failure frequency and the contour lines are the space mean speed errors. The figure demonstrates evidently that there is less than 10% effect on the space mean speed errors resulted due to change in polling intervals from 20 to 30 and less than 15% due to change in polling intervals from 20 to 60 seconds. Table 23 shows the calibrated coefficient for each model.

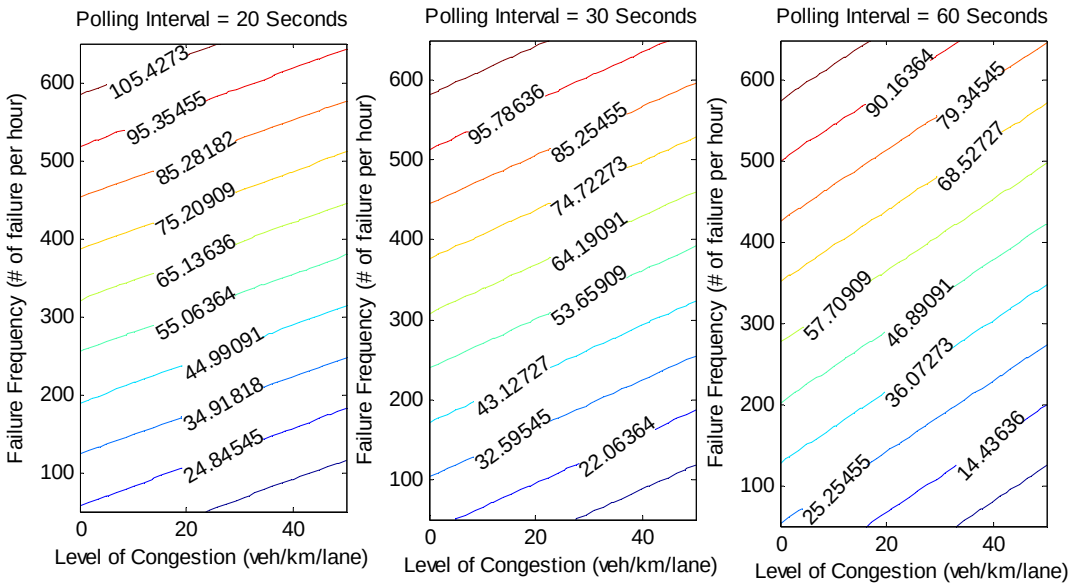

Figure 26: Speed Errors using Different Polling Intervals.

Table 23: Calibrated Coefficient for Space Mean Speed Models for Different Polling Intervals.

	20	30	60
C1	0.153	0.154	0.145
C2	3.21	3.35	3.51
C3	-0.38	-0.469	-0.64

Table 24 shows the confidence limits of the three coefficients for the three models. In spite of that there is no overlap between the three models coefficients, implying that there appears to be a significant difference between the three regression models. Nevertheless, the non-existent overlap could be attributed to the small differences between the limits of the coefficients.

Table 24: Upper and Lower Limits for the Polling Intervals Coefficient for Space Mean Speed Models.

SPEED	MODELS					
	20SEC		30SEC		60SEC	
	LL	UL	LL	UL	LL	UL
C1	0.1504	0.155	0.1511	0.156	0.1423	0.1476
C2	3.1464	3.2586	3.292	3.4116	3.447	3.5748
C3	-0.413	-0.327	-0.515	-0.422	-0.69	-0.59

Regression models were developed on the three coefficients that result from the three polling interval models in order to statistically determine if the polling interval resulted in different models. As demonstrated in Table 25, a linear regression line was fit to the failure frequency coefficient considering the polling interval as the independent variable. Given that the slope of the line was not significant (p-value = 22%) there is insufficient evidence to conclude that the

polling interval affects the space-mean speed error. Similar results are observed for coefficients C_2 and C_3 as summarized in Table 26 and Table 27.

Table 25: ANOVA Table of the Failure Frequency Parameter.

ANOVA						
	df	*SS*	*MS*	*F*	*Significance F*	
Regression	1	768.04	768.04	7.79	0.22	
Residual	1	98.63	98.63			
Total	2	866.67				
	Coefficients	*Standard Error*	*t Stat*	*P-value*	*Lower 95%*	*Upper 95%*
Intercept	635.21	214.57	2.96	0.21	-2091.12	3361.53
Slope	-3972.60	1423.60	-2.79	0.22	-22061.20	14115.99

Table 26: ANOVA Table of the Failure Duration Parameter

ANOVA						
	df	*SS*	*MS*	*F*	*Significance F*	
Regression	1	816.67	816.67	16.33	0.15	
Residual	1	50.00	50.00			
Total	2	866.67				
	Coefficients	*Standard Error*	*t Stat*	*P-value*	*Lower 95%*	*Upper 95%*
Intercept	-415.19	111.88	-3.71	0.17	-1836.77	1006.39
Slope	134.62	33.31	4.04	0.15	-288.61	557.84

Table 27: ANOVA Table of the Level of Congestion Parameter

ANOVA						
	df	*SS*	*MS*	*F*	*Significance F*	
Regression	1	857.87	857.87	97.52	0.06	
Residual	1	8.80	8.80			
Total	2	866.67				
	Coefficients	*Standard Error*	*t Stat*	*P-value*	*Lower 95%*	*Upper 95%*
Intercept	-41.13	8.06	-5.10	0.12	-143.56	61.31
Slope	-156.74	15.87	-9.88	0.06	-358.41	44.94

4.7 Study Conclusions

This research attempted to quantify the accuracy of loop detector measurements (density (k), flow (q), and space-mean speed (u)) by introducing failures into raw loop detector actuations using a Monte Carlo simulation approach. The research concluded, as would be expected, that

the polling interval density, flow, and space mean speed RMSEs increase as the frequency and duration of failures increase. Furthermore, the research demonstrated that the density and flow RMSEs increase as the level of congestion increases while the space-mean speed RMSE decreases. Finally, the research developed regression models that predict the accuracy of loop detector measurements. The input parameters to these models are the failure frequency, the failure duration, and the traffic stream density.

A sensitivity analysis of the models revealed that the errors are insensitive to the error function, location, (speed and density), the lane, or the polling interval that is used to aggregate the data. Alternatively, the location had the same trend but the magnitude of the flow RMSE increased by 7.5 to 15%.

Chapter 5: Inclement Weather Impact on Freeway Traffic Stream Free-flow Speed

Hesham Rakha [1], Mazen Arafeh [2], Mohamadreza Farzaneh[3], and Hossam ElDin Hablas

Abstract

The research reported in this paper quantifies the impact of inclement weather (precipitation and visibility) on traffic stream free-flow speeds along freeway sections. The analysis is conducted using weather data (precipitation and visibility) and loop detector data (speed) obtained from Baltimore, Minneapolis/St. Paul, and Seattle, US. The results demonstrate that visibility alone has minimum impact on free-flow speed with reductions in the range of 1 to 3%. These reductions only appear as the visibility level falls below 1.2 km. The study demonstrates that the impact of snow is more significant than that of rain for similar intensity levels. Reductions caused by rain are in the neighborhood of 2 to 5% depending on the precipitation intensity while reductions caused by snow are in the neighborhood of 6 to 20%. Finally, the paper derives free-flow speed reduction factors that vary as a function of the precipitation type and intensity level. These reduction factors can be incorporated within the Highway Capacity Manual's procedures.

5.1 Introduction

Low visibility, precipitation, high winds, and extreme temperature can affect driver capabilities, sight distances, vehicle performance, and infrastructure characteristics. For example, the Highway Capacity Manual [7] (HCM) asserts that adverse weather can significantly reduce operating speeds and identifies when and how these effects occur. The manual references several studies in its discussion of weather effects. For example Lamn et al. [11]concluded that speeds are not affected by wet pavement until visibility is affected, which suggests that light rain does not impact operating speeds, but heavy rain does and can be expected to have a noticeable effect on traffic flow.

Similarly, Ibrahim and Hall [10] found minimal reductions in operating speeds in light rain, but significant reductions in heavy rain. The HCM states that, in light rain, a 1.9 km/h (1.9%)

[1]Hesham Rakha is a Professor with the Charles Via Jr. Dept. of Civil and Environmental Engineering at Virginia Tech and the Director of the Center for Sustainable Mobility at the Virginia Tech Transportation Institute, Blacksburg, VA 24061 (e-mail: hrakha@vt.edu).

[2]Mazen Arafeh is a Senior Research Associate at the Virginia Tech Transportation Institute, Blacksburg, VA 24061 (e-mail: amazen@vt.edu).

[3] Mohamadreza Farzaneh is an Assistant Research Scientist in the group of Air Quality Studies, Texas Transportation Institute College Station, TX 77843-3135 (e-mail: M-Farzaneh@ttimail.tamu.edu).

reduction in speed during free-flow conditions is typical. In heavy rain, a 4.8 to 6.4 km/h (4.8 to 6.4%) reduction in free-flow speed can be expected. The HCM, however, does not define the intensity ranges associated with light and heavy rain and light and heavy snow.

As was the case with rain, light snow was found to have minimal effects, while heavy snow was found to have a potentially large impact on operating speeds[10]. Light snow resulted in a statistically significant drop of 0.96 km/h (1%) in free-flow speeds. Heavy snow resulted in a 37.0 to 41.8 km/h free-flow speed reduction (or 35 to 40%).

A recent study quantified the impact of rain, snow, and low visibility on operating speeds using data from the Minneapolis/St. Paul region [30]. The study concluded that rain (more than 0.635 cm/h), snow (more than 1.25 cm/h), and low visibility (less than 0.4 km) showed operating speed reductions of 4–7%, 11–15%, and 10–12%, respectively. Speed reductions due to heavy rain and snow were found to be significantly lower than those specified by the HCM [7]. The study, however, suffers from several drawbacks. First, the study considers traffic stream behavior over the entire uncongested regime as opposed to isolating the traffic stream behavior during free-flow conditions. Second, the study removes all speed estimates below 96 km/h (60 mi/h) from the analysis. Such screening of data may result in the removal of valid data especially during inclement weather conditions. Third, the study utilizes hourly weather data to conduct the analysis and thus does not capture sub-hourly variations in weather, which are critical for such an analysis. Finally, the study erroneously scaled the precipitation rates based on the duration of precipitation, which resulted in unrealistically high precipitation rate observations.

5.2 Paper Objectives and Layout

The paper investigates the impact of visibility, the type of precipitation, and precipitation intensity on traffic stream free-flow speeds along freeway sections. The study differs from a recent study [21]in that this study isolates traffic stream behavior within free-flow conditions, conducts the analysis using 5-min. as opposed to hourly data, and develops rain and snow free-flow speed adjustment factors that can be easily incorporated within the HCM level of service (LOS) procedures. These factors are sensitive to the precipitation type (rain versus snow) and intensity.

In terms of the paper layout, initially the field data that were utilized for the study are described. The data fusion and construction is also described. Subsequently, the results of the analysis are

presented. Finally, the conclusions of the study are presented together with recommendations for further research.

5.3 Field Data Description

This section describes the data sources that were utilized to conduct the analysis. These data sources include two weather stations and over 4000 available single loop detectors located along the major freeways in the study area. The analysis was conducted using two years worth of data. These data included data for 2004, which was the latest year for which weather data were available, and 2002, which represented the highest total precipitation since 1990, as illustrated in Figure 27.

5.3.1 Weather Data

Two sources of weather data existed within the study area at the time of the study, namely, the Road Weather Information System (RWIS) stations operated by MnDOT and the Automated Surface Observing System and Automated Weather Observing System (ASOS/AWOS) stations located at airports. The National Climatic Data Center (NCDC) collects and archives data from the stations. An initial analysis of RWIS data showed that the precipitation and visibility records within the Twin Cities Area were either missing data or inaccurate and therefore the ASOS data were utilized for the analysis. The weather data reported by ASOS were of METAR type (Aviation Routine Weather Reports) and contained precipitation type, precipitation intensities (inch/h), visibility readings (mile) for the past 5-min interval. The ASOS data also provided information on other climatic factors such as temperature and wind, however these factors were not considered in this study. The following paragraphs briefly describe the ASOS system [31, 32].

ASOS visibility measurements were performed at 30-s increments using a forward scatter sensor to compute one-minute average extinction coefficients (sum of the absorption and the scattering coefficients). For this purpose, a photocell that identified the time of day (day or night) was used to select the appropriate equation for use in the procedure. The ASOS system computed a one-minute average visibility level that was used to compute a 10-minute moving average (MA) visibility level. This value was then rounded down to the nearest reportable visibility level. ASOS visibility was reported in 0.4-km (0.25-mi) increments up to 3.2 km (2 mi) then at 1.6 km

(1 mi) increments to a maximum of 16 km (10 mi). Visibilities greater than 16 km were reported as 16 km and values less than a 0.4 km were recorded as a 0.4 km visibility level.

ASOS used precipitation identification sensors to determine the type of precipitation (rain, snow, or freezing rain). Precipitation intensity was recorded as liquid-equivalent precipitation accumulation measurements using a heated Tipping Bucket (HTB) gauge. The HTB has a resolution of 0.025 cm (0.01 in) and an accuracy of ±0.05 cm (±0.02 in) or 4% of the hourly total; whichever is greater.

A set of five detector stations were initially considered for the analysis. These sites were considered based on the following criteria:

1. The recorded data provided sufficient coverage for all traffic conditions, i.e. uncongested, around capacity, and congested conditions to allow a full analysis over all traffic regimes. This paper, however, only considers behavior during free-flow conditions.
2. Not within the influence area of merge, diverge, or weaving sections in order to ensure that changes in behavior were not impacted by lane-changing behavior.
3. Lanes were neither a shoulder nor median lane because behavior in shoulder lanes are impacted by traffic merge and diverge behavior while traffic stream behavior in median lanes can be affected by High Occupancy Vehicle (HOV) restrictions.
4. Outside the influence of any incidents. This objective was achieved by screening data using incident information obtained from Mn/DOT. The incident information included time of detection, time of clearance, and the location of the incident.
5. As close as possible to ASOS stations.

Of the five detectors only four were selected and included in the analysis because one site only had a single year's worth of data. All four detectors were in the vicinity of an ASOS station at the Minneapolis-St. Paul International Airport. The closest detector was 5.4 km from the ASOS station while the farthest detector was 15 km from the weather station.

Table 28 provides further information on the Twin Cities loop detectors used in this study and also Table 29 provides more information on the Seattle loop detectors used in the study. In addition, Figure 28 shows the study area and the locations of four loop detector stations that were considered together with the two ASOS stations. All selected detectors were located on the middle lane of 3-lane sections. Two of the detectors (D2463 and D2390) were in different directions of the same section of freeway.

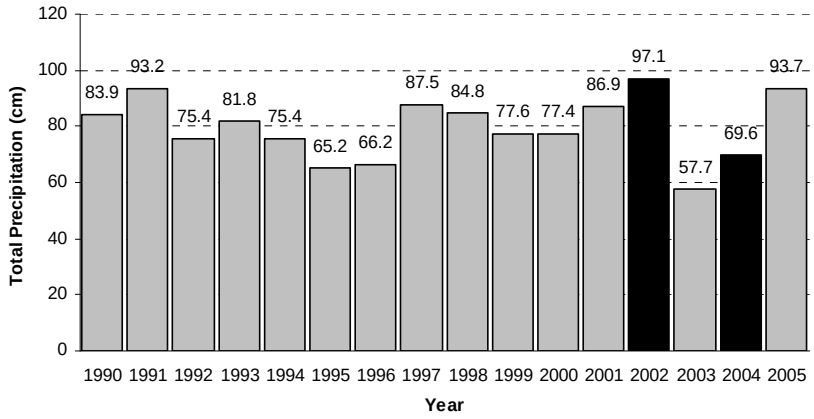

Figure 27: Minneapolis/St. Paul annual precipitations

Table 28: Twin Cities Loop Detector Summary Information.

Detector	Lane	No. of lanes	Distance to Int'l Airport	Distance to St. Paul
D3294	Middle lane	3	5.4 km	17.5 km
D2463	Middle lane	3	15 km	2.4 km
D2390	Middle lane	3	15 km	2.4 km
D2387	Middle lane	3	14.6 km	1.6 km

Table 29: Seattle Loop Detector Summary Information.

Detector	Lane	No. of lanes	Distance to Int'l Airport
059 DS-T5	5th from shoulder	6+HOV	3.2 km
059 DS-T4	4th from shoulder	6+HOV	3.2 km
042 DS-T2	Middle lane	3+HOV	4.7 km
042 DN-T2	Middle lane	3+HOV	4.7 km
333 DN-T2	Median lane	2+HOV	7.0 km
333 DS-T2	Median lane	2+HOV	7.0 km
024 DN-T2	3rd from shoulder	4+HOV	11.8 km

Five-minute weather data were only available for the Minnesota/St. Paul International Airport ASOS station and thus was utilized in the analysis. In order to ensure that no local weather effects were present, a comparison of hourly precipitation and visibility reports from both ASOS stations was conducted. The analysis demonstrated a high level of consistency in the data despite the fact that the stations were approximately 10 km apart.

The rain and snow data were divided into three and four intensity categories, respectively, as recommended by Agarwal et al. [21, 30]. Furthermore, the visibility data were divided into 4 groups (equal to or greater than 4.8 km, between 1.6 and 4.8 km, between 0.8 and 1.6 km, and less than or equal to 0.8 km).

5.3.2 Loop Detector Data

Traffic data were available from around 4000 single loop detectors installed on freeway lanes within the Twin cities area. Each detector recorded the volume and occupancy of the traffic stream at 30 s intervals. The data from selected detectors were converted to 5-min. averages in order to be consistent with the weather data temporal aggregation level. The traffic parameters were calculated using the following relationships (Equations(1),(2) and(3)).

$$q = 3600\frac{n}{T} \quad (1)$$

$$k = 1000\frac{O}{D \times 100} = 10\frac{O}{D} \quad (2)$$

$$u = \frac{q}{k} \quad (3)$$

where q is the traffic stream flow rate (veh/h/lane), k is traffic stream density (veh/km/lane), u is the space-mean speed (km/h), T is the polling interval (s), n is the number of vehicles observed during a polling interval, O is the detector occupancy during a polling interval (%), and D is the calibrated detector field length which includes the length of the detection zone plus an average vehicle length (m).

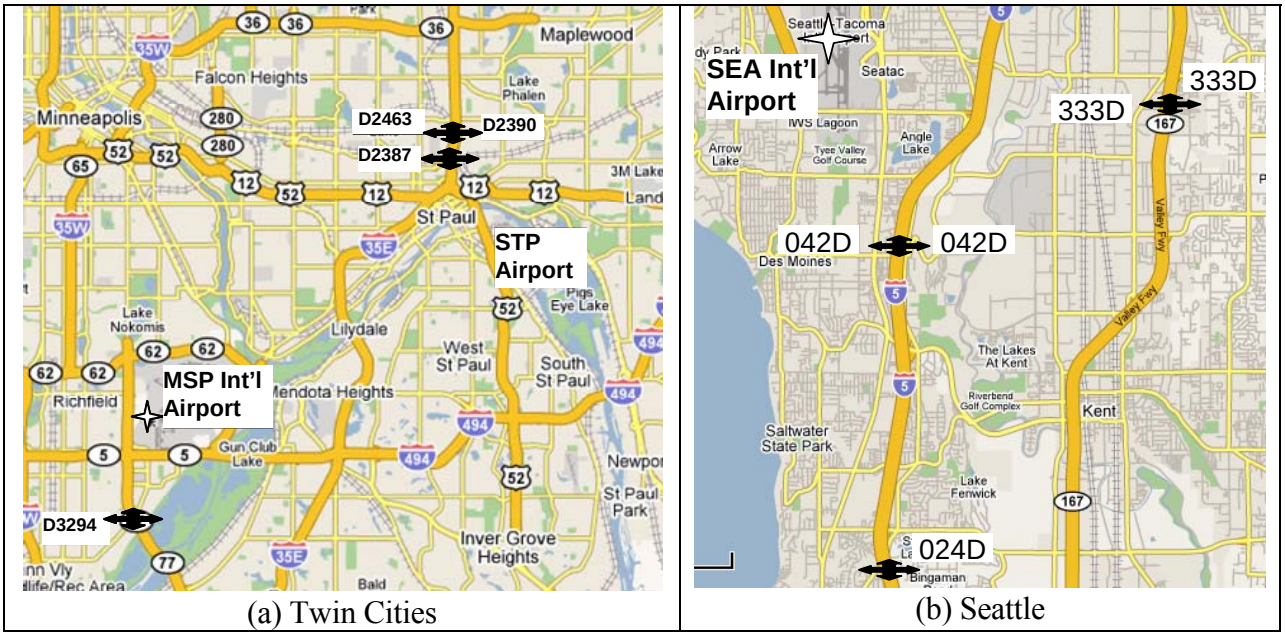

(a) Twin Cities (b) Seattle

Figure 28: Detector and weather station layout

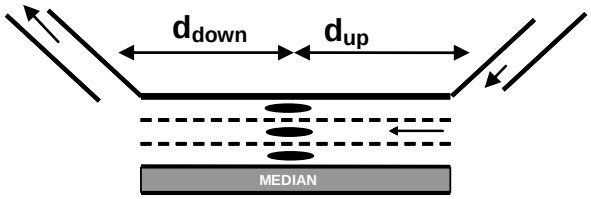

Detector	d_{down} (km)	d_{up} (km)
D3294	2.00	1.50
D2390	0.40	1.35
D2463	1.35	0.40
D2387	0.90	0.45

(a) Twin Cities

Detector	d_{down} (km)	d_{up} (km)
042DS_T2	1.40	1.30
042DN_T2	0.90	1.40
333DS_T2	1.90	1.00
333DN_T2	0.45	2.10
024DN_T2	1.10	2.60

(b) Seattle

Figure 29: Detector location relative to adjacent on- and off-ramps

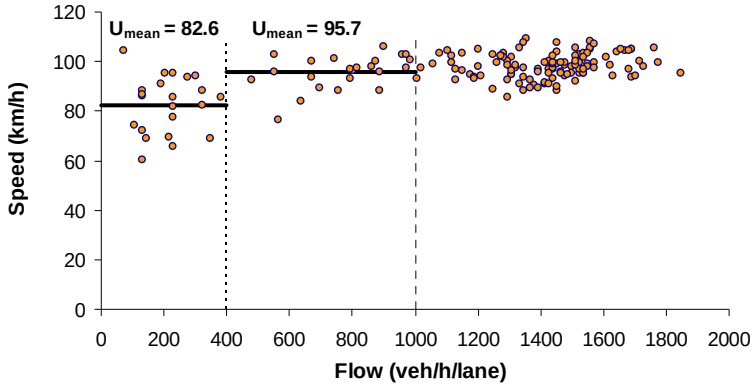

Figure 30: Example illustration of speed reduction at low flows

5.4 Data Fusion and Dataset Construction

Prior to conducting the data analysis, speed estimates for different precipitation and visibility level combinations were visually inspected in an attempt to identify any potential data problems. This inspection revealed an increase in the average traffic stream speed in the uncongested regime for an increase in the flow rate (from 400 veh/h/lane or less to 400 to 1000 veh/h/lane), as depicted in Figure 30. This uncharacteristic behavior was caused by the fact that the loop detectors were single loop detectors and thus did not measure speed explicitly. In computing the traffic stream speed a constant average vehicle length was assumed, as was depicted earlier in Equation(2). Consequently, a long truck was considered to be a slow moving car. These errors were more pronounced at low flow rates when the sample size within a polling interval was small. Further inspection of the data showed that for all cases the speed remained fairly constant in the uncongested regime (upper arm of speed-flow relationship), which is typical of traffic

stream behavior on freeways that are constrained by a speed limit rather than by physical or traffic control constraints. Free-flow speed is typically considered when the flow rate and traffic stream density approaches zero, however, because of the identified problems with the data; the free-flow speed was estimated as the average speed in the 400 to 1000 veh/h/lane range.

Two criteria were used to identify valid free-flow speed data; first, speed estimates for flow rates between 400 and 1000 veh/h/lane were considered, and second, traffic stream densities less than 22 veh/km/lane were only considered. The second condition was used to ensure that all observations were associated with the uncongested regime.

Data screening techniques were applied to the data in order to remove any outlier observations. Data screening was performed by computing the difference between the 75th and 25th quartiles. This difference was then divided equally and multiplied by 1.5 to compute the lower and upper bounds validity ranges. Any data outside these bounds were considered outliers, as illustrated in Figure 31.

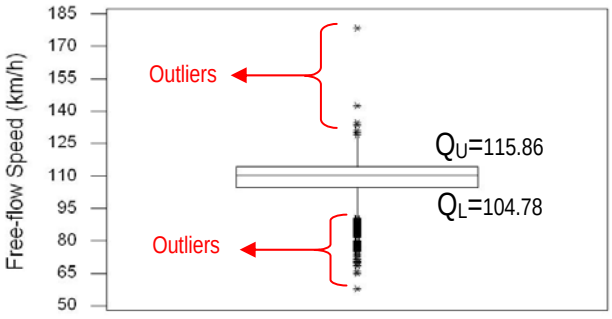

Figure 31: Sample data screening (D3294)

5.5 Data Analysis and Results

This section describes the data analysis procedures together with a summary of the study findings. Initially, the effect of visibility on traffic stream free-flow speed is characterized. Subsequently, the effect of rain, freezing rain, and snow intensity on free-flow speed is described.

5.5.1 Impact of Visibility

As was mentioned earlier, the visibility data were divided into 4 groups (equal to or greater than 4.8 km (the control group), between 1.6 and 4.8 km, between 0.8 and 1.6 km, and less than or equal to 0.8 km).

Typically to study the effect of visibility on the traffic stream free-flow speed considering no precipitation, an Analysis of Variance (ANOVA) test is performed on the data, data for all detectors in each city was combined into one data set. The use of ANOVA tests is based on the assumptions that residual are normally and independently distributed with mean zero and constant variance. A test for equal variances between clear conditions and different rain intensity levels was executed in MINITAB. MINITAB calculates and displays a test statistic and p-value for both Bartlett's test (used when the data come from a normal distribution) and Levene's test (used when the data come from continuous, but not necessarily normal, distributions). High p-values indicate that there is no difference between the variances, while low p-values indicate that there is a difference between the variances (inequality of variances) [33]. Data from Twin Cities and Baltimore satisfied these assumptions as shown in Figure 32a and 32b. Moderate departures from these assumptions are found not to affect the analysis. For datasets that did not satisfy the normality or the equal variance tests, as in the case of the Seattle dataset shown in Figure 32c, the datasets were grouped in bins and analysis was performed on the averages of the bins. Bins were chosen such that the variance is statistically constant, as shown in Figure 32d.

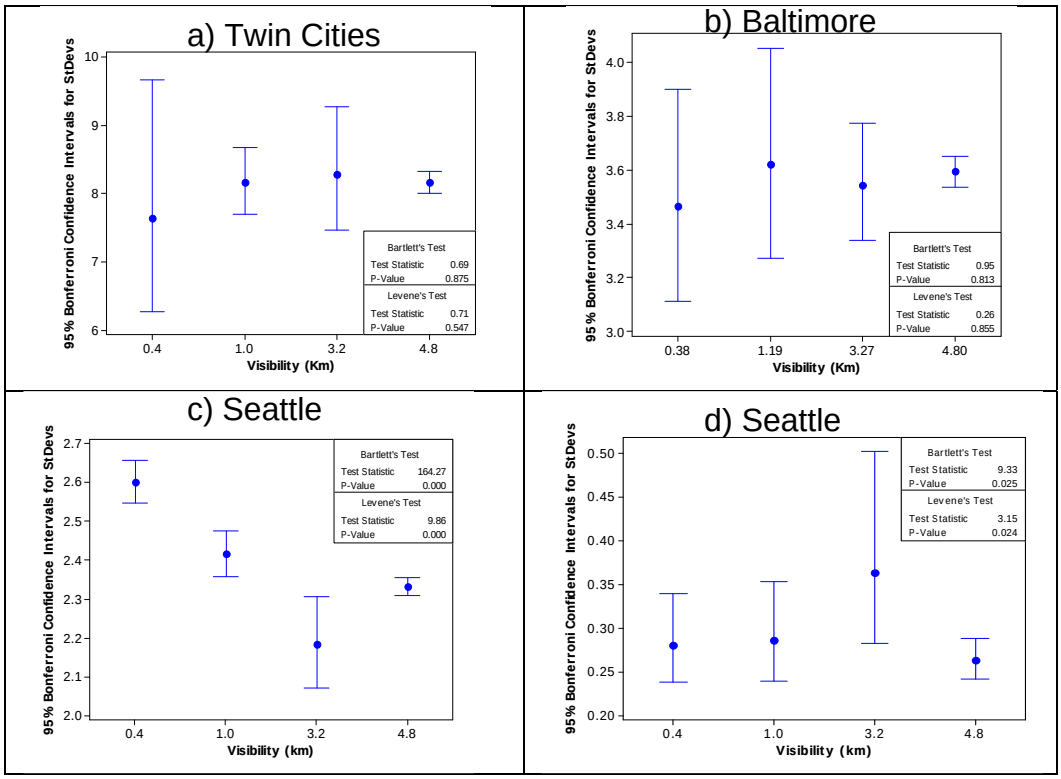

Figure 32: Test for Equal Variances (Visibility)

Table 30 summarizes the ANOVA results for the different cities. A p-value of 0.05 or less implies that there is sufficient evidence to reject the null hypothesis. Consequently, the results of

Table 30 indicate that visibility alone results in reductions in traffic stream free-flow speed for the three cities.

Table 30: ANOVA for Visibility Effect.

City	Source	DF	SS	MS	F	P
Twin Cities	Visibility	3	3625.8	1208.6	18.16	0.000
	Error	8902	592468.3	66.6		
	Total	8905	596094.2			
Seattle	Visibility	3	9.95	3.318	43.58	0.000
	Error	621	47.28	0.076		
	Total	624	57.24			
Baltimore	Visibility	3	1961.0	653.7	50.75	0.000
	Error	13304	171351.2	12.9		
	Total	13307	173312.2			

Although the ANOVA results indicate that the visibility level has a statistical significant effect on traffic stream free-flow flow speed, this difference is minor and does not exceed 4.0 km/h, which corresponds to a reduction of only 3.7% as shown in Figure 33 for Twin Cities. Similar results were observed for other cities as shown in Table 31, with Twin Cities having the highest reductions.

Table 31: Summary Results for Visibility Effect.

City	Visibility (Km)	Number of Obs.	Mean (km/h)	Std. Dev. (km/h)	Reduction (%)
Twin Cities	4.80	7680	111.82	8.16	
	3.20	267	110.01	8.28	1.62%
	1.00	890	110.29	8.16	1.37%
	0.40	69	107.72	7.63	3.67%
Seattle	4.80	400	112.338	0.263	
	3.20	40	112.186	0.364	0.14%
	0.97	85	112.141	0.286	0.18%
	0.40	100	112.012	0.280	0.29%
Baltimore	4.80	11957	122.08	3.59	
	3.27	828	120.99	3.54	0.89%
	1.19	275	121.16	3.62	0.75%
	0.38	248	120.11	3.46	1.61%

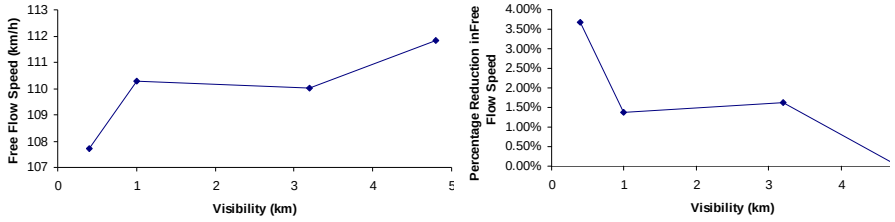

Figure 33: Impact of visibility on free-flow speed (Twin Cities)

5.5.2 Impact of Rain

Having established that reductions in visibility below 1.2 km produce statistically significant, but minor reductions in free-flow speed (reductions of less than 4%), the next step was to investigate the effect of rain intensity on traffic stream free-flow speed. The details of the analysis are presented in this section.

Statistical tests on the variances were also conducted to determine if these trends were statistically significant. The results clearly demonstrate that the observed differences are statistically significant for Twin Cities, Seattle, and Baltimore, as illustrated in Figure 34a, c, and e, and also that the free-flow speed variance increases as the rain intensity. For example, the standard deviation increases by 2.0 to 6.0 km/h (or 24 to 94%) for a rain intensity of about 1.5 cm/h relative to clear conditions.

Since the datasets did not satisfy the equal variances tests, the datasets were grouped in bins and analysis was performed on the averages of the bins. Figure 34b, d, and f shows the result of the equal variances tests after grouping.

Again, ANOVA tests were performed on the data with a null hypothesis that rain has no effect on traffic stream free-flow speed.

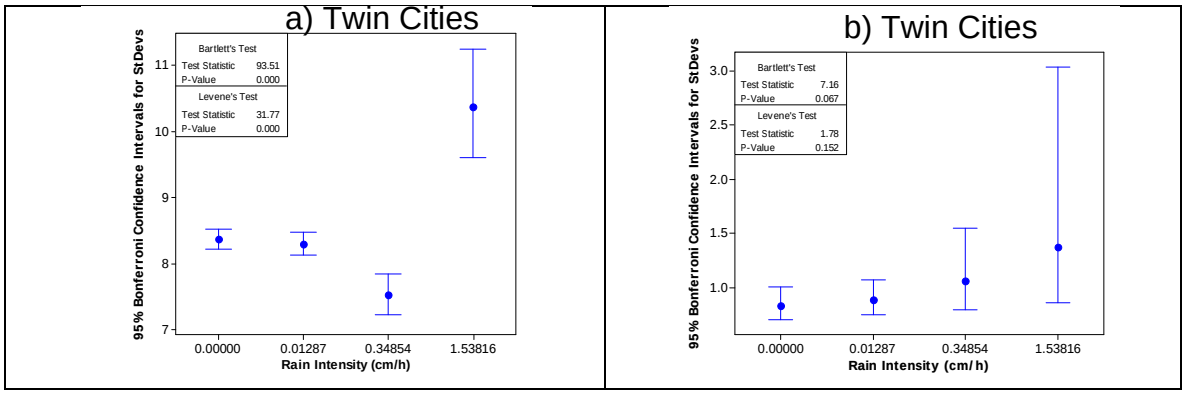

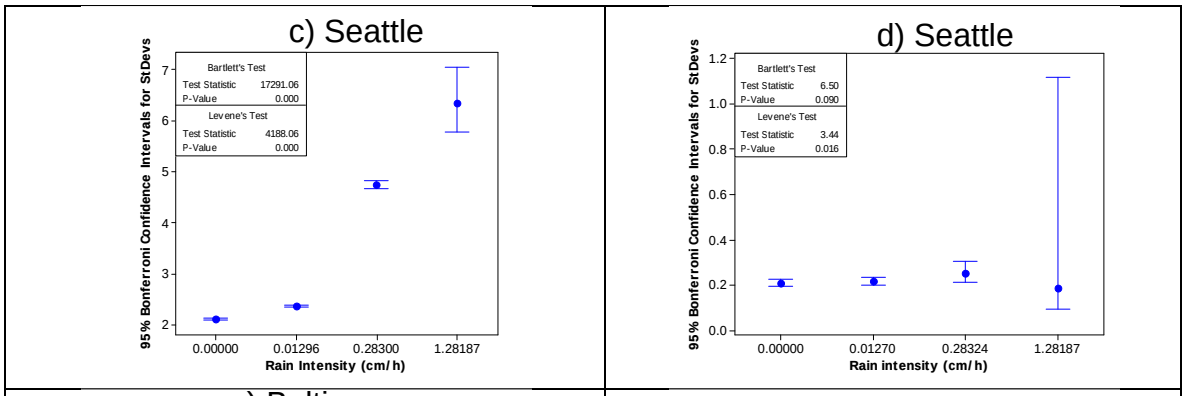

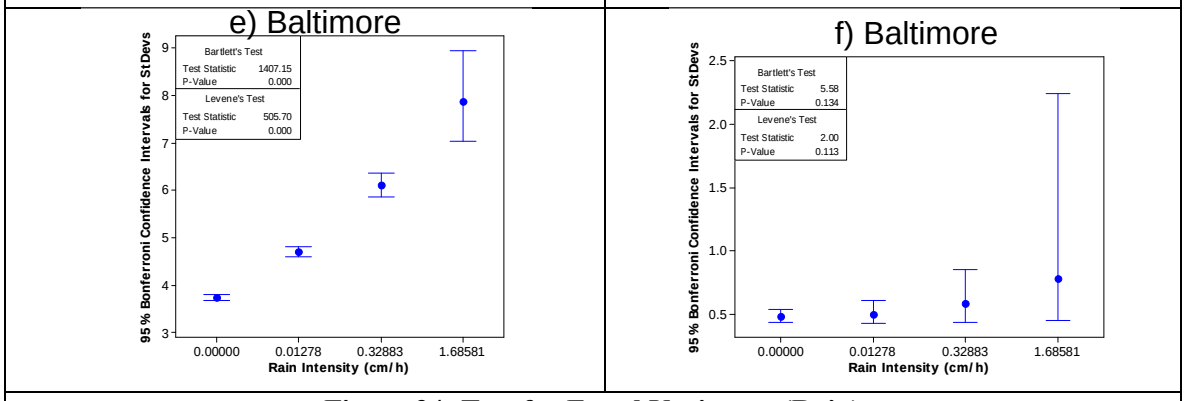

Figure 34: Test for Equal Variances (Rain)

Table 32 summarizes the ANOVA results for Twin Cities, Seattle, and Baltimore. As was the case with visibility levels, the results demonstrate that rain intensity has a significant impact on traffic stream free-flow speed.

Table 32: ANOVA Results for Rain.

City	Source	DF	SS	MS	F	P
Twin Cities	Rain	3	551.573	183.858	223.30	0.000
	Error	236	194.318	0.823		
	Total	239	745.891			
Seattle	Rain	3	2723.367	907.789	19461.40	0.000
	Error	1001	46.646	0.047		
	Total	1003	2770.013			
Baltimore	Rain	3	3948.205	1316.068	5294.07	0.000
	Error	383	95.211	0.249		
	Total	386	4043.416			

The summary results of Table 33 clearly demonstrate reductions that range between 5.2 and 11.2 km/h (4.7 to 9.1%) between clear conditions and a rain intensity of about 1.5 cm/h.

Table 33: Summary Results of Rain Intensity Effects.

City	Intensity (cm/h)	Number of Obs.	Mean (km/h)	Std. Dev. (km/h)	Reduction (%)
Twin Cities	0.00000	100	109.80	0.83	
	0.01287	100	107.32	0.882	2.26%
	0.34854	30	106.44	1.056	3.06%
	1.53816	10	104.63	1.371	4.71%
Seattle	0.00000	500	112.75	0.208	
	0.01297	400	110.84	0.216	1.69%
	0.28325	100	107.38	0.253	4.76%
	1.28187	5	107.32	0.187	4.82%
Baltimore	0.00000	250	123.04	0.478	
	0.01278	100	118.67	0.500	3.55%
	0.32883	30	113.30	0.581	7.92%
	1.68581	7	111.86	0.784	9.09%

The free-flow speeds were normalized across the three sites by dividing the mean at each rain intensity level by the mean for the corresponding clear conditions at the specific city. Using the normalized data an inclement weather free-flow speed reduction factor was developed as

$$F = ai^b, \qquad (4)$$

Where F is the inclement weather free-flow speed reduction factor, i is the precipitation intensity (cm/h), and a, and b are calibrated model coefficients. Nonlinear regression analysis is performed. This model has proven to produce better results in terms of R^2 and ANOVA p-value than other linear models.

The various calibrated model coefficients are tabulated in Table 34, and the shape of F as a function of the rain intensity is illustrated in Figure 35.

Table 34: Calibrate Model Coefficients.

Precept.	City	N	*a*	*b*	*Pseaudo-R^2*	*P*-value
Rain	Baltimore	*3*	*0.9122*	*-0.0125*	98.36	*0.0032*
	Twin Cities	3	0.9588	-0.0048	83.64	0.0043
	Seattle	3	0.9495	-0.0075	90.64	0.0046
Snow	Baltimore		0.5988	-0.0971	98.93	0.0132
	Twin Cities	3	0.6946	-0.0546	99.97	0.0012
	Seattle		0.7266	-0.0205	80.75	0.0134

The figure demonstrates a 2.3% reduction in the free-flow speed at the onset of rain (wet roadway surface with no rain). The inclement weather adjustment factor continues to decrease as the rain intensity increases for a maximum reduction of 9% at a rain intensity of about 1.5 cm/h. It should be noted that the function is only valid up to a maximum precipitation of 1.69 cm/h.

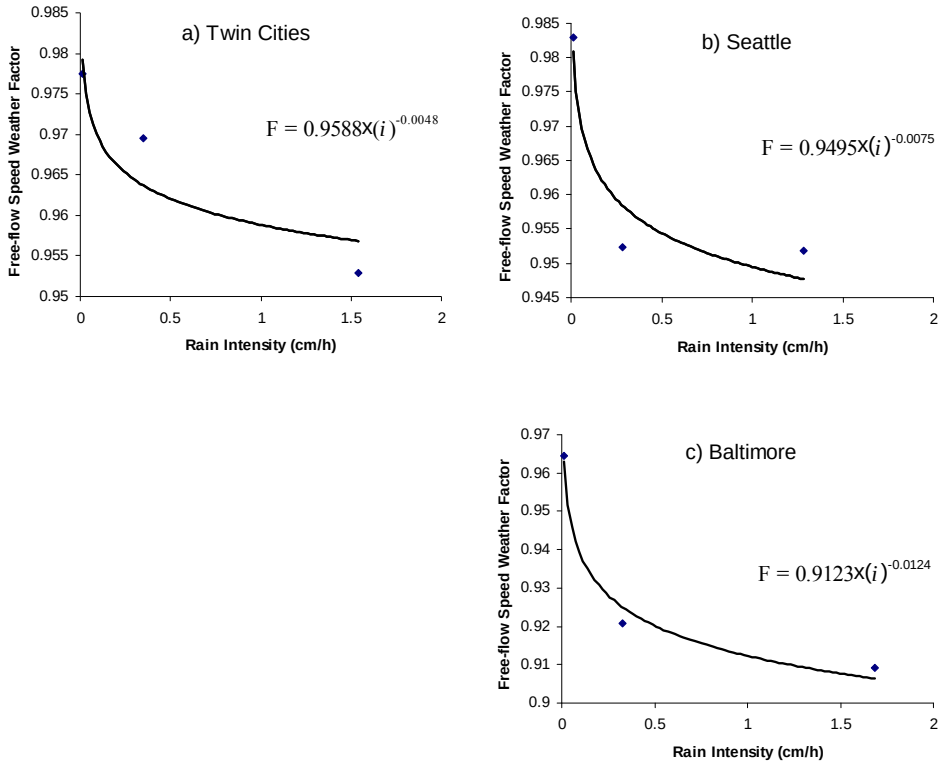

Figure 35: Variation in the free-flow speed inclement weather factor as a function of rain intensity

By comparing the reduction of free flow speed due to rain on the three cities, it can be found the onset reduction for Seattle and the Twin cities is almost the same (2.3%), and as for Baltimore the reduction on the onset was more than 3% On the other hand the maximum reduction was 5.5% for both Minneapolis and Seattle and 9% for Baltimore.

5.5.3 Impact of Freezing Rain

This section investigates the impact of freezing rain intensity on traffic stream free-flow speed. Data was available from Seattle and Baltimore only. ANOVA tests are used to conduct the analysis. The null hypothesis is that freezing rain intensity has no impact on traffic stream free-flow speed. Again, as was the case with the rain intensity analysis, the free-flow speed variance appears to increase as the freezing rain intensity increases as shown in Figure 36 a & c. As explained in earlier sections, binning was performed to homogenize the data with respect to the variance. The results are shown in Figure 36 b & d.

Results for the two cities clearly demonstrates that the null hypothesis is rejected and that indeed there is sufficient evidence to conclude that an increase in freezing rain intensity results in reductions in traffic stream free-flow speeds, as summarized in Table 36. The results in Table 36 demonstrate that significant reductions in free-flow speed are observed for minor freezing rain intensity levels. Specifically, reductions in Free Flow Speed of 32 km/h (31%) & 30 km/h (27%) are observed for a freezing rain intensity of 0.3 cm/h & 0.58 cm/h compared to Free Flow Speed in clear condition for Seattle and Baltimore respectively.

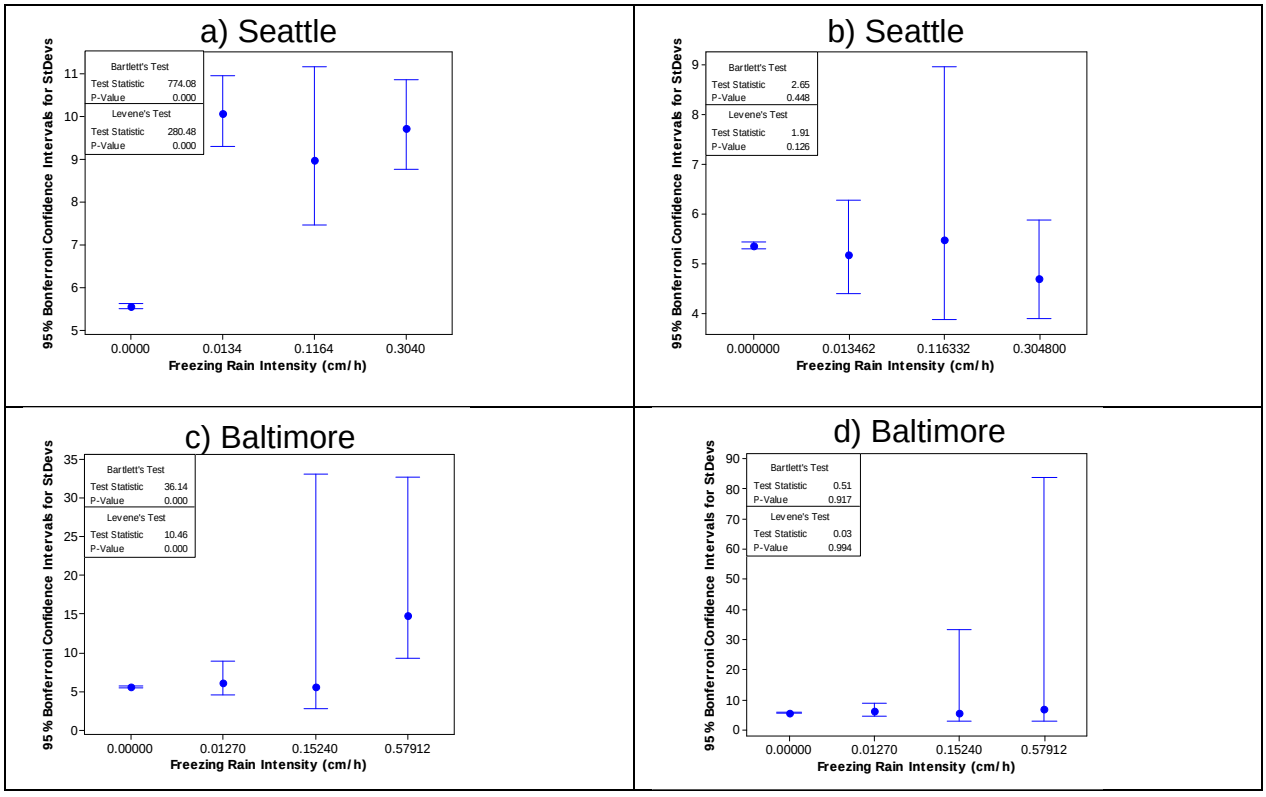

Figure 36: Test for Equal Variances (Freezing Rain)

Table 35: **ANOVA Results for Freezing Rain.**

City	Source	DF	SS	MS	F	P
Seattle	Freezing Rain	3	208621.0	69540.3	2426.91	0.000
	Error	15192	435310.3	28.7		
	Total	15195	643931.3			
Baltimore	Freezing Rain	3	16847.3	5615.8	183.60	0.000
	Error	10221	312630.6	30.6		
	Total	10224	329477.9			

Table 36: Summary Results of Freezing Rain Intensity Effects.

City	Intensity (cm/h)	Number of Obs.	Mean (km/h)	Std. Dev. (km/h)	Reduction (%)
Seattle	0.000	15000	103.76	5.36	
	0.013	100	70.12	5.17	32.42
	0.120	20	72.75	5.46	29.89
	0.305	76	71.53	4.69	31.06
Baltimore	0.000	10189	112.28	5.53	
	0.013	29	91.07	6.01	18.89
	0.152	4	95.60	5.52	14.86
	0.579	3	82.01	6.63	26.96

Similarly to the rain data, the Free Flow Speed were normalized across the two cities by dividing the mean at each rain intensity level by the mean of the corresponding clear conditions at the specific city. Using the normalized data an inclement weather free-flow speed reduction factor was developed as

$F = a + bi$

Where F is the inclement weather free-flow speed reduction factor, *i* is the precipitation intensity (cm/h) and *a*, and *b* are calibrated model coefficients.

Table 37 shows the calibrated model coefficient for the freezing rain for the city of Baltimore.

Table 37: Calibrate Model Coefficients for Freezing Rain.

Precept.	City	N	*a*	*P-value (a)*	*b*	*P-value (b)*	R^2
Freezing Rain	Baltimore	3	*-0.162*	0.36	*0.84*	0.38	*68.6 %*

Figure 37 shows the model for the freezing rain in both Seattle and Baltimore, as for Seattle the reduction is found to be constant with 31 % of reduction in free flow speed, on the other hand in Baltimore the reduction ranges between 14 to 26 %.

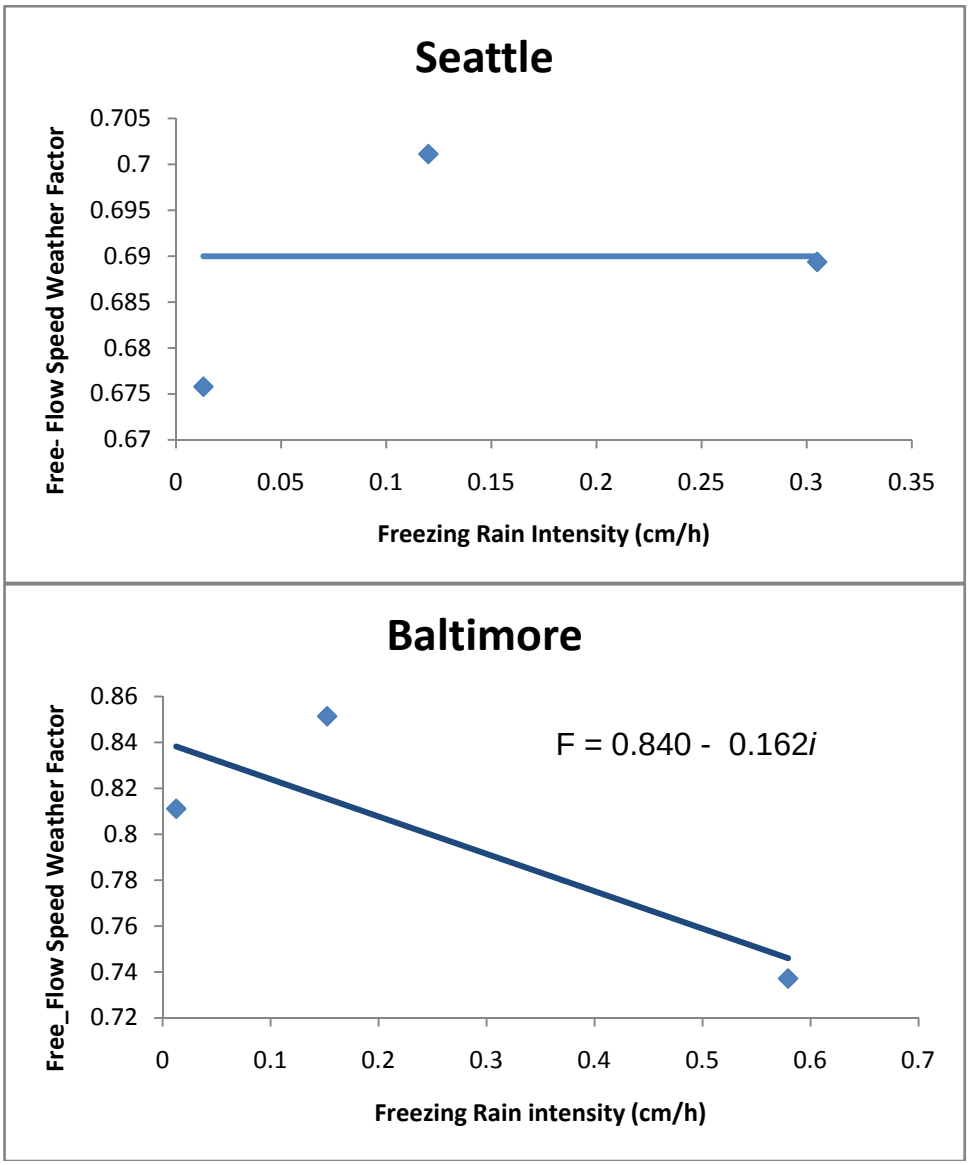

Figure 37: Variation in the free-flow speed inclement weather factor as a function of freezing rain intensity

By comparing the reduction of free flow speed due to freezing rain on the two cities, it can be found the reduction for Seattle was constant for all different freezing rain intensities (31%), and as for Baltimore the reduction on the onset was found to be 14% and maximum reduction was 27%

5.5.4 Impact of Snow

This section investigates the impact of snow intensity on traffic stream free-flow speed. ANOVA tests are used to conduct the analysis. The null hypothesis is that snow intensity has no impact on traffic stream free-flow speed.

Statistical tests of the variances were conducted to determine if the variance is constant for each city. The results that are summarized in Figure 38 a, c, and e demonstrates that the free-flow speed variance appears to increase as the snow intensity increases. Consequently, the results demonstrate that the free-flow standard deviation increases in the range of 3 to 8 km/h for a snow intensity of 0.3 cm/h compared to clear conditions. This increase is equivalent to an increase of 28 to 100% in the free-flow speed standard deviation. Since the data did not satisfy the equal of variance test, data was grouped into bins and the analysis was performed on the average of the bins Figure 38 b, d, & F show the result of the equal variance test after grouping.

Results for the three cities clearly demonstrates that the null hypothesis is rejected and that indeed there is sufficient evidence to conclude that an increase in snow intensity results in reductions in traffic stream free-flow speeds, as summarized in Table 35. The results also demonstrate that significant reductions in free-flow speed are observed for minor snow intensity levels, as demonstrated in Table 38. Specifically, reductions in free flow speed in the range of 25 to 35 km/h (or 22 to 29%) are observed for a snow intensity of about 0.3 cm/h compared to free-flow speeds in clear conditions.

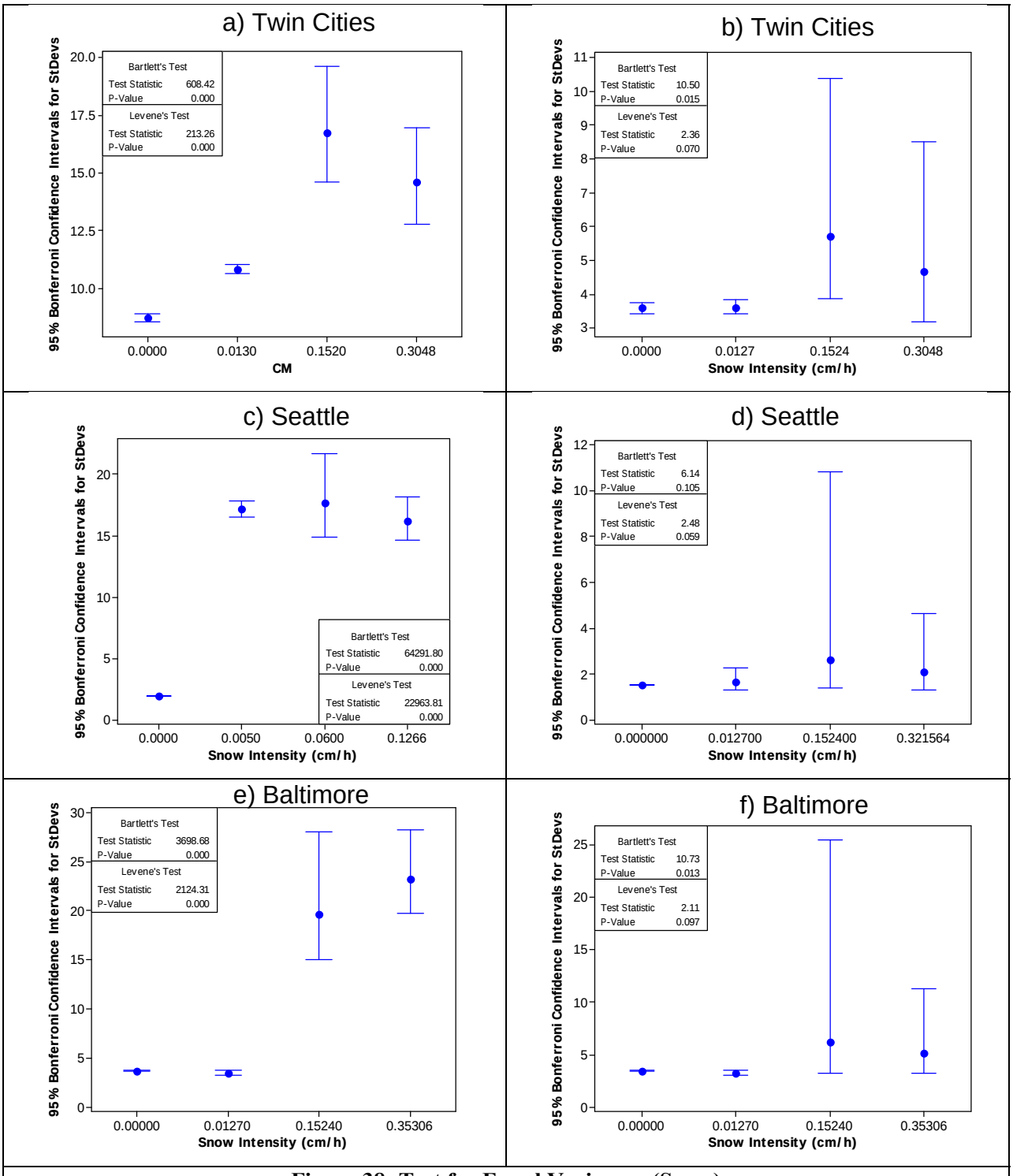

Figure 38: Test for Equal Variances (Snow)

Table 38: ANOVA Results Snow.

City	Source	DF	SS	MS	F	P
Twin Cities	Snow	3	51083.0	17027.7	1306.15	0.000
	Error	2526	32930.3	13.0		
	Total	2529	84013.3			
Seattle	Snow	3	27552.52	9184.17	3965.23	0.000
	Error	25051	58022.48	2.32		
	Total	25054	85575.00			
Baltimore	Snow	3	15227.2	5075.7	438.96	0.000
	Error	10511	121540.5	11.6		
	Total	10514	136767.7			

Table 39: Summary Results of Snow Intensity Effects.

City	Intensity (cm/h)	Number of Obs.	Mean (km/h)	Std. Dev. (km/h)	Reduction (%)
Twin Cities	0.000	1500	112.22	3.58	
	0.013	1000	104.12	3.60	7.22%
	0.152	15	90.74	5.71	19.14%
	0.305	15	87.63	4.68	21.91%
Seattle	0.000	25000	111.3	1.52	0.00%
	0.013	40	90.5	1.66	18.69%
	0.152	5	84.11	2.61	24.43%
	0.322	10	85.6	2.1	23.09%
Baltimore	0.000	10000	122.30	3.41	
	0.013	500	122.12	3.22	0.15%
	0.152	5	98.04	6.14	19.84%
	0.353	10	87.22	5.08	28.68%

As was done in the previous analysis, the mean speeds for each snow intensity level were normalized relative to their respective clear conditions mean speed. These data were then utilized to develop free-flow speed reduction factors as a function of the snow intensity, as illustrated in Figure 39. The model was developed as

$$F = ai^b \quad (5)$$

Similar to the rain data and the results were presented in Table 40.

Figure 39 demonstrates that the free-flow speed is reduced by approximately 6% at the onset of snow and continues to decrease as the snow intensity increases. The free-flow speed is reduced by approximately 20% for a maximum snow intensity of 0.3 cm/h. Again, the model is only valid for a snow intensity that ranges from 0.0 to 0.3 cm/h given that the dataset did not include higher precipitation rates.

From Figure 40 it is evident that snow produces larger reductions in the traffic stream free-flow speed. Furthermore, the rain reduction factor appears to be fairly constant for rain intensities of 1 cm/h or greater.

Table 40: Calibrate Model Coefficients of Snow.

Precept.	City	N	*a*	*b*	*Pseaudo-R*^{2}	*P*-value
Snow	Baltimore	3	0.5988	-0.0971	98.93	0.0132
	Twin Cities		0.6946	-0.0546	99.97	0.0012
	Seattle		0.7266	-0.0205	80.75	0.0134

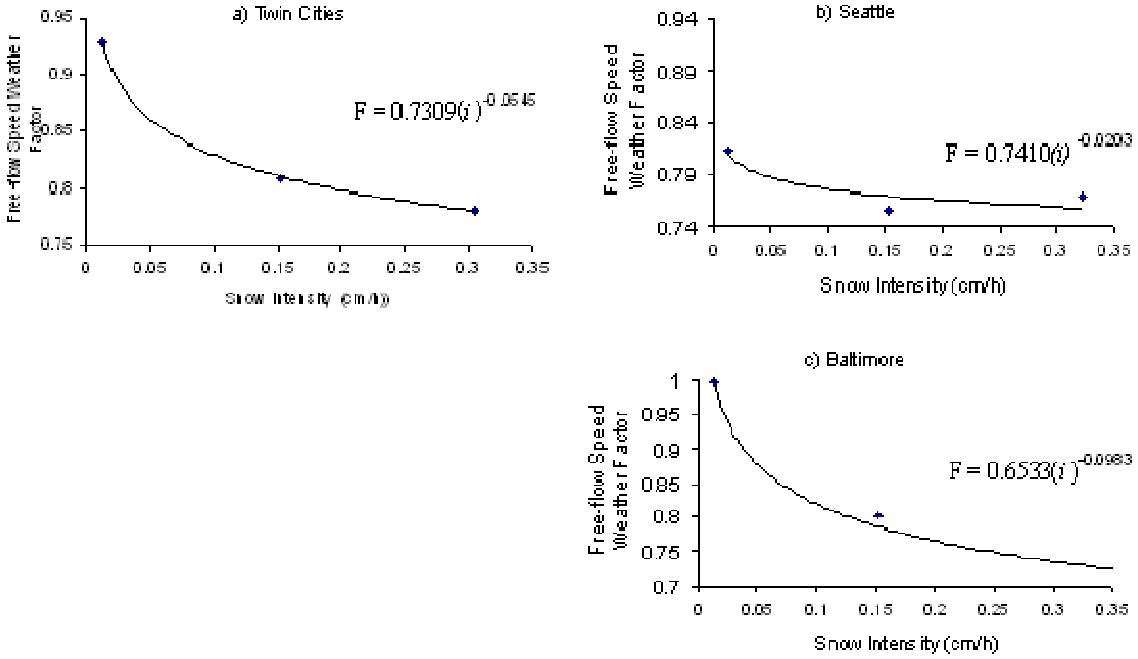

Figure 39: Variation in the Free-Flow Speed Inclement Weather Factor as a Function of Snow Intensity

Although Twin cities had the biggest average annual snow precipitation of the three cities, (73 cm/hr) the max reduction was the least among the three cities which indicates that drivers are used to snow and they can update their driving behavior according to snow. Conversely Baltimore had the least average annual snow precipitation (11 cm/hr) but it had the biggest reduction on free flow speed.

By comparing the reduction of free flow speed due to snow on the three cities, it can be found the onset reduction was different along the three cities with a maximum reduction at Seattle (20%) and for tthe case of the max reduction; Seattle and Baltimore were almost the same with (21) and a max reduction for Baltimore almost (26%)

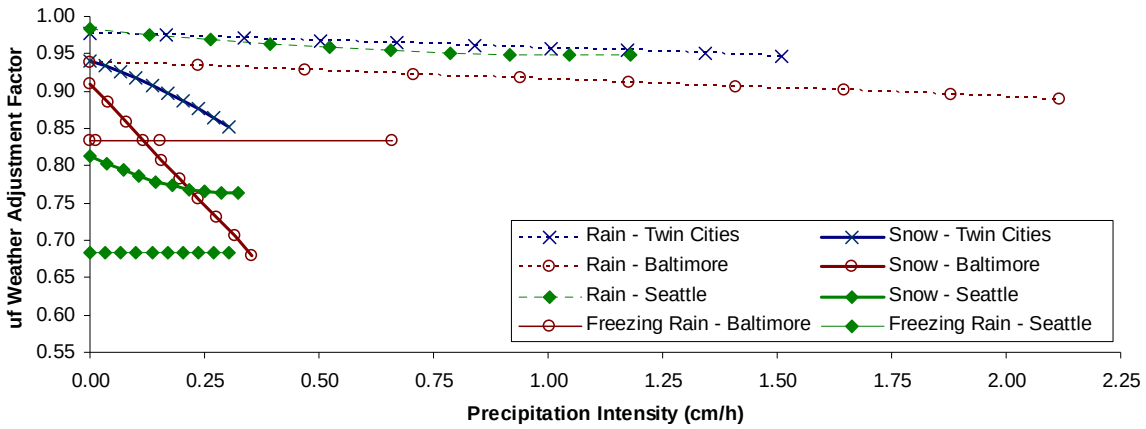

Figure 40: Comparison of rain, snow, and freezing rain inclement weather factors

5.6 Concluding Remarks

The study quantified the impact of inclement weather on traffic stream free-flow speed. The study demonstrated that impaired visibility had minimal impacts on free-flow speed with reductions in the range of 1 to 3%. Furthermore, these reductions were only observed when the visibility decreased below 1.2 km. With regards to rain, the onset of rain produced reductions in free-flow speeds in the range of 2.3%. The free-flow speed continued to decrease as the rain intensity increased reaching a maximum reduction of 4.8% at a rain intensity of 1.5 cm/h. The analysis also demonstrated that free-flow speed standard deviation increased in the range of 14 to 100% for a rain intensity of 1.5 cm/h relative to the clear scenario. With regards to snow, higher reductions in free-flow speed were observed when compared to rain. Specifically, the free-flow speed was reduced by 6% at the onset of snow precipitation with a maximum decrease of 20% at a snow intensity of 0.3 cm/h. The free-flow speed standard deviation also increased in the range of 28 to 100% at the maximum snow intensity of 0.3 cm/h. With regards to freezing rain, higher reductions in free-flow speed were observed when compared to rain and snow. Specifically, the free-flow speed was reduced by 14% at the onset of freezing rain precipitation with a maximum decrease of 27% at freezing rain intensity of about 0.53 cm/h for Baltimore and as the case of Seattle the reduction was found to be constant with 31%.

Acknowledgement

The authors acknowledge the help of Daniel Krechmer and Vijay Kovvali of Cambridge Systematics for providing the data and for their valuable input on the analysis. Further acknowledgements are due to Alfelor Roemer, Paul Pisano, James Colyar, and Lynette Goodwin

for their input on the data analysis. This research effort was funded by the FHWA, the Mid-Atlantic University Transportation Center (MAUTC), and the Virginia Department of Transportation (VDOT).

Chapter 6: Conclusions and Recommendation for Further Research

6.1 Summary Conclusions

The research presented in this thesis attempted to investigate the impact of detector failure frequency and duration on the accuracy of loop detector space mean speed, flow, and density measurements using a Monte Carlo simulation approach. The inputs to the model are the number of failures per hour (frequency) and failure duration. The second part of the research effort attempted to quantify the impact of inclement weather (precipitation and visibility) on traffic stream free-flow speeds along freeway sections. The analysis is conducted using weather (precipitation and visibility) and loop detector data (speed) obtained from Baltimore, Minneapolis/St. Paul, and Seattle, US. The following sections summarize the study conclusions.

6.1.1 Loop Detectors

This research attempted to quantify the accuracy of loop detector measurements (density (k), flow (q), and space-mean speed (u)) by introducing failures into raw loop detector actuations using a Monte Carlo simulation approach. The research concluded, as would be expected, that the polling interval density, flow, and space mean speed RMSEs increase as the frequency and duration of failures increase. Furthermore, the research demonstrated that the density and flow RMSEs increase as the level of congestion increases while the space-mean speed RMSE decreases. Finally, the research developed regression models that predict the accuracy of loop detector measurements. The input parameters to these models are the failure frequency, the failure duration, and the traffic stream density.

A sensitivity analysis of the models revealed that the errors are insensitive to the error function, location, (speed and density), the lane, or the polling interval that is used to aggregate the data. Alternatively, the location had the same trend but the magnitude of the flow RMSE increased by 7.5 to 15%.

6.1.2 Inclement Weather

The study quantified the impact of inclement weather on traffic stream free-flow speed. The study demonstrated that impaired visibility had minimal impacts on free-flow speed with

reductions in the range of 1 to 3%. Furthermore, these reductions were only observed when the visibility decreased below 1.2 km. With regards to rain, the onset of rain produced reductions in free-flow speeds in the range of 2.3%. The free-flow speed continued to decrease as the rain intensity increased reaching a maximum reduction of 4.8% at a rain intensity of 1.5 cm/h. The analysis also demonstrated that free-flow speed standard deviation increased in the range of 14 to 100% for a rain intensity of 1.5 cm/h relative to the clear scenario. With regards to snow, higher reductions in free-flow speed were observed when compared to rain. Specifically, the free-flow speed was reduced by 6% at the onset of snow precipitation with a maximum decrease of 20% at a snow intensity of 0.3 cm/h. The free-flow speed standard deviation also increased in the range of 28 to 100% at the maximum snow intensity of 0.3 cm/h. With regards to freezing rain, higher reductions in free-flow speed were observed when compared to rain and snow. Specifically, the free-flow speed was reduced by 14% at the onset of freezing rain precipitation with a maximum decrease of 27% at freezing rain intensity of about 0.53 cm/h for Baltimore and as the case of Seattle the reduction was found to be constant with 31%.

6.2 Recommendations for Further Research

In chapter 4 an initial attempt to quantify the accuracy of loop detector data was presented. It is recommended that further research be conducted on the following:

- The methodology should be extended, implemented, and tested using data from different sites in order to generalize the study findings.
- Further research is required to characterize the typical spacing behavior of detector failures as a function of failure frequency.

6.2.1 Lessons learned from Completed Research

High-quality traffic and weather data is critical to accurate analysis of the effects of inclement weather on traffic flow and driver behavior. The data must be accurate, complete and representative of the geographic, functional (i.e., freeways, arterials), and geometric (i.e., grades, curves) areas of interest. In this phase, researchers were limited by the extent of existing traffic and weather data collection. Better, more comprehensive data will result in better modeling and analysis.

In addition, information on roadway surface conditions is critical to an accurate analysis of inclement weather impacts on traffic flow and driver behavior. Consequently, video or roadway sensors are required to gather roadway surface conditions.

In many major metropolitan areas, traffic sensor data are collected and archived. However data quality is not always as high as desired. It is important that the sensors and communications equipment are maintained and data are reviewed regularly for quality control.

Weather data collected by state DOT's and other transportation agencies are typically not as robust as the traffic data. While meteorological concerns are often considered in the siting of Environmental Sensor Stations (ESS), they are most often used for winter maintenance activities, and as a result, are located with those needs in mind. The availability of communications and power are also important considerations and compromises from the ideal location may be necessary. Some agencies are now trying to colocate new ESS with traffic counting stations, but for the most part they are not found in the same locations. One of the major problems with using DOT ESS data in this project was that many ESS only report the presence of precipitation, not the rate. Therefore the data have limited utility

The study has shown that while traffic and weather data sets are often sufficient for day-to-day operations, the combination of the two data sets is lacking for analysis of this detail and sensitivity. Therefore, it is recommended that the current study – evaluating the macroscopic traffic flow parameters – be replicated with better, complimenting, sets of traffic, weather, and roadway surface data.

6.2.2 Enhancement of Macroscopic Analysis

The macroscopic analysis conducted for this project should be enhanced through a data collection procedure as outlined below:

- Select sites with dual loop detectors that collect high-quality and robust traffic data elements of volume, speed, and occupancy. The set of locations should provide enough uniformity to have a large data set and enough variety of functional classification or geometric configuration to provide direction for further research.
- Place ESS near traffic loop detectors. The ESS should have a weather sensors, a roadway surface sensor, and a video detection system to collect atmospheric

(temperature, precipitation, visibility, wind) and pavement condition (pavement temperature, surface condition) environmental data. It is important to use roadway surface conditions when evaluating the impact of inclement weather on traffic flow to capture the true conditions of the roadway (e.g., wet, slushy, icy) and consider splash from vehicles.

- Collect traffic and weather data during dry, rainy, and winter conditions. A potential source of both traffic and weather data is VTTI's Mobile Traffic Laboratory (MTL), a fully self-contained modular laboratory that provides real-time traffic data, such as traffic volume, vehicle speed, lane occupancy, and pedestrian detection. The MTL van is equipped with a weather station that measures wind speed, direction, temperature, relative humidity, and rainfall. In addition, the van is equipped with an Autoscope Solo Pro™ wide-area video vehicle detection system, an Autoscope Image Sensor™ (AIS), a pneumatic mast (13.71-meter maximum raised height) with color pan/tilt/zoom cameras, a computer system, and a videocassette player/recorder. The equipment racks are easily configurable and the MTL has a modular design that allows for extension and enhancement. A mobile collection approach will enable the collection of relevant field data at multiple geographic locations.

6.2.3 The impact of Precipitation on Traffic Stream Free-flow Speed

After a review of existing sources during the development of the data collection plan it did not appear that arterial data could be obtained that meet the criteria above. Most arterial detectors are located at intersections making it difficult to calculate average speeds along a stretch of highway. Speed and volume data are also difficult to obtain on nonurban stretches of arterial roadway. While only freeways are included in this analysis, different types of freeway facilities will be incorporated into the study. One potential categorization is by function, with the hypothesis that radial and circumferential/cross-town freeways may experience different impacts from adverse weather. More likely is that the size of the facility will result in different traveler responses to weather events. As a result, the study tried to incorporate different freeway capacities into the analysis, including four-lane, six-lane and eight-lane sections. While there was some variation in the freeways sampled, including both radial and circumferential highways,

the number of stations observed was not adequate to identify differences in behavior. A good research goal for the future would also be to analyze adverse weather impacts on different types of roadway geometry. Given the relatively sparse distribution of RWIS in most metropolitan areas this analysis would require collection and analysis of additional observations from a dense network such as the NWS Cooperative Observer program.

6.2.4 Study of Regional Differences

The limitation of this study to three cities limited the ability to draw conclusions about regional differences in driver response to adverse weather. Given the limited number of cities and detector stations, it was difficult to isolate the impact of weather events from other factors such as roadway geometry, signing and in the case of snow, winter maintenance. A more thorough analysis of regional differences will require a larger sample of cities with more detailed data from each.

6.2.5 Study the Macroscopic Impacts of Reduced Visibility

Some of the RWIS stations identified for this study included visibility sensors. The findings related to visibility are documented in Section 5 but conclusions are limited due to the limited number of locations studied and lack of refinement in some of the sensor data. More detailed analysis is needed in the future to separate the impact of fog from other factors. This is clearly an important area of emphasis but it is not clear whether there are adequate data to support this analysis.

6.2.6 Microscopic and Human Factors Analysis

In addition to refining the macroscopic analysis with better data, future research on weather-sensitive traffic flow modeling should focus on individual driver behavior and resulting vehicle movements under different weather and pavement conditions. Proposed microscopic and human factors analyses are outlined below.

Empirical evidence regarding the microscopic effects of weather on individual drivers is deficient in the literature. Similarly, research into human factors has been limited to vehicle safety investigations, with minimal consideration of traffic flow. These gaps in research provide a need and motivation to study both microscopic parameters (i.e., desired speed, acceleration, minimum gap acceptance, and lane changing) and human factors (i.e., reaction times,

demographics, driver workload). The following tasks will focus on enhancing knowledge in this field.

6.2.7 Use of Existing Naturalistic Driving and NGSIM Data

The Federal Highway Administration is collecting a significant amount of detailed vehicle trajectory and driver behavior data as part of the Next Generation Simulator (NGSIM) Project. Additionally, previous work in developing driver behavior models has resulted in numerous, detailed vehicle data. Subsets of this data can be extracted and analyzed to characterize driver longitudinal motion in clear, rainy, and snowy weather conditions. The trajectory data should be augmented with historical ASOS weather data. If the dataset includes inclement weather conditions then an analysis of driver behavior during inclement weather conditions could be compared to driver behavior during clear conditions to establish differences in driver behavior.

In addition to the NGSIM data, a number of naturalistic Field Operational Test (FOT) data sets are available. The 100-Car Study was the first instrumented-vehicle study undertaken with the primary purpose of collecting large-scale naturalistic driving data. Drivers were given no special instructions, no experimenter was present, and the data collection instrumentation was unobtrusive. In addition, the majority of the drivers drove their own vehicles (78 out of 100 vehicles). The dataset contains data at 10 HZ for many extreme cases of driving behavior and performance, including severe drowsiness, impairment, judgment error, risk taking, willingness to engage in secondary tasks, aggressive driving, and traffic violation.

The data collection effort resulted in the following dataset contents: a) approximately 2 million vehicle miles of driving, b) almost 43,000 hours of data, c) 241 primary and secondary driver participants, d) 12- to 13-month data collection period for each vehicle; 18-month total data collection period, e) 15 police-reported crashes, f) 67 non-police-reported crashes (some producing no damage), g) 761 near-crashes, h) 8,295 incidents, and i) five channels of video and many vehicle state and kinematics variables.

If the naturalistic driving data are augmented with weather and pavement data, it will be possible to study the effect of inclement weather on driver behavior.

Acceleration, lane changing and gap acceptance models should be evaluated for differences based on varying precipitation and visibility conditions.

6.2.8 Controlled Field Studies

In addition, vehicle trajectory data and driver behavior/response data should be collected from instrumented vehicles in a controlled field study to model individual decisions drivers make under different weather conditions. We recommend that a combination of controlled field and naturalistic driver studies be conducted as part of the next phase of the project.

The Smart Road, a 3.5 kilometer fully instrumented two-lane road in southwest Virginia, is a joint project of the Virginia Department of Transportation (VDOT), VTTI, and the FHWA. The facility is an operational test-bed for detailed, real-world performance of vehicles in a controlled environment. It is a real roadway environment that has the capability to generate and monitor all types of weather and pavement conditions. Data will be collected on drivers under generated weather conditions of rain, snow, and dense fog. DGPS will be utilized to track exact trajectories of test vehicles and in-vehicle camera systems will be used to record driver reactions. Environmental monitoring stations will record conditions on the roadway. The facility has the following unique capabilities:

- **All-weather Testing Capability.** The facility is capable of producing rain, snow, and a fog-like-mist over a one-half-mile stretch of roadway. At maximum output, the system produces up to five inches of rain per hour and 10 inches of snow per hour. A 500,000-gallon water tank feeds the system and allows for multiple research events. The all-weather testing towers are automatically controlled and can produce rain and snow at multiple intensities. In addition, water can be sprayed by the towers onto freezing pavement to create icy conditions.
- **Environmental Monitoring.** VTTI has installed a permanent visibility sensor and three weather stations to provide direct data for operational conditions to the research staff. Available data includes temperature, humidity, wind speed, wind direction, and visibility measured in miles. These data are used in conjunction with the All Weather Testing section to provide quantitative measurements of test conditions as subjects complete research tasks.
- **On-site Data Acquisition Capabilities.** The roadway has an underground conduit network with manhole access every 60 meters. This network houses a fiber optic data network and interfaces with several on-site data acquisition systems. The facility also has a complement of Road Weather Information

Systems (RWIS) stations connected to the data network. The fiber network has an interface with a card that will allow RWIS data to be transmitted via wireless communications.

- **Wet Visibility Section.** VTTI recently constructed a Wet Visibility road section that runs alongside a section of the Smart Road. This roadway section is a "crownless" road: it has no arch in the middle and runs as flat across as is possible. On such a road, water will not drain off onto the sides and will pool in the middle. This section of roadway is being used to test pavement markings in wet-weather conditions. This two-lane road connects with the Smart Road intersection. It joins the intersection on the opposite side of the Smart Road and runs parallel to the Smart Road up to the first turnaround. In addition, 35 portable rain towers were constructed to be used along the wet visibility section.
- **In-house Differential GPS System**. Precise vehicle location can be tracked on the road with a military-grade global positioning systems (GPS) base-station. This system can track the location of a vehicle on the road to 2.0-centimeter accuracy at four samples per second, or 5.0-centimeter accuracy at 10 samples per second.
- **Surveillance Camera Systems.** In 2001, VTTI installed a complete video surveillance system consisting of nine permanently mounted, low-light color cameras. Also on hand are two portable cameras that can be moved to any location on the roadway for project-specific needs. Six of the cameras use dedicated fiber optic links to transmit video and data signals to the control room. The cameras are fed directly to the Smart Road Control Room and monitored by staff. VTTI has the ability to pan/tilt/zoom all of the cameras via custom software on the video wall computer.
- **Variable Lighting Testbed.** VTTI and Virginia DOT, in conjunction with FHWA, developed a highway lighting test bed on the Smart Road. The system consists of overhead light poles with the following spacing: 40-20-20-40-40-20-20-40-40-20-20 meters. This spacing, combined with wiring the poles on three separate circuits, allows for evaluating lighting systems at 40, 60, or 80 meters. The poles incorporate a modified design to allow for easy height adjustment of

the bracket arm. In addition to evaluating spacing and bracket height, various luminaries are available as well, including metal halide and high-pressure sodium. If desired, differing levels of roadway lighting also can be simulated concurrently with the variation in visibility produced by the all-weather testing equipment. This allows a multitude of visibility conditions to be created, on demand, for testing purposes.

Figure 41: Image of Smart Road Weather Making Capabilities

These data will be used to estimate differences in microscopic models in varying weather conditions, especially different precipitation and visibility combinations.

6.2.9 Pretrip Driver Decisions

A survey should be developed and conducted to determine how weather events and forecasts impact driver's pretrip decisions, including departure time, route choice, expected travel time, and aggressiveness. There are several options for conducting such a survey. One is a traditional telephone survey that would identify regular commuters and ask them about their use of pretrip information. A survey conducted by Cambridge Systematics for Michigan DOT asked commuters in the Detroit region whether they used pretrip information to change their time of departure or route of travel. The survey found bad weather to be one of the major factors in the decision to change departure time but much less of a factor in changing route choice. It also

indicated that the sensitivity to weather information is much greater during the a.m. peak commute than the p.m. peak commute. This is an expected result since weather is less likely to vary by route than traffic conditions.

Table 41 Reasons for Changing Routes
West Sector (Washtenaw, Livingston and Westen Wayne Counties, Michigan)

Reasons for Changing Routes	a.m. Commute	p.m. Commute
Traffic Accident or Incident	57%	51%
Roadway Construction	38%	40%
Normal Traffic Congestion	23%	27%
Bad Weather	4%	2%
Business or Personal Reasons	2%	5%
Don't Know/No Reason	–	2%

Source: Michigan ITS Predeployment Study: West Sector Report, prepared by Cambridge Systematics and Kimley-Horn Associates for Michigan DOT, 2003.

Table 42 Reasons for Changing Departure Time
West Sector (Washtenaw, Livingston and Westen Wayne Counties, Michigan)

Reasons for Changing Departure Time	a.m. Commute	p.m. Commute
Traffic Accident or Incident	51%	35%
Roadway Construction	22%	35%
Normal Traffic Congestion	29%	39%
Bad Weather	24%	8%
Business or Personal Reasons	10%	4%
Don't Know/No Reason	2%	4%

Source: Michigan ITS Predeployment Study: West Sector Report, prepared by Cambridge Systematics and Kimley-Horn Associates for Michigan DOT, 2003.

This survey was focused on general uses of ITS and also obtained information on how commuters might value different types of emerging technology and new information sources. The following table, for example, summarized commuters' ranking of various technologies and information sources on a scale of 1 to 10.

Table 43 Stated Importance

Total Sample (Oakland, Genessee, Washtenaw, Livingston, Monroe, Western Wayne and southern Wayne Counties, Michigan) and West Sector (Washtenaw, Livingston and Westen Wayne Counties, Michigan) Results

	Total Sample	West Sector
Obtaining traffic information from a variety of sources, like the radio and TV	8.3	8.3
Obtaining information about alternate routes as a result of accidents, congestion or weather	8.3	8.5
Having a device in your vehicle to automatically call an emergency number during an accident	8.1	7.7
Providing continuous traffic advisory information on a dedicated radio station	8.0	7.9
Having immediate access to traffic information in your vehicle	7.8	7.9
Using electronic highway message signs to obtain traffic information	7.5	7.4
Having immediate access to traffic information at home	7.3	7.1
Having a collision avoidance device in your vehicle	7.2	7.1
Providing automatic traffic and accident reports on a device in your vehicle	6.9	7.0
Having a device in your vehicle that gives maps and directions	6.8	6.9
Obtaining information on public transportation at home or at work	6.2	6.0
Using a toll-free mobile phone to obtain traffic information	5.8	5.4
Offering a customized paging service that gives traffic information about routes you take	5.6	5.2
Accessing traffic information on the Internet	4.4	4.2

Source: Michigan ITS Predeployment Study: West Sector Report, prepared by Cambridge Systematics and Kimley-Horn Associates for Michigan DOT, 2003.

This chart indicates the importance of alternate route information to commuters and also indicates that it is the information that is important, not the technology that delivers it.

A survey focused on weather response would expand on some of these questions and use some of the questions used in previous studies that are documented in the literature search in Section 2. In particular, the survey effort should attempt to obtain more detail on what type of weather

phenomena impact pretrip decisions and what level of detailed information is desired. For example, do commuters respond to generalized regional forecasts or are they more likely to respond to maps showing estimated snowfall totals around the region? What is the best way to express the impact of weather on road conditions? One method may be to read a weather forecast or road weather information scenario to the respondent and ask them whether they would modify their trip based on that forecast. This method could be used in a focus group setting as well as a phone survey.

It is important to note that other methods are now available for collecting data on traveler pretrip preferences. While most of them would not achieve the statistical validity found in a survey sample, they could be less expensive and still provide strong insight into customer preferences:

- **Web site surveys –** Volunteers may be solicited from regular users of traveler information web sites. They would be asked to report any changes in their trip patterns based on weather and traffic information. The data could provided directly over the Internet.
- **E-mail surveys –** A preselected group of commuters could be e-mailed on a daily basis to obtain information on their use of pretrip information and their travel habits.
- **In-vehicle devices –** Volunteers could be solicited among subscribers to in-vehicle information and navigation services. They could report their trip patterns, such as time of departure on a daily basis, and this could be matched against weather data for that time period.

Another important consideration is the geographic scope of such surveys. They may be more effective if concentrated in a small number of cities that represent a range of climates. While this study may be location-specific, it also may identify some overlying trends in how weather impacts driver behavior prior to entering the vehicle.

References

[1] B. Coifman, "Using Dual Loop Speed Traps to Identfy Detector Errors," *Tranportation Research Record,* vol. 1683, pp. 47-58, 1999.

[2] R. E. Turochy and B. smith, ""A new Procedure for Detector Screening in Traffic Management System" " *Tranportation Research Record,* vol. 1727, pp. pp 127-131.

[3] L. N. Jacobson, N. L. Nihan, and J. D. Bender, "Detecting Erroneous Loop Detector Data in a Freeway traffic Management System," *Tranportation Research Record,* vol. 1287, pp. 151-160, 1990.

[4] B. Coifman and S. Dhoorjaty, "Event Data Based Traffic Detector Validation Tests," in *Transportation Research Board* Washington D.C., 2002.

[5] C. Chen, J. Kwon, J. Rice, A. Skabardonis, and P. Varaiya, "Detecting Errors and Imputing Missing Data for Single Loop Sureveillance Systems," in *Transportation Research Board* Washington D.C., 2003.

[6] S. Ishak, "" Quantifying Uncertainties of Freeway Detector Observations using Fuzzy-Clustering Approach"," in *Transportation Research Board (TRB)* Washington D.C, 2003.

[7] TRB, *Highway Capacity Manual*: Transportation Research Board, 2000.

[8] "Economic Impact of Highway Snow and Ice Control Final Report," Federal Highway Administration U.S. DOT FHWA-RD-77-95, 1977.

[9] P. D. Prevedouros and P. Kongsil, "Synthesis of the Effects of Wet Conditions on Highway Speed and Capacity," 2003.

[10] A. T. Ibrahim and F. L. Hall, "Effect of adverse weather conditions on speed-flow-occupancy relationships," *Transportation Research Record,* vol. 1457, pp. 184-191, 1994.

[11] R. Lamm, E. M. Choueiri, and T. Mailaender, "Comparaison of Operating Speeds on Dry and Wet Pavements of Two-lane Rural Highways," *Tranportation Research Record,* vol. 1280, pp. 199 - 207, 1990.

[12] W. Brilon and M. Ponzlet., "Variability of Speed-Flow Relationships on German Autobahns," *Transportation Research Record,* vol. 1555, pp. 91-98, 1996.

[13] K. K. Knapp and L. D. Smithson, "The Use of Mobile Video Data Collection Equipment to Investigate Winter Weather Vehicle Speeds," in *Transportation Research Board (TRB)* Washington D.C.

[14] A. D. May, "Capacity and Level of Services for Freeway Systems," Third Interim Report Phase C - Tasks C1 through C10, June 12 1998.

[15] R. K. Hawkins, "Motorway Traffic Behaviour in Reduced Visibility Conditions," in *The 2nd International Conference in Vision in Vehicles*, Elsevier, Amesterdam, 1988.

[16] D.Galin, "Speeds on Two Lane Rural Roads - A Multiple Regression Analysis.," *In Traffic Engineering and Control,* vol. 22, pp. 453 -460, 1981.

[17] P. L. Olson, D. E. Cleveland, P. S. Fancher, L. P. Kostyniuk, and L. W. Schneider., "Parameters Affecting Stopping Sight Distance," National Research Council 1984.

[18] M. Kyte, Z. Khatib, P. Shanon, and F. Kitchener, "Effect of Environmental Factors on Free-Flow Speed.," in *the Fourth International Symposium on Highway Capacity*, Maui, 2001.

[19] M. Kyte, Z. Khatib, P. Shanon, and F. Kitchener, "Effect of Weather on Free-Flow Speed," *Transportation Research Record,* vol. 1776, pp. 61-68, 2001.

[20] W.L. Liang, M. Kyte, F. Kitchener, and P. Shannon, "Effect of Environmental Factors on Driver Speed," *Tranportation Research Record,* vol. 1635, 1998.
[21] M. Agarwal, T. H. Maze, and R. R. Souleyrette, II., "The weather and its impact on urban freeway traffic operations.," *85th Transportation Research Board Annual Meeting,* 2006.
[22] Federal Highway Administration. Road Weather Management. U.S. DOT.
[23] D. Unrau and J. Andrey, "DRIVER RESPONSE TO RAINFALL ON AN URBAN EXPRESSWAY," in *Transportation Research Board* Washington D.C.
[24] "www.en.wikipedia.org/wiki/Weather."
[25] "http://www.nws.noaa.gov/ost/asostech.html."
[26] "ASOS Guide For Pilots." vol. 2006.
[27] "http://shadow.agry.purdue.edu/sc.hly-faq.html."
[28] "http://www.nws.noaa.gov/om/brochures/asosbook.shtml."
[29] "http://www.globalspec.com/FeaturedProducts/Detail/RainWise/Industrial_Tipping_Bucket_Precipitation_Gauge/3273/0."
[30] M. Agarwal, T. H. Maze, and R. Souleyrette, "The weather and its impact on urban freeway traffic operations," in *85th Transportation Research Board Annual Meeting*, Washington D.C., 2005.
[31] I. S. C. Office, "http://shadow.agry.purdue.edu/sc.hly-faq.html," 2006.
[32] NWS, "ASOS User's Guide." vol. 2005: National Weather Service.
[33] MINITAB, "User's Guide2: Data Analysis and Quality Tools. ."

Vita

Hossam ElDin Hablas was born on January 18, 1974 in Alexandria, Egypt. He received his bachelor degree from the department of civil Engineering, Alexandria University, Egypt in 1996. After graduation, Hossam worked as a marketing engineer at a Belgium company in its branch in Egypt (Schréder Egypt) for 6 years, Hossam Travelled in January 2003 to the United States of America to accompany his wife who got accepted in the EDP program at Virginia Tech. Hossam got a job at Blacksburg Transit (BT).

While working at Blacksburg Transit, Hossam decided to apply to the Master program of the The Charles Edward Via, Jr. Department of Civil and Environmental Engineering at Virginia Tech, which earned him a Master degree in 2007 under the supervision of Dr. Hesham Rakha. During the same period Hossam worked as a Graduate Research Assistant with the Center for Sustainable Mobility at the Virginia Tech Transportation Institute.